University of Alberta

Solubility Modeling of Athabasca Vacuum Residue

by

Maryam Zargarzadeh

A thesis submitted to the Faculty of Graduate Studies and Research
in partial fulfillment of the requirements for the degree of

Master of Science
in
Chemical Engineering

Department of Chemical and Materials Engineering

Fall 2010
Edmonton, Alberta

Examining Committee

William C. McCaffrey, Chemical and Materials Engineering

Murray R. Gray, Chemical and Materials Engineering

Rick Chalaturnyk, Civil and Environmental Engineering

Abstract

The solubility parameters for ten fractions of Athabasca vacuum residue were calculated from molecular representations via group additivity methods. Two methods were used; Marrero-Gani and Fedors. The calculated parameters were compared between the fractions for consistency, and also compared with other literature sources. The results from the Marrero-Gani method were satisfactory in that the values were in the expected range and the results were consistent from fraction to fraction. The final stage of the work on group additivities was to estimate the solubility parameter values at the extraction temperature of 473 K, and then compare the solutes to the solvents. The solubility parameters of the solvents were calculated from correlations and from the molecular dynamic simulation; the latter method did not result in fulfilling values. The most reasonable solvent and solute solubility parameters were used to assess the utility of the solubility models to explain the trends. The solubility models were not suitable for these types of materials. Stability of heavy oil fractions undergoing mild thermal reactions were predicted computationally for limited sample cracked molecules.

Acknowledgements

My appreciation is extended to Professors McCaffrey and Gray for their supervisions during the project.

My special thanks to Dr. Katell Le Lannic from Total for providing me with the opportunity to enrich my research by her support and guidance during my study-leave at Total Research Centre of Gonfreville, Le Havre and for their financial support.

I would also like to thank all my colleagues, friends and staffs at the Department of Chemical and Materials Engineering and acknowledge Dr. Shaofeng Yang’s help in running the molecular dynamic simulations with Materials Studio.

Finally I express my recognition to God and my deepest gratitude to my parents, brother and sister for their boundless love, encouragement and moral support.

Table of Contents

List of Tables

List of Figures

Nomenclature

A	asphaltene
AC	amorphous cell
asph	asphaltene
F-H	Flory-Huggins
FiMj	molecule #j of fraction i
H	heavy phase/ hydrogen wt%
H/C	hydrogen/carbon ratio
ig	ideal gas
L	non-solvent/ light phase
M	maltenes
MD	molecular dynamics
MG	Marrero-Gani
N	Nitrogen wt%
N/A	not available
N/C	not calculated
PR EOS	Peng-Robinson equation of state
MW	molecular weight
S	solvent/ sulphure wt%
SCF	supercritical fluid
SP	solubility parameter
Wt%	weight percent

Symbols

C_P	heat capacity
ΔH_{fus}	enthalpy of fusion
ΔH^{mix}	enthalpy of mixing
ΔH_V	molar enthalpy of vaporization
ΔS^{mix}	entropy of mixing
δ (MPa$^{1/2}$ or [cal/cc]$^{1/2}$)	Hildebrand solubility parameter
$\bar{\delta}$	average solubility parameter
δ_r	reduced solubility parameter
f	fugacity
f^0	standard fugacity
φ	volume fraction
γ	activity coefficient
K	equilibrium K-value
μ	chemical potential
μ^*	standard chemical potential
P_C	critical pressure
R	gas constant
ρ	density
ρ_r	reduced density
T(K)	temperature
T_m	melting temperature
T_r	reduced temperature
U	internal energy
$\overline{U}$	mean internal energy
U^*	standard internal energy
v	molar volume
xi	mole fraction of component i in liquid phase/solubility
yi	mole fraction of component i in vapor phase

1 Introduction

1.1 Importance of property estimation methods for engineering design for processing of heavy petroleum

Physical and thermodynamic properties of heavy petroleum fractions are important for production, transportation, storage, and process design for upgrading and refinery processes. The boiling curve of any complex hydrocarbon mixture is important because it indicates how much of the heavy petroleum can be distilled, leaving behind undesirable heavy components. Determination of molecular weight (MW) is important as an alternative to boiling point, and is crucial for calculation of phase behaviour.

Process design for upgrading of heavy petroleum fraction requires a number of separations based on vapor-liquid equilibrium, including flashing vapor from liquid, degassing produced fluids and distillation. At the heart of vapor-liquid equilibrium calculations is the K-value defined as follows:

$$K_i = y_i / x_i \qquad [1]$$

Where y_i is the mol fraction of component i in the vapor phase and x_i is the mol fraction of component i in the liquid phase. The use of K-value definition requires that a mixture be defined in terms of its components on a molar basis. In heavy petroleum, the number of components is far too great to uniquely identify each one. Consequently, oils are characterized by pseudo-components for the purposes of these calculations by grouping together components of similar behaviour. This grouping is done by boiling point, so that oil is characterized as a series of narrow boiling cuts.

The most efficient method for vapor-liquid calculations is to use an accurate equation of state such as Peng-Robinson to calculate all the thermodynamic properties of heavy petroleum, including K-values. In order to use cubic equations of state for pseudo-components, the critical properties and the acentric factor must be estimated. Several correlations are available and are built into the software packages (for example the work of Twu (1984)). In general, boiling point and specific gravity are sufficient to use these correlations. Additional correlations allow conversion between molecular weight, boiling point and specific gravity (e.g. Twu, 1984). Difficulties arise for vacuum residue fractions for two simple reasons. Because the material cannot be distilled, data are no longer available for correlation of properties. These fractions are rich in aromatic compounds and polar species; therefore, correlations that use n-alkanes as a reference series, such as Twu (1984) pointed out in Gray (2008), become less and less relevant as boiling point increases.

Methods based on boiling curves are clearly not sufficient for characterizing residue fractions, because they cannot be distilled. Two methods have been suggested, depending on the type of calculation required. If all of the oil remains in the liquid phase, then it can be treated as a single pseudo-component. If the heavier fractions of the oil are vaporizing, then the residue must be more fully characterized. Riazi (2005) presents a comprehensive discussion of fitting and extrapolating data for petroleum fractions. His approach and an example for fitting data to ASTM D1160 data for Athabasca bitumen and extrapolation to get a boiling curve for the vacuum residue can be found in Gray (2008).

1.2 Importance of liquid-liquid and liquid-solid behaviour in production and upgrading

The other type of phase behaviour that is critical in the behaviour of heavy petroleum fractions is liquid-solid or liquid-liquid equilibrium, depending on the temperature of the operation. The formation of new liquid or solid phases in vacuum residue may also be accompanied by chemical reactions. Examples of such phase behaviour include precipitation of components, which are called asphaltenes, from the crude oil during production or refining, fouling of heat transfer surfaces by organic deposits and formation of coke during thermal cracking.

Some of these phase separations are related to the stability of liquid products, which is an important concern for every refinery for storage and transportation. Unstable blends, that produce solid precipitates, are of concern for fouling of pipelines and heat-transfer equipment. Stability is of concern in thermal cracking processes, such as visbreaking for product stability, and in delayed cokers for the fouling of process furnaces. During thermal conversion or visbreaking the asphaltenes become increasingly more and more aromatic, due to cracking of alkyl chains, aromatization of naphthenes and condensation reactions, so the stability decreases with increasing conversion (524°C+ residue fraction conversion) or process severity (equivalent reaction time (Yan, 1990)). Conversion is limited by asphaltene instability and coke formation and it is important to control it to avoid fouling.

The prediction of liquid-liquid and liquid-solid phase behaviour is difficult due to the complexity of both of the phases. Given time, thermodynamic equilibrium will be established between the solid and the liquid solutions. This condition can be analyzed as a thermodynamic phase equilibrium problem using solution theories. One of the most successful methods is based on regular solution theory, which defines the mutual solubility of components based on the difference in the solubility parameters between the solute and the solvent. The solubility parameter is defined as a function of enthalpy of vaporization and molar volume, and it can be estimated for solvents and for petroleum fractions.

1.3 Value of molecular representations for petroleum

The pseudo-component methods explained above are based on extrapolation of empirical physical property methods for petroleum fractions, to represent the residue fraction. A completely different approach is to represent vacuum residue as a mixture of actual chemical components such that each component will have a concentration, allowing a mixture of components to fit the analytical data available for the vacuum residue. This approach was used by Sheremata et al. (2004) to quantitatively represent the asphaltenes in Athabasca using elemental compositions, molecular weights, and proton and carbon-13 NMR data. Jaffe et al. (2005) illustrated how large molecules can be used to systematically represent vacuum residues for reactions during processing, and to estimate thermodynamic and physical properties. The attraction of molecular representations is the ability to span from computational chemistry through to refinery design with a single representation of petroleum fractions as mixtures of defined components.

Once a molecular representation of a mixture is available, then a group contribution method can be used to determine the critical properties for use in an equation of state. McFarlane (2007) analysed data from Sheremata et al. (2008) and found that the Marrero and Gani (2001) contribution method gave the most consistent results for critical properties and acentric factors for large bitumen molecules. This group-contribution approach is also valuable for estimating the solubility parameters of heavy fractions, in order to perform solubility calculations based on thermodynamic models. In principle, the group contribution method can be combined with reaction models to predict stability of products from processes such as visbreaking and hydroconversion.

1.4 Statement of objective and hypotheses

The objective of this work is to test group-contribution methods for the estimation of the solubility parameter of fractions of vacuum residue. The modeling approach consists of two steps; the fractions are represented as mixtures of molecules that are consistent with experimental data for molecular weight, elemental analysis, and NMR spectrometric analysis (Sheremata, 2008), then the properties of the molecules are calculated from group additivity. Two methods for group-additivity calculations were examined; Marrero and Gani (2001) and Fedors (1974). The latter method has been suggested for solubility parameter calculations (Rogel, 1997, Jaffe et al., 2005). The fractions considered by Sheremata (2008) had been separated by supercritical fluid extraction. The consistencies of the results were examined for a series of fractions separated from Athabasca bitumen by extraction with supercritical pentane at successively increasing pressures. The solubility parameters of the solvents were calculated from correlations and from the molecular dynamic simulation. The solubility parameters of the extracts and the solvents were compared through the series of fractions. A thermodynamic model was used to estimate the solubilities of each of the vacuum residue materials in the extracting super critical solvents. The input parameters for the model were the mole fraction, molar volume and the solubility parameter of the solvents and the extracts. Trends between the solubility parameter obtained and the elemental compositions were also investigated.

This scope of research supports ongoing efforts to represent the behaviour of vacuum residue on a molecular basis. Given a molecular representations, then cracking of the molecules can be simulated computationally based on the known reaction mechanisms and different cracking propensities such as breakage of the C-C and C-S bonds. As the reactions progress, the group additivity methods developed here can be used to evaluate the stability of the reaction products as a function of severity (number of cracks in the favored cracking locations and the amount of aromatization), again on a molecular basis, to determine the limits of conversion.

2 Literature Review

2.1 Phase behaviour from corresponding states methods and equations of state

Equation-of-state methods provide one of the most useful techniques used in chemical engineering practice for modeling phase equilibria of multicomponent systems. For cubic equations of state, suitable estimates of the constants in an equation of state are usually found from values for the critical constants T_C and P_C. The Peng-Robinson (PR) equation, in which the acentric factor enters through function $\alpha(T_r,\omega)$ as an additional parameter, yields three-parameter corresponding-states correlations. Critical properties can be estimated from a set of correlations developed by Twu (1984), using the properties of the n-alkanes as a reference for properties of petroleum fractions of a given boiling point, T_b, in degree R and specific gravity. The agreement is excellent even for the aromatic compounds, even though the n-alkane series is used as a reference set. The difficulty with heavy petroleum fractions is that the fractions become extremely aromatic and enriched in polar components. The critical properties cannot be measured and T_b cannot be measured. In order to compensate for the difficulties in dealing with these fractions, interaction parameters are commonly adjusted to match predictions to experimental data.

2.2 Solution models for liquid-solid and liquid-liquid equilibrium

The solubility of a solute in a solvent can be modeled based on the enthalpy and entropy of solution. The regular solution theory, developed by Hildebrand & Scott (1964), represents the enthalpy and entropy of mixing as simple functions of concentration as follows for two components *1* and *2*:

$$\Delta H^{mix} = (v_1 x_1 + v_2 x_2)(\delta_1 - \delta_2)^2 \phi_1 \phi_2 \qquad [2]$$

Where v_i is molar volume, x_i is mol fraction and ϕ_i is volume fraction of component *i*. The parameter δ is the Hildebrand solubility parameter which is defined as follows:

$$\delta = \left[\frac{\Delta H_V - RT}{v} \right]^{1/2} \qquad [3]$$

where ΔH_V is molar enthalpy of vaporization (to an ideal gas) and v is molar volume. Recalling that ΔH_V - RT = ΔU_V , we see that the solubility parameter is the square root of the internal energy per unit volume, which can also be considered the cohesive energy per unit volume. The greater the density of cohesive energy, the stronger the solvent for heavy fractions of bitumen and petroleum. Total energy of vaporization of a liquid consists of several individual parts. These arise from (atomic) dispersion forces, (molecular) permanent dipole-permanent dipole forces and (molecular) hydrogen bonding (Hansen, 2000). The entropy of mixing is:

$$\Delta S^{mix} = -R\left[x_1 \ln(x_1) + x_2 \ln(x_2)\right] \qquad [4]$$

A shortcoming of the Hildebrand solubility parameter is that it was limited to regular solutions, as defined by Hildebrand & Scott, and does not account for associations between molecules, such as those that polar and hydrogen –bonding interactions would require (Hansen, 2000). At reaction conditions, these forces may be negligible and Hildebrand solubility parameter may be a good approximation.

The simplest model for the entropy of mixing of chain molecules is the Flory-Huggins equation:

$$\Delta S^{mix}_{F-H} = -R\left[x_1 \ln(\phi_1) + x_2 \ln(\phi_2)\right] \qquad [5]$$

From these mixing relationships, the chemical potential of an asphaltene (A) in solution in maltenes (M) and non-solvent (L) can be written as follows:

$$\begin{aligned}\frac{\mu_A - \mu_A^*}{RT} = {} & \ln(\phi_A) + (1-\phi_A) - \phi_M\left(\frac{v_A}{v_M}\right) - \phi_L\left(\frac{v_A}{v_L}\right) + \left(\phi_M \frac{v_A(\delta_A - \delta_M)^2}{RT} + \phi_L \frac{v_A(\delta_A - \delta_L)^2}{RT}\right)(\phi_M + \phi_L) \\ & - \phi_M\phi_L\left(\frac{v_A}{v_M}\right)\frac{v_M(\delta_M - \delta_L)^2}{RT}\end{aligned}$$

[6]

Flory (1953) derived this equation from differentiation of Gibbs free energy for polymer mixed with a solvent and nonsolvent. Similar equations can be written for the chemical potential of the maltenes and the non-solvent, which would usually be an n-alkane such as heptane. At equilibrium, the chemical potential of each component is the same in each phase. There are three equations (for asphaltene, maltene and non-solvent) and four unknowns (three volume fractions sum to one in each phase). Simplifying approximations are needed for solving the unknowns.

Hirschberg et al. (1984) were the first to apply the regular Flory-Huggins model to petroleum mixtures. The simplifying assumption they made was to consider the solvent as the mixture of maltenes and the liquid and hence reducing the tertiary mixture of asphaltene, maltenes and solvent to a pseudo-binary mixture:

$$v_S = x_M v_M + x_L v_L \quad [7]$$

$$\delta_S = \phi_M \delta_M + \phi_L \delta_L \quad [8]$$

$$\frac{\mu_A - \mu_A^*}{RT} = 0 = \ln(\phi_A) + \left(1 - \frac{v_A}{v_S}\right)\phi_S + \phi_S^2 \frac{v_A(\delta_A - \delta_S)^2}{RT} \quad [9]$$

Equation 6, mentioned before, was derived by an extension of the procedure used to obtain equation 9.

They also assumed that the asphaltenes are dilute at the flocculation point, so that $\phi_A \ll 1$ and $\phi_S = 1$. Hence the maximum volume fraction of asphaltenes that is soluble in the oil-solvent mixture is:

$$\phi_A^{\max} = \exp\left[\frac{v_A}{v_S} - 1 - \frac{v_A}{RT}(\delta_A - \delta_S)^2\right] \quad [10]$$

The equivalent maximum weight percent of asphaltenes is:

$$Wt\%_A = \frac{(1-\phi_A^{\max})\dfrac{MW_S}{v_S}}{(1-\phi_A)\dfrac{MW_A}{v_A} + \phi_A \dfrac{MW_S}{v_S}} \quad [11]$$

Although solubility parameters were devised as part of the regular solution model, very few liquid mixtures are found to be described by the regular solution model (Wiehe, 2008). Nevertheless, the solubility parameter is extremely useful for analyzing and interpreting the solubility behaviour of asphaltenes and other petroleum components as used in numerous cases in literature (Anderson 1999, Wiehe 2008, etc).

As indicated in equation [8], the solubility parameter for a mixture is defined as the volumetric average of the mixture components:

$$\delta_{mix} = \sum_{i=1}^{n} \phi_i \delta_i$$
$$\phi_i = \frac{x_i v_i}{\sum x_i v_i} \qquad [12]$$

Yarranton et al. (1996, 2002, 2005) used similar approximation as Hirschberg et al. (equation [9]) for the regular Flory-Huggins model except that Yarranton et al. increased the number of pseudo-components to include n-paraffin, saturates, aromatics, resins and associated asphaltenes with a molecular weight distribution, and included resins with asphaltenes in the precipitated phase. The multi-component regular Flory-Huggins model for the chemical potential of component *i*, μ_i, is given by:

$$\frac{\mu_i - \mu_i^*}{RT} = \ln(\phi_i) + 1 - \sum_{j=1}^{n} \frac{v_i}{v_j}\phi_j + \frac{v_i(\delta_i - \delta_{mix})^2}{RT} = \ln(x_i \gamma_i) \qquad [13]$$

With the same assumptions discussed in Hirschberg model, Yarranton et al. (1996) determined that the ratio of the equilibrium mole fractions of each of the asphaltene and resin species in light (L) and heavy (H) phases is given by

$$K_i = \frac{x_i^H}{x_i^L} = \gamma_i^L = \exp\left[\ln\frac{v_i^L}{v_{mix}^L} + 1 - \frac{v_i^L}{v_{mix}^L} + \frac{v_i^L}{RT}\left(\delta_i - \delta_{mix}^L\right)^2\right] \qquad [14]$$

A liquid–liquid equilibrium is assumed between the heavy liquid phase (asphaltene-rich phase including asphaltenes and resins) and the light liquid phase (oil-rich phase including all components). It is still not certain that asphaltenes ‘precipitate’ as a liquid phase or a solid phase. The above formulation is equivalent to solid-liquid phase equilibrium where the contribution of the heat of fusion to the equilibrium expression is negligible (Akbarzadeh et al., 2004, 2005).

The regular Florry-Huggins model is extremely sensitive to the values of the solubility parameters with differences in the fourth significant figure being important. This requires higher accuracy than is typically measured for solubility parameters. Yarranton et al. calculated solubility parameters of n-paraffins from a correlation based on heat of vaporization and molar volume data (Wiehe, 2008).

2.3 Solubility of pure solids

The solubility behaviour can be explained as an equilibrium solubility of a solute in a liquid solution (based on the assumption that there is no appreciable solubility of the liquid solvent in the solid phase):

$$\begin{aligned} f_{a(pure solid)} &= f_{a(solute in liquid solution)} \\ f_a^S &= \gamma_a x_a f_a^0 \end{aligned} \qquad [15]$$

where x_a is the solubility (mol fraction) of the solute in the solvent, γ_a is the activity coefficient of the solute in the liquid phase and f_a^0 is the standard-state fugacity to which γ_a refers. The standard-state fugacity f_a^0 can be defined as the fugacity of pure, subcooled liquid at the temperature of the solution and at some specified pressure.

The pure solute fugacity ratio can be determined from a thermodynamic cycle (assuming that Δc_p is constant over the temperature range $T \rightarrow T_m$) to give:

$$\ln \frac{f_a^0}{f_a^S} = \frac{\Delta H_{fus}}{RT_m}\left(\frac{T_m}{T} - 1\right) - \frac{\Delta c_p}{R}\left(\frac{T_m}{T} + 1\right) + \frac{\Delta c_p}{R} \ln \frac{T_m}{T} \qquad [16]$$

One simplification can be made, which is the first term on the right hand side of equation [16] is the dominate one and the two terms of opposite signs approximately cancel each other especially if T and T_m are not far apart (Prausnitz, 1999).

The ratio of the standard state fugacities was considered to be near unity for asphaltenes in toluene-hexane mixtures because the asphaltenes do not appear to precipitate in a crystalline form, but rather as an amorphous solid and the enthalpy of fusion at the point of precipitation may well be small in such circumstances (Yarranton & Masliyah, 1996).

In order to measure the solubility from equation [15], an estimation of the activity coefficient from Flory-Huggins theory for the infinitely dilute case of a solute in a solvent can be used. The resulting equation is:

$$\ln\frac{1}{x} = -\ln x = 1 - \frac{v_a}{v_S} + \ln\frac{v_a}{v_S} + \frac{v_a}{RT}\left[(\delta_a - \delta_S)^2\right] + \frac{\Delta H_{fus}}{RT_m}\left(\frac{T_m}{T} - 1\right) \qquad [17]$$

where x is the mole fraction solubility, ν molar volume, R the universal gas constant, T the absolute temperature, ρ the density.

Table 2-1 shows the solubilities (mole fractions) of five model compounds in pure n-heptane at 20 °C when $\Delta\delta = \delta_a - \delta_S = 4$ MPa$^{1/2}$ is assumed. X_a is the solubility when $\ln\frac{f0}{fs} = \frac{\Delta H_m}{RT_m}\left(\frac{T_m}{T} - 1\right)$ term is not included and x_a^* is the correct solubility. There is an error in the order of about 10^{-4} for most of the compounds as a result of the fugacity ratio term. Dechaine et al. (2009) had to consider the ratio of the standard state fugacities (enthalpy of fusion term) in order to obtain good solubility predictions for the model compounds in heptane-toluene and DCM-heptane mixtures.

Table 2-1. Solubility of model compounds (first five columns taken from Dechaine et al., 2009)

Name	MW g/mol	Density g/ml	Tm, °C	ΔH_m KJ/mol	$\ln\gamma_a$	Ln(f0/fs)	x_a	x_a^*
H2TTP	614.74	1.34	452	38.4	2.02	9.39	0.132	1.109E-05
VOTPP	679.66	1.31	504	55.5	2.13	14.18	0.119	8.231E-08
H2OEP	534.78	1.19	342	42.6	2.01	9.15	0.135	1.143E-05
VOOEP	599.70	1.25	351	38.2	2.06	8.31	0.127	3.122E-05
PBP	612.77	1.34	227	52.2	2.02	8.86	0.133	1.874E-05

Petroleum fractions melt over a wide range of temperatures as they are such complex mixtures. In modeling the petroleum fractions solubilities, this problem of complexity rules out the application of the ratio of the standard state fugacities of pure solutes based on enthalpies of fusion.

2.4 Solubility parameters of petroleum fractions

Several correlations have been developed for solubility parameters of petroleum fractions, based on fitting solubility models by adjusting solubility parameters. For example, Rogel et al. (1997) gave a correlation for fractions in terms of elemental composition:

$$\delta = 35.87 - 10.477\ (H/C) \qquad [18]$$

It should be noted that Fedors' method is incorporated in the Rogel's, i.e. Rogel used Fedors' to calculate the solubility parameters and to derive her correlation of solubility parameter with H/C ratio.

Sundaram et al. (2008) modeled sediment formation in hydroconversion, using equation [17] without the enthalpy of fusion term, to predict the maximum amount of asphaltene precipitated. In this equation, all parameters except the molar volume (ν_a) and the solubility parameter of asphaltene (δ_a) are known. Given a correlation for the density of the asphaltene, the calculated sediment content (asphaltene concentration) and the measured sediment content value in ppm were used to estimate the asphaltene solubility parameters. The asphaltenes solubility parameter was related to the solubility parameter of the surrounding heavy oil (solvent in their system), which varied for each run. The following equation was derived from the best fit of all experimental data:

$$\delta_{asph} = 1.33\,\delta_{heavyoil} \qquad [19]$$

For a perfect fit of the measured sediment values, the molecular weight of asphaltenes can be found from equation [17] by an iterative procedure, since the sediment content (left hand side of equation [17]) is in wt% instead of mol%, i.e. it includes the molecular weight of asphaltene.

2.5 Solubility-based separation of vacuum residues at elevated temperature and pressure

Much of the modeling effort for asphaltene solubility has focussed on ambient temperatures, which are relevant to production and product stability. Commercial separation processes, such as solvent deasphalting, use high-pressure solvents at elevated temperature. In some of these processes, such as supercritical extraction (Chung et al., 1997) or the Residual Oil Supercritical Extraction (ROSE) process (developed by M. W. Kellogg Technology Co. , figure given in Gray, 2008), the solvents may be supercritical. Separation and recovery of the solvent from the deasphaltened-oil is less energy intensive when the solvent is above its critical point. Little work has been published on solubility of petroleum fractions as a function of temperature. Akbarzadeh et al. (2005) modeled asphaltene precipitation from n-alkane diluted heavy oils and bitumens at a range of temperatures and pressures using regular solution theory with liquid-liquid equilibrium. The solubility parameter of the asphaltenes (and resins) was determined from the following correlation:

$$\begin{aligned} \delta_a &\approx \left(A(T)\rho\right)^{1/2} \\ A(T) &= -6.667\times10^{-4}T + 0.5614 \end{aligned} \qquad [20]$$

The common Hildebrand formula is meaningless at supercritical conditions because the vaporization is undefined. The energy of the compressed fluid phase is the sole contributor to the cohesive energy. At the critical temperature, the heat of vaporization of the liquid is zero and the equation wrongly leads to a negative value of δ. There is no simple relationship for the solubility parameter of supercritical fluids. Giddings et al. (1968) proposed an empirical correlation based on studies in liquid chromatography as follows:

$$\delta = 1.25 P_C^{1/2} \frac{\rho_{r\,SCF}}{\rho_{r\,liq}} \qquad [21]$$

Here P_C is the critical pressure and ρ_{rSCF} is the reduced density of the SCF, $\rho_r = \rho/\rho_C = V_C/V$, where ρ_C is the critical density. The reduced density of the fluid in the liquid state, ρ_{rliq}, pertains to $T_r < 1$ and $P < P_C$. The numerical constant 1.25 corrects for the unit of the critical pressure, P_C, in atmosphere (1 atm = 0.101325 MPa) yielding the solubility parameter in $(cal/ml)^{1/2}$ (where 1 $(cal/ml)^{1/2}$ = 2.0455 $MPa^{1/2}$). The approximation $\rho_{rliq} = 2.66$ was suggested by Giddings et al. (1968).

Although this relation predicts trends qualitatively in the right direction, its quantitative predictions were found to be poor (Allada, 1984). Allada (1984) proposed a solubility parameter concept for supercritical fluids which uses the internal energy of the supercritical gas relative to isothermally expanded ideal state as the cohesive energy of the gas.

$$\delta = \left[\left(U^{*} - U\right)/v\right]^{1/2} \qquad [22]$$

Where U and ν are the internal energy and molar volume of the supercritical or dense gas at temperature T and pressure P, and U^* is the internal energy of the gas isothermally expanded to zero pressure where intermolecular cohesive force is zero (ideal gas).

The above equation was modified to express δ in terms of temperature and pressure. Further, to make it available to any gas, the equation was expressed in terms of reduced parameters, hence:

$$\begin{aligned} \delta_r &= \left[\frac{C_1}{R}\frac{\left(U^{ig} - U\right)}{T_C}\frac{P_r}{T_r}\frac{1}{Z}\right]^{1/2} \\ \delta_r &= \delta/\sqrt{P_C} \qquad [23] \\ \frac{U^{ig} - U}{T_C} &= \frac{H^{ig} - H}{T_C} - (1 - Z)RT_r \end{aligned}$$

where δ_r is the reduced or generalized solubility parameter, T_r is the reduced temperature, P_r is the reduced pressure, Z is the compressibility factor, R is the gas constant (calmol^{-1} K^{-1}), and C_1 is the conversion factor ($\frac{cal/cm^3}{atm}$). The reduced solubility parameter was given as an explicit function of P_r and T_r by Allada (1984).

2.6 Solubility parameter from group contribution methods

There are several group-contribution based methods for estimation of pure component properties. The two methods used in the literature for petroleum fractions are Fedors (1974) and Marrero and Gani (2001). Marrero and Gani's method was shown to be successful for estimation of the boiling point, T_b (McFarlane, 2007).

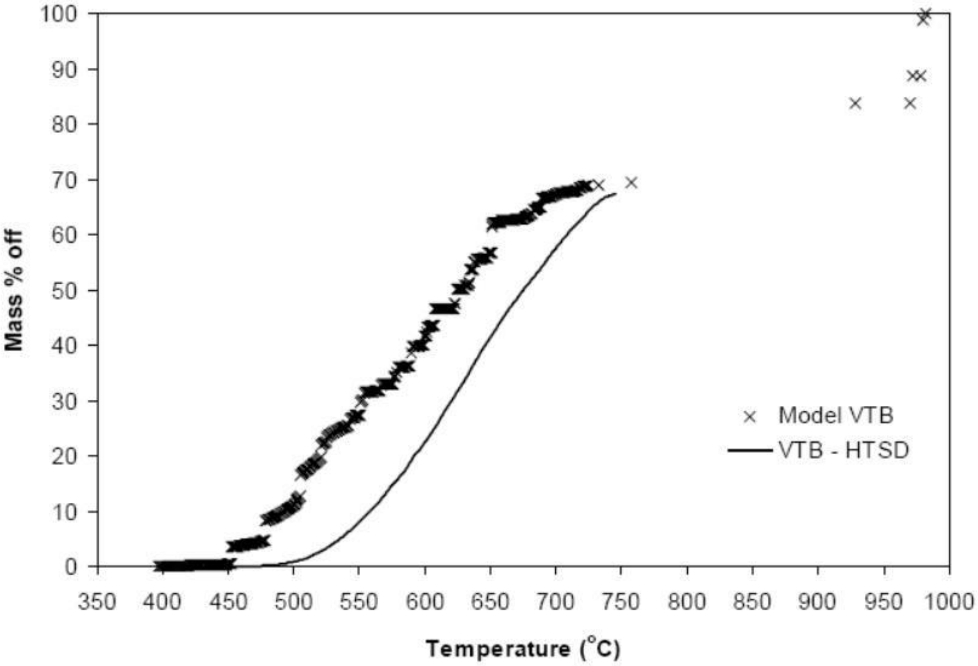

Figure 2-1. **Comparison of measured high temperature simulated distillation curve for VTB and that calculated from the molecular representations (taken from McFarlane, 2007)**

One of the early versions of group contribution method for solubility parameter is Fedors's (1974). He calculated molar vaporization energy contributions, $\Delta U_i = \Delta H_V - RT$, and molar volume contributions, ν_i, for structural components. The group contributions to the molar vaporization energy (kJ mol^{-1}) and molar volume at 25 °C ($\text{cm}^3\ \text{mol}^{-1}$), can be found in the *CRC Handbook of Solubility Parameters and Other Cohesion Parameters*.

$$\delta = \left(-\frac{U}{v}\right)^{1/2} = \left(-\sum_i U_i \Big/ \sum_i v_i\right)^{1/2} \qquad [24]$$

Although it is considered that the contributions give less accurate estimates of the cohesive energy than other sets of data, this compilation was remarkable because of the great number of groups considered (116 groups), and because of the inclusion of metals for use in calculations on organometallic compounds. Jaffe et al. (2005) recommended Fedors' method for the estimation of properties of vacuum residue fractions using molecular representations.

Many of the Fedors groups are related to halogens and metals which may not occur considerably in the petroleum molecules. In this work, the following ten groups were used to present the petroleum fractions:

Table 2-2. Group contributions to the molar vaporization energy and molar volume at 25 °C from Fedors (1974)

Groups	ΔU_i, kJ mol^{-1}	ν_i, cm^3 mol^{-1}
–CH3	4.71	33.5
–CH2–	4.94	16.1
>CH–	3.43	-1.0
–CH=	4.31	13.5
>C=	4.31	-5.5
Ring closure, 5 or more atoms	1.05	16
Conjugation in ring, for each double bond	1.67	-2.2
–NH– (NH cyclic)	8.4	4.5
–S– (S cyclic)	14.15	12
–O– (O cyclic)	3.35	3.8

Marrero and Gani (2001) developed a group contribution method based on three levels of molecular structure. First order, second order and third order groups were defined in the model. The proposed model was:

$$f(x) = \sum_i N_i C_i + \omega \sum_j M_J D_J + z \sum_k O_k E_K \qquad [25]$$

where C_i is the contribution of the first-order group that occurs N_i times and other variables are contribution and occurrence for the second and the third order groups. In the first level of estimation, the constants ω and z are assigned zero values. In the second, the constants ω and z are assigned unity and zero values and so forth. The left hand side functions for eight different properties, including normal boiling point, standard enthalpy of vaporization at 298 K, standard enthalpy of fusion and melting point are given in the paper. For example, for the standard enthalpy of vaporization at 298 K (H_V):

$$f(x) = H_V - H_{V0} = \sum_i N_i H_{V1i} + \sum_j M_j H_{V2j} \qquad [26]$$

The values of the additional adjustable parameters are also given, e.g. H_{V0} = 11.733 kJ/mol.

Gani has developed a package called ProPred, for property prediction, under the ICAS software. In ProPred, solubility parameter is given as one of the primary properties (with third level of estimation) also in the book by Kontogeorgis and Gani (2004); however, the function for this property and the value of the additional adjustable parameter, are not published in the literature. In this work the solubility parameter is considered as a secondary property, using the two elements of the common Hildebrand formula, enthalpy of vaporization and molar volume, for its calculation. The standard enthalpy of vaporization at 298 K can be calculated, as a primary property, from equation [26]. The molar volume was calculated from the density, as discussed below.

2.7 Estimation of molar volume

The thermodynamics equations for density are poor for calculating the density of high boiling, heavy petroleum fractions. The Lee-Kesler equation is commonly used, but requires estimates of acentric factors. The acentric factors, from the group contribution methods, are not available or consistent for the larger molecules (MW > 450 g/mol).

For molar volume, a density correlation with elemental composition (Gray, 2002) can be used as follows:

$$\rho = 1033 - 13.69H + 13.85S + 115.7N \qquad [27]$$

where ρ is density in kg/m^3 at 298 K, H, S and N are elemental content in wt%. The correlation is for the density of Alberta heavy oils and bitumens and may not be suitable for lighter molecules. The above correlation allows calculation of the density and hence the molar volume from the molecular weight and chemical formula.

These molar volumes were also used as initial guesses for calculating the solubility parameters using the molecular dynamic simulation.

2.8 Model compounds and hydrocarbon thermal cracking and free radical chain mechanism

The good feature of the molecular approach to upgrading processes such as visbreaking is that it links feed composition to product yield and quality via defined fundamental chemical steps. The most challenging aspect of implementing this modeling approach is to incorporate the addition reactions and the hydrogen transfer reactions. The addition reactions dominate the formation of sediment and coke and the hydrogen transfer reactions convert the olefins in the heavy fractions (Gray and McCaffrey, 2002).

In the simplest possible terms, residue conversion concerns the liquid-phase behaviour of saturated compounds, alkyl-aromatic and reactive sulfur groups at thermal reaction conditions. Although several authors have suggested that alkyl-aromatic materials such as heavy oils undergo cracking via free-radical chain mechanism, the work of LaMarca et al. (1993) was the most remarkable. They first represented the mechanisms of liquid-phase cracking of complex feeds that incorporated free-radical chain reaction mechanism. A complete literature review on the role of chain reactions and olefin formation in several related chemical processes was given by Gray and McCaffrey (2002). They also developed a mechanist framework for conversion of petroleum and bitumen residues. This framework is based on the LaMarca model with the explicit addition of coke formation, donor solvent and heterogeneous catalytic reactions, and the removal of the radical-hydrogen transfer step. This framework was partly used by Sheremata et al. (2004) in the computer kinetic modeling.

The sulfur compounds have weaker bonds than hydrocarbons. Alkyl sulfides are likely initiators of free-radical chain reactions in residues. The coke formation is preceded by phase separation in the liquid phase, driven by cracking reactions that leave behind more aromatic components than in the initial oil mixture. Coking is a disproportionation process, where most of the feed reacts to form lower molecular weight species, while a portion reacts to give a much higher molecular weight material than the initial feed. Most models in the literature assume that coke forms by termination reactions between large aromatic radicals. If this reaction is dominant and rapid, the total concentration of radicals in the remainder of the mixture would drop rapidly as soon as phase separation occurs. A reasonable mechanism for coke formation from hydrocarbons is free-radical chain polymerization followed by rearrangement to give a more thermally stable product. A second mechanism for formation of stable toluene-insoluble material is intermolecular addition reactions. All these mechanisms were based on the real reaction rates observed in the experiments. The activation energy of cracking and coke formation can range from 22 to 83 kcal/mol. The average value is 50 kcal/mol which is the thermal cracking energy for C_{15} compound (Joshi et al., 2008).

The related model compounds are listed below. Cracking happens at C-S bond and at C-C bond one carbon away from the aromatic ring. Ring opening is less probable in the absence of catalyst.

Sulfur containing model compounds (didodecyl sulfide, 1-dodecanethiol)

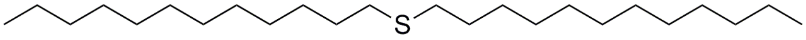

Phenyl model compounds (1-phenyldodecane, pentadecyl benzene)

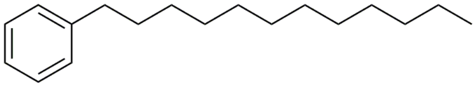

2-n-pentadecylpyridine

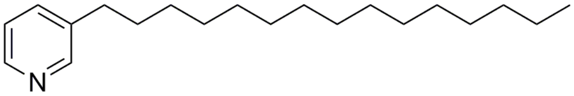

1-dodecylpyrene

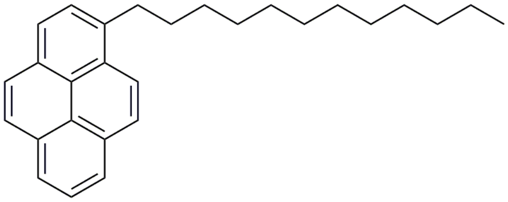

2-(3-phenylpropyl) naphthalene

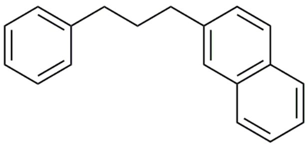

1, 3-bis (1-pyrene) propane

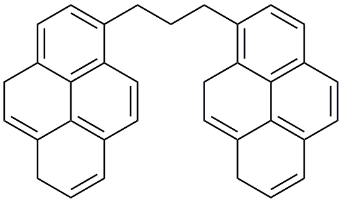

Solubilities of reaction products in this context were not discussed in the literature for a liquid-liquid phase.

3 Methods

The molecules from Sheremata (2008) were used as a test of the group additivity method. Sheremata proposed molecular representations for bitumen, its vacuum residue and the vacuum residue fractions using a Monte Carlo construction method which are consistent with the available NMR, molecular weight, aromaticity and SARA fraction data by building molecular models on the basis of just ten sub-structures. Seven of these sub-structures are the same as the 150 ones identified in the work of Jaffe et al. (2005). These molecules were from a series of fractions of Athabasca bitumen that had been prepared by supercritical extraction of vacuum residue by n-pentane (Chung et al. 1997, 1998, Zhao et al. 2005, 2007).

Table 3-1. Experimental properties of fractionated Athabasca Vacuum Residue (Sheremata, 2008)

Fractions	Yield, wt%	Yield, cum wt%	Density (g/ml)	MW	V (m^3/mol)	H/C	% aromaticity
1	12.7	12.7	0.9745	506	519	1.61	27.5
2	9.8	22.5	0.9930	755	760	1.59	29.7
3	7.6	30.1	1.0061	711	707	1.56	28
4	10.6	40.7	1.0228	800	782	1.52	34
5	6.5	47.2	1.0427	825	791	1.47	36
6	4.4	51.6	1.0543	948	899	1.43	40
7	3.3	54.9	1.0646	1138	1069	1.39	40
8	2.6	57.5	1.0678	1210	1133	1.39	42
9	2.1	59.6	1.0737	1520	1416	1.37	46
10	40.4	100	N/A	4190	N/A	1.23	50

This set of molecular representations includes 60 representative molecules for the narrow fractions extracted and fractionated from the Athabasca vacuum residue using n-pentane as a supercritical solvent at 200°C and pressure of 4-12 MPa (6 molecules for each fraction).

In the preparation of these fractions, the pressure of n-pentane was increased step by step. First it was increased from 3.5 to 5 MPa and whatever could be extracted was collected as fraction 1, then it was changed to 5.5 MPa with a step change and fraction 2 was collected. The cumulative weight percents are given in Figure 3-1.

The mol fractions of all the molecules are also available from the fitting of the molecules to the analytical data for each fraction (Table 9-2) (McFarlane, 2007, Sheremata, 2008).

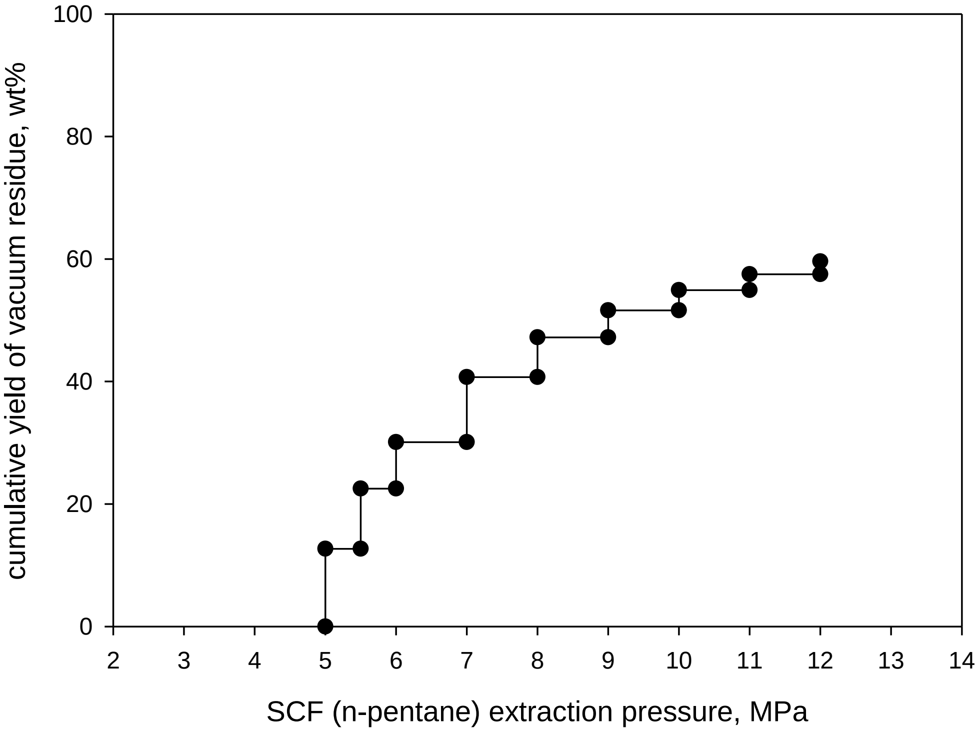

Figure 3-1. **Fractionation-pressure curve for the fractions of vacuum residue**

The predicted distillation curve and measured high temperature simulated distillation curve for these fractions were shown in Figure 2-1.

Winning successful boiling point calculations from the molecular representations for the Athabasca vacuum residue fractions, the simulated distillation data was incorporated in the molecular generation of the Athabasca bitumen and vacuum residue besides other analytical chemistry data.

The 60 representative molecules of these 10 SCFE fractions were chosen for three reasons. First, it was a rich set of molecular representations for the calculation methods. Second, the series of ten fractions allowed a check of the estimation methods for an incremental set of linked fractions, which should exhibit monotonic trends in all properties; as they were fractionated using the same supercritical solvent at constant temperature and varying pressures. Third, the solubility parameters of the solvent used at different pressures to extract the corresponding fractions could be calculated and compared to the solubility parameters of the extracted material.

Molecular weights and elemental compositions were obtained from the chemical formulas. Then each molecule was imported into ProPred Software (developed by Gani's group, Technical University of Denmark) to obtain the assignment of the groups for the Marrero-Gani method. Calculation of the enthalpies of vaporization was done manually from the groups and their contributions to the standard enthalpy of vaporization. In ProPred, the third order groups that describe molecular fragments in polycyclic compounds are also considered for calculating the standard enthalpy of vaporization but since the contribution value (z) are missing for some of the groups we did not consider the third order groups in general.

Groups obtained from ProPred were mapped to get the groups for the Fedors estimation method. As Fedors method uses fewer groups, it is a subset of the Marerro-Gani groups. The mapping (association) was as follows:

Table 3-2. Mapping form the Marrero-Gani groups to the Fedors groups

Fedors groups	Marrero and Gani associated groups
CH3	CH3 + aC-CH3
CH2	CH2 + aC-CH2 + CH2 (cyc)
CH	CH + CH(cyc)
–CH=	aCH + CH=C(cyc)
>C=	aC + (CHn=C)cycCH2 + aC-CH2 + aC-CH3
–S–	S(cyc)
–NH–	NH(cyc)

The number of rings and conjugations in rings for Fedors calculation were read from each molecule by observation.

The rule for calculating the solubility parameter for a mixture is well established to be the volumetric average (Hildebrand & Scott, 1964). The volumetric mixing rule is used to calculate the solubility parameter of each fraction from the solubility parameters of its representative molecules (equation [12]).

3.1 Illustration of group additivity method on an example molecule

Figure 3-2 gives an example of a large molecule. The ProPred software for the Marrero and Gani method cannot accept such large molecules; hence it is divided into two portions. Considering the basic of the group contribution method, the summation of the groups and their contributions to the two portions should almost be equal to those of the original molecule (there is for example the reduction of two aromatic carbons and addition of two other types, when the molecule is broken from a biphenyl bridge).

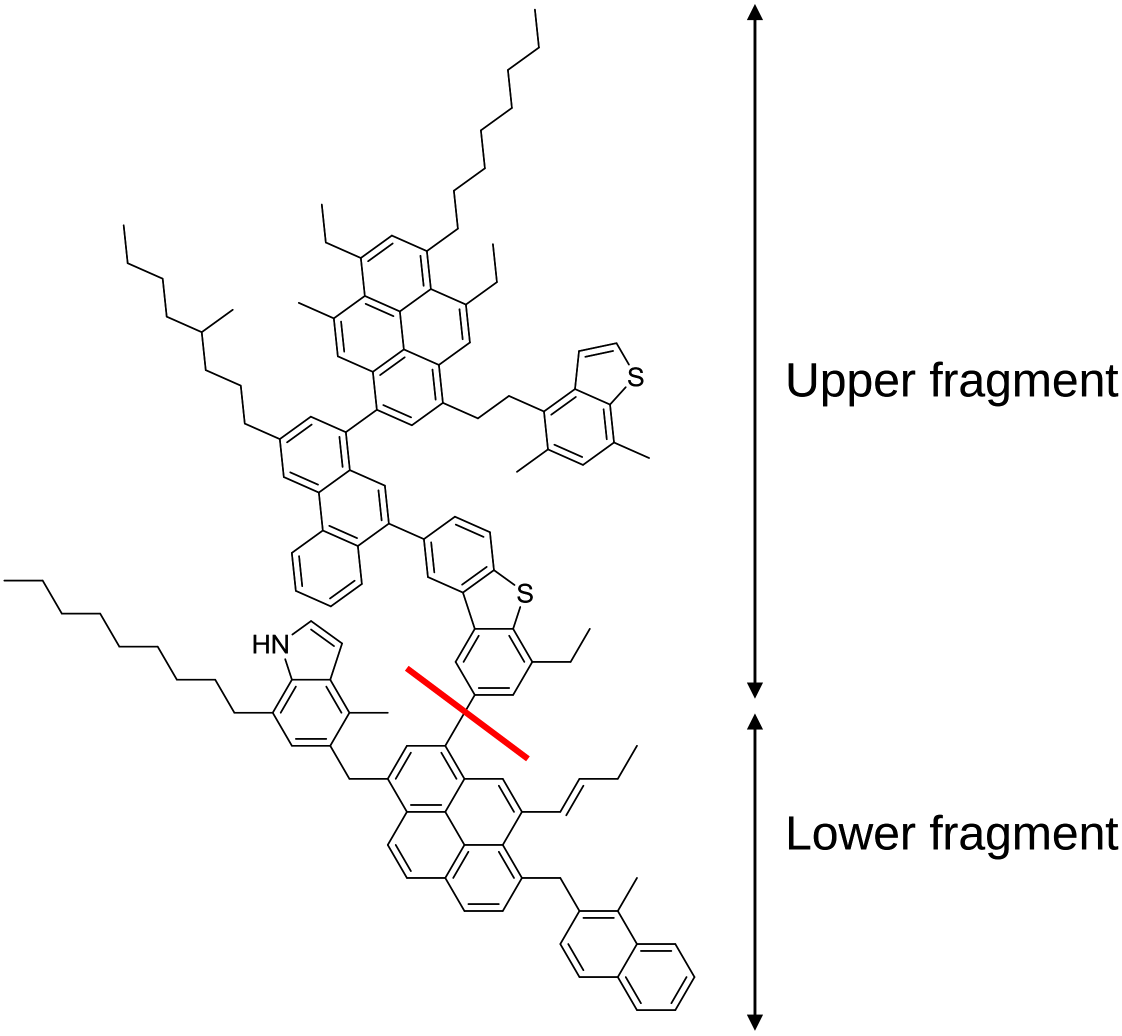

Figure 3-2. Example molecule (taken from Sheremata (2008) Athabasca bitumen molecular representation, molecule summa #10 ($C_{129}H_{135}NS_2$))

If we break the molecule in Figure 3-2 at the biphenyl bridge between the dibenzothiophene and the pyrene ring groups (shown as a red line), then the following first order groups exist in the upper and lower resulting portions:

Table 3-3. Marrero and Gani first order groups for the molecule from Figure 3-2

1st order groups	Upper fragment	Lower fragment
CH3	6	2
CH2	11	8
CH	1	0
aCH	17	14
aC fused with aromatic ring	10	8
aC fused with non-aromatic ring	6	2
aC except as above	4	2
aC-CH3	4	2
aC-CH2	7	3
aC-CH=CH	0	1
CH=CH(cyc)	1	1
NH(cyc)	0	1
S(cyc)	2	0

CH_3 groups are at the end of the chain attachments. The bridge between benzothiophene and pyrene in the upper portion is considered as two aC-CH_2 groups. Thiophene and pyrrole are considered as non-aromatic rings and the aromatic carbons attached with their non-aromatic carbons fall into the 2nd aC groups (fused with non-aromatics). Six of these aromatic carbons (aCs) exist in the upper portion. Other aCs in the upper portion are fused with aromatic rings like the six aCs in pyrene, except the four biphenyl-type bridge aCs. In the lower portion, the bridge between naphthalene and pyrene or benzothiophene and pyrene, each has one aC-CH2 and one aC (third type/except as above) group.

Table 3-4. Types of aromatic carbon groups in the Marrero and Gani method

Sample Increments	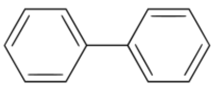	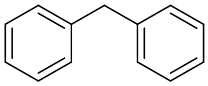	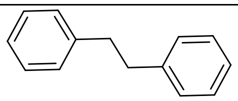
Types of aromatic carbons in connecting bridges	aC third type (2)	aC-CH2 (1) aC third type (1)	aC-CH2 (2) aC third type (0)

aC third type is a non-fused aromatic carbon. It is not fused to the aromatic or non-aromatic ring immediately i.e. there is a bridge between them.

Calculation of the solubility parameters at 473 K required estimation of the internal energy/enthalpy of vaporization and the molar volume. The mean internal energy for each fraction was calculated as follows:

$$\Delta\overline{U}_V^{298K} = \Delta\overline{H}_V^{298K} - RT = \left(\overline{\delta}^{298K}\right)^2 \times v \qquad [28]$$

$\overline{\delta}^{298K}$ is the solubility parameter of the fraction calculated from the volume average mixing rule and ν is the experimental molar volume of the fraction. The enthalpy of vaporization can then be calculated from the internal energies and the heat capacities:

$$\Delta\overline{H}_V^{473K} = \left(\frac{\Delta\overline{U}_V^{298K} + 8.314 \times 298}{1000}\right) + \int_{473}^{298} C_{P_l}\,dT + \int_{298}^{473} C_{P_V}\,dT \qquad [29]$$

where $\Delta\overline{H}_V^{473K}$ is in KJmol^{-1}.

Isobaric heat capacity of petroleum fraction liquids and vapors were estimated using the API procedures 7D2.2 (for $T_r \leq 0.85$) and 7D4.2, where Watson K = $T_b^{1/3}$/sp.gr, 60F/60F.

$$\delta^{473K} = \sqrt{\frac{\Delta H_V^{473K} \times 1000 - 8.314 \times 473}{1.12 \times v}} \qquad [30]$$

3.2 Supercritical solvent enthalpies and solubility parameter calculation

A non reduced form of the Allada correlation (equation 22) was used for solubility parameter calculation of the solvent.

$$\delta = \left[\frac{\left(H^{ig} - H\right) - (1 - Z)RT}{v}\right]^{1/2} \qquad [31]$$

$H^{ig} - H$, Z and v were calculated from PR EOS at 473 K and different pressures.

ν calculated from PR EOS was also used in Giddings correlation to calculate the solubility parameters.

3.3 Molecular dynamics (MD) simulation

Another computational method for calculating the cohesive energy density/ solubility parameter is molecular dynamics (MD) simulation. MD simulations were performed using a commercially available software package, Materials Studio (MS version 4.2, Accelrys) run on a workstation cluster.

In molecular dynamics a set of same molecules (for example 4 to 15), packed into the constructed amorphous cell (AC), are used for simulation. The density is needed for the AC construction. Amorphous Cell is a suite of computational tools that allows construction of representative models of complex amorphous systems and prediction of key properties. Among the properties that can be predicted and investigated are cohesive energy density and equation-of-state behavior. MD involves the stepwise integration of Newton's equations from a given starting point. It is the most natural method of performing equilibrium statistical-mechanical calculations via simulation.

All initial amorphous structures were subjected to energy minimization step using the conjugate gradient method in order to remove strong van der Waals overlaps. NVT MD simulations were carried out at 298 K and 473 K. The velocity Verlet method, with a time step of 0.001 pico-second (ps), was used as an integrator in all simulations. Simulations were carried out until the total energy of the system was stabilized. Each simulation was carried out for a total of 2000 ps. The properties of interest were calculated by averaging over the last three hundred ps of the corresponding trajectory file.

The calculations were done for the molecules at ambient condition and for selected molecules at process condition. The standard densities, at ambient condition, were obtained computationally from the correlation with the elemental composition (Gray, 2002). In order to acquire the density values at process temperature (473 K), MD simulation was done in isobaric-isothermal (NPT) statistical ensemble using the density values from the elemental composition correlation as the initial values. The temperature and pressure of the systems were controlled by Andersen thermostat and Brendsen barostat algorithms, respectively. In the NPT MD simulation, the volume of the periodic unit cell (i.e. density) was allowed to flocculate. These density values were used in the subsequent canonical (NVT) MD simulations at 473 K using the Brendsen thermostat to determine the cohesive energy densities. The rational behind using NVT rather than NPT MD simulation was to reduce the computational time.

Solubility parameters of representative molecules at 298 K

After the cell construction and minimization, molecular dynamics task (NVT ensemble) of the amorphous cell module was used for simulation. Amorphous cell analysis/ Energetic/ Cohesive energy density was selected for analyzing after running to get the cohesive energy density and hence solubility parameter.

Molecular dynamics task (NVT ensemble) of the discover module was also used for some of the main molecules and the same results were obtained for the solubility parameter.

Solubility parameters at process condition

The densities, needed for AC construction, are not available at process condition.

Molecular dynamics task (NPT) of the Discover module was first used to obtain the density and that density was used for a new AC construction and molecular dynamics task (NVT ensemble) of the Discover module for running to get SP.

Table summarizes the computed density values.

The solubility parameter at process condition was calculated for selected molecule having highest mol fractions.

Solubility parameters of n-pentane from MD

The solubility parameter for n-pentane was calculated at the associated supercritical pressure and the molar volume (density) calculated from the PR EOS.

3.4 Self compatibility from molecular representation

For analysing the self compatibility of the oil from the molecular representation instead of the S-value method, we may consider the molecule, or small series of molecules, with the highest solubility parameter(s), also having relatively high mol fraction(s), as asphaltene(s) and the rest as a solvent. Then we can calculate the maximum volume fraction of asphaltene from equation 10 and 11 and compare it with the calculated volume fractions. The same approach can be used to study the compatibility of the resulting products considering them as mixture of molecules with identical mole fractions. The molecule(s) with largest solubility parameter can be considered as asphaltene representative (s).

3.5 Cracking

Simple study of the effect of aromaticity and alkyl chains on solubility parameter

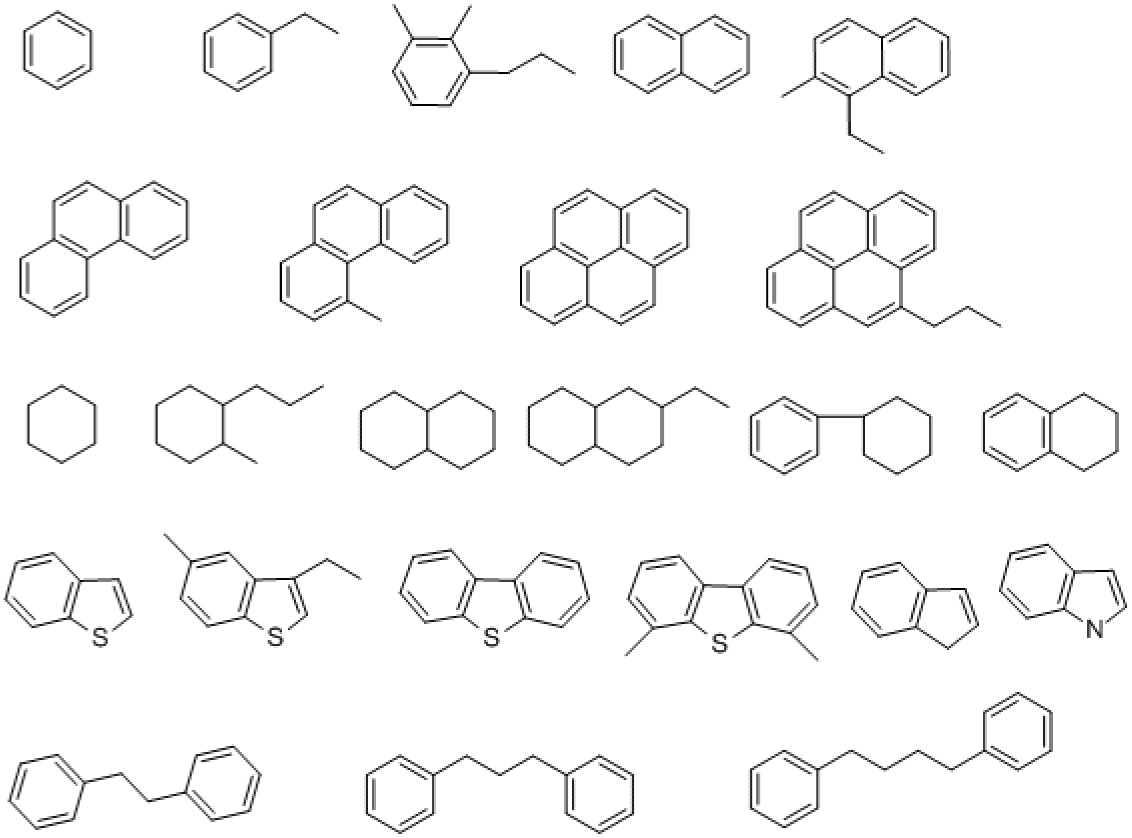

Figure 3-3. Sample compounds for studying the trend of solubility parameter

The following trends can be understood from Table 3-5 below:

1) Solubility parameter increases considerably with aromaticity (naphthalene, tetralin, and decaline; benzene and cyclohexane))
2) Solubility parameter changes slightly with increasing number of aromatic rings from benzene to pyrene.
3) Solubility parameter decreases with branches as a result of increase in the molar volume. Alkyl compounds have larger solubility parameters.
4) Solubility parameter increases considerably with the presence of heteroatom.

5) Solubility parameter decreases with increase in the length of the bridge between two benzene rings.

Table 3-5. List of solubility parameters of the sample compounds (the MG group contribution method and the density correlation with elemental composition were used for SP calculations)

Name	H/C	δ
Benzene	1	20.78
Ethyl benzene	1.25	19.66
Alkyl benzene	1.45	18.68
Naphthalene	0.80	20.62
Alkyl naphthalene	1.08	19.37
Phenanthrene	0.71	20.55
Alkyl phenanthrene	0.80	20.20
Pyrene	0.63	20.82
Alkyl pyrene	0.84	19.99
Cyclohexane	2	18.57
Alkyl cyclohexane	2	17.16
Decalin	1.8	17.75
Alkyl decalin	1.83	17.22
Naphthenic benzene	1.33	18.74
Tetralin	1.2	19.85
Benzothiophene	0.75	24.33
Alkyl benzothiophene	1.09	21.25
DBT	0.67	23.49
Alkyl DBT	0.86	22.45
Indene	0.89	19.96
Indole	0.88	Error*
Two benzenes with C2 bridge	1.07	19.15
Two benzenes with C3 bridge	1.13	19.01
Two benzenes with C4 bridge	1.18	18.89

* The density correlation gives a large density value, hence very large SP value.

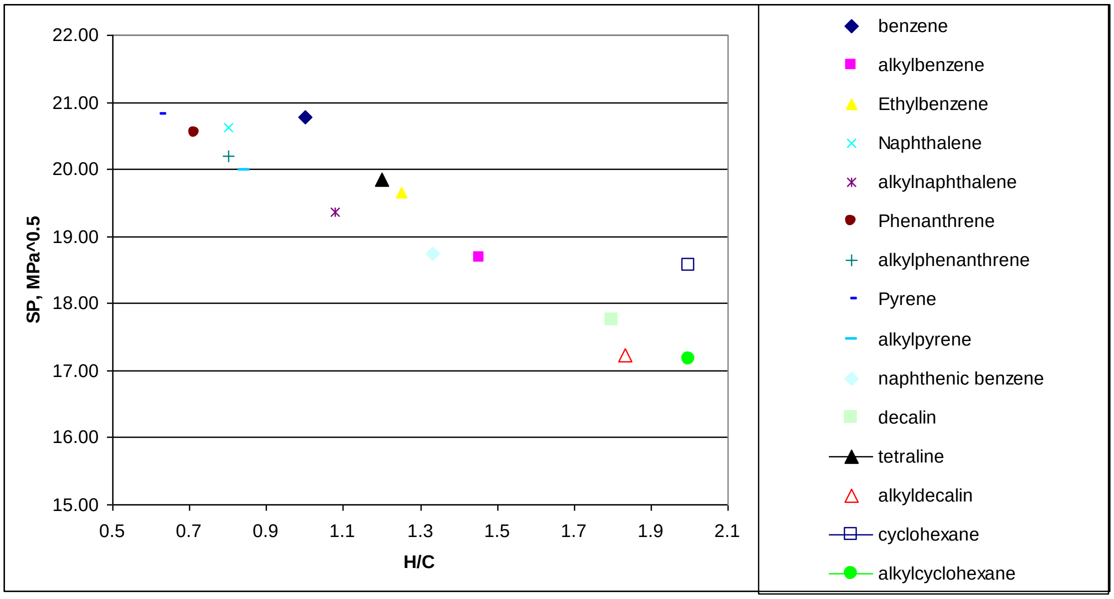

Figure 3-4. **Aromatic rings and aromatic rings with branch attachments**

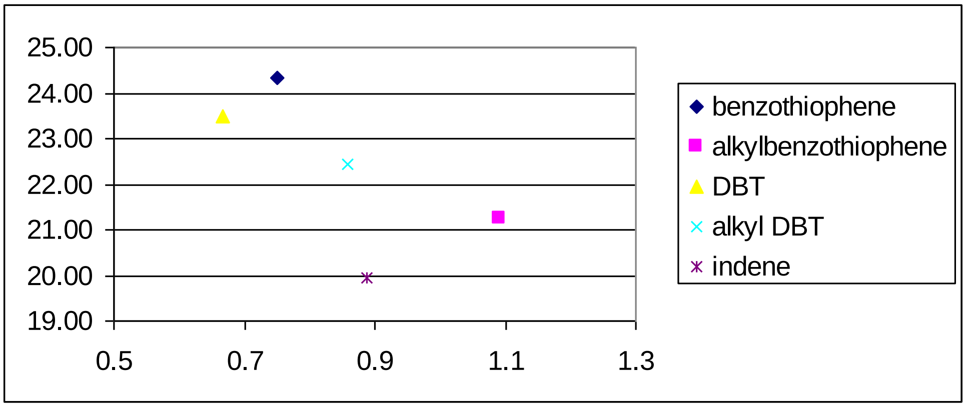

Figure 3-5. **Heteroatom compounds and heteroatom compounds with branch attachments (indene given for comparison)**

During mild thermal cracking the solubility parameter can change as a result of three changes:

1) Cracking of alkyl chains at favored locations
2) Aromatization of naphthenic rings
3) Condensation reactions

Two sample archipelago and pericondensed asphaltene molecule were selected for studying the cracking of alkyl chains. The other two changes mentioned above were not considered. The favored cracking locations were determined based on the information from thermal cracking of the model compounds.

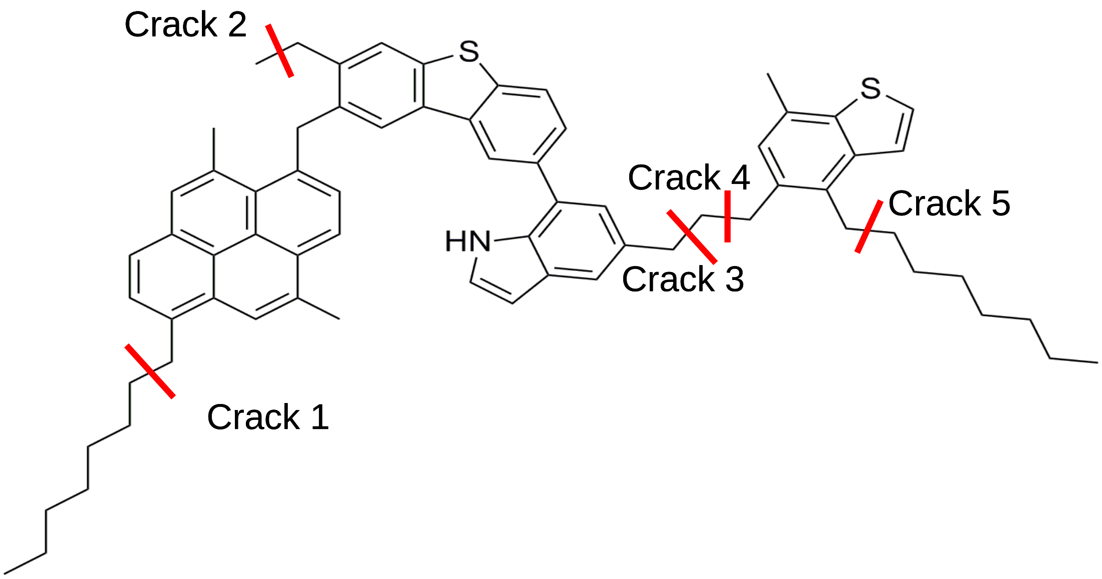

Chemical Formula: $C_{69}H_{75}NS_2$
Molecular Weight: 982.47

Figure 3-6. **Archipelago molecule (taken from Sheremata (2008) Athabasca bitumen molecular representation, molecule Summa # 3)**

Different cracking combinations

With five favored cracking locations for the archipelago molecule and hence the cracking amount from one to five cuts, the possible numbers of combinations for the different amount of cracking of the archipelago molecule presented are:

Table 3-6. Possible number of combinations for the different amount of cracking of the archipelago molecule

1 cut	2 cuts	3 cuts	4 cuts	5 cuts
$\frac{5!}{1!4!}=5$	$\frac{5!}{2!3!}=\frac{5\times 4}{2}=10$	$\frac{5!}{3!2!}=10$	$\frac{5!}{4!1!}=5$	$\frac{5!}{5!0!}=1$

The solubility parameters of the cracked products from this archipelago molecule are shown in the appendix. The table has five rows with two columns (for the SP of the two products from 2 cracks), ten rows with three and four columns respectively and five rows with five columns.

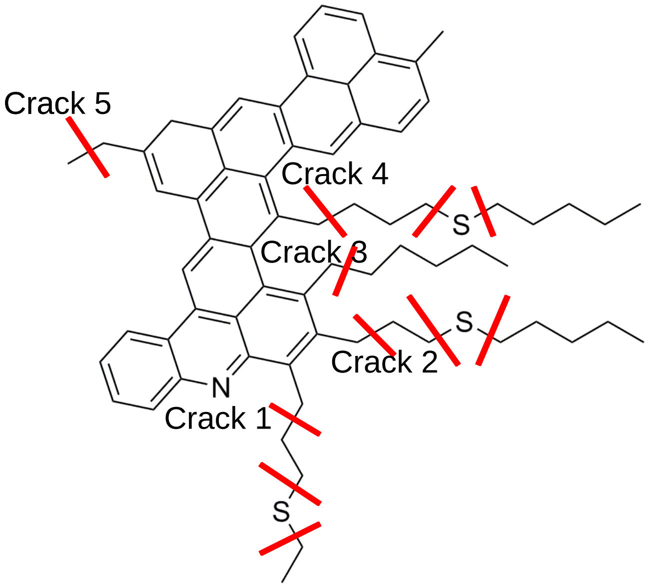

Chemical Formula: $C_{69}H_{85}NS_3$
Molecular Weight: 1024.61

Figure 3-7. **Pericondensed molecule (taken from Boek's quantitative molecular representation of Athabasca asphaltenes, 2009)**

In the pericondensed model, there are five main cracking locations (crack 1-5) for the detachment of the chains from the main core aromatic group. Location five was ignored as CH4 is a small fragment. Hence with four locations, there are 4 possible combinations for one cut, 6 possible combinations for two cuts and 4 possible combinations for three cuts shown in Table 9-23 in the appendix.

The solubility parameter distributions of the cracked products are shown in the results.

4 Results

Physical and thermodynamic properties were calculated for both supercritical n-pentane and for molecular representations of fractions of Athabasca vacuum residue prepared using supercritical n-pentane. The results from each material will be presented separately. The average solubility parameter of the Athabasca bitumen and its vacuum residue and their self compatibilities were investigated. Different solubility parameter distributions of cracked products from an archipelago and a pericondensed molecule are also presented.

4.1 Calculated properties of super critical n-pentane

The densities of the nine solvents used for vacuum residue extraction and fractionation are shown in a scatter form in Figure 4-1. The data in the figure were calculated using PR EOS in the VMGSim software. Density to a first approximation is proportional to the solvent power of the super critical fluid.

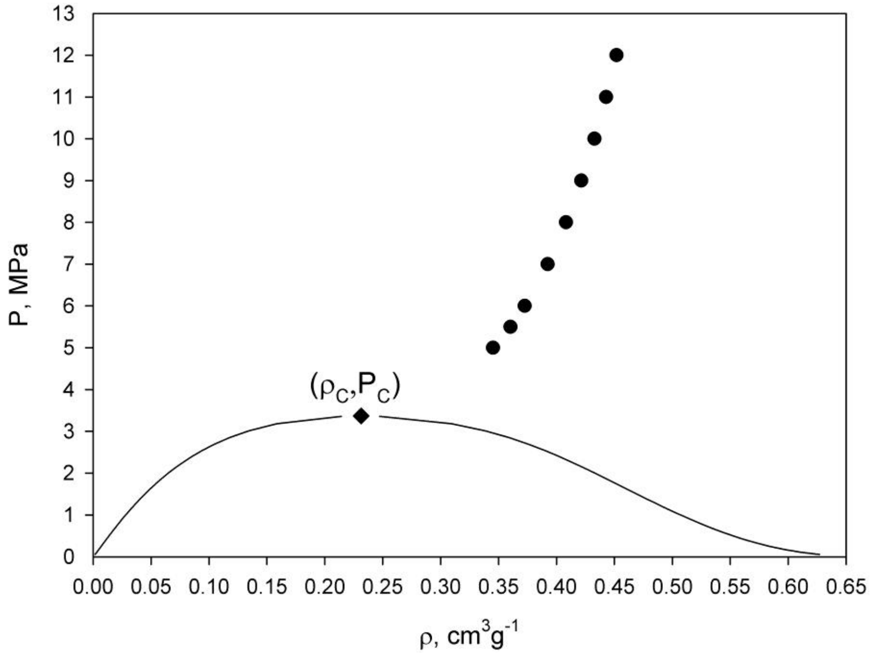

Figure 4-1. n-pentane pressure-density phase diagram (T = 473 K, $T_r \cong 1$)

The solubility parameters of the n-pentane solvent at slightly supercritical temperature of 473 K and supercritical pressures of 5-12 MPa were calculated from three methods: Giddings correlation (equation 20), Allada correlation (equation 22) shown in Figure 4-2 and MD simulation. In the Giddings correlation, $\rho_{r\ SCF}$ $(=V_C/V)$ was obtained from PR EOS, knowing the external pressure and temperature that were used to produce the supercritical fractions for these nine fractions. In the Allada correlation, C_1 is 1 in term of $(\frac{MJ/m^3}{MPa})$ and gives δ in term of $(MJ/m^3)^{1/2}$ or $MPa^{1/2}$ if P_C is in MPa. Any of the equations of state can be used to evaluate $(U^{ig} - U)$ so we used PR EOS in our calculations. H^{ig}-H, Z and ν calculations are shown in Figure 4-2 and Table 9-4. The critical properties of n-pentane are as follows (Smith et al., 2005):

T_C = 469.7 K, P_C = 3.369 MPa, ν_C = 311.815 cm^3mol^{-1}.

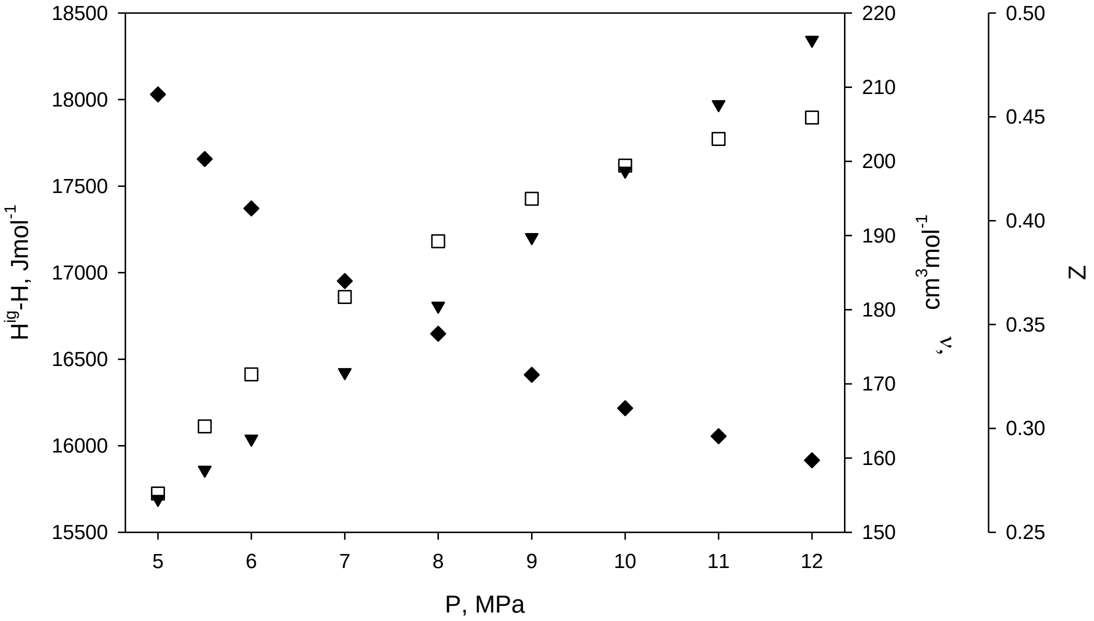

Figure 4-2. **Allada solubility parameter calculations: ♦ molar volume, ▼ Z, □ H^{ig} – H for supercritical n-pentane at 473 K**

Having the densities from PR EOS, the NVT MD simulations were also performed for analyzing the cohesive energy densities and hence solubility parameters.

The results from the different methods are presented in Figure 4-3 below and Table 9-5.

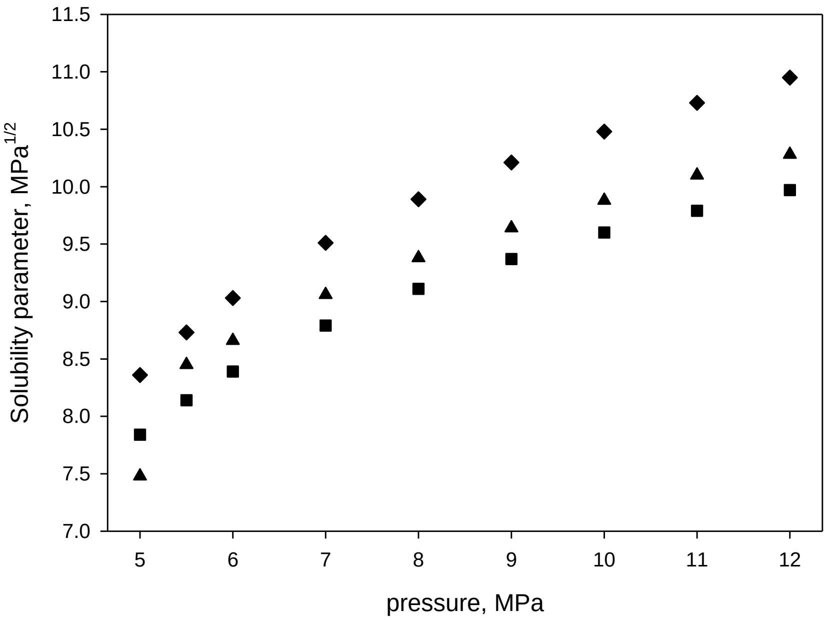

Figure 4-3. Solubility parameters of n-pentane at 473 K: ■ Allada, ♦ Giddings, ▲ MD

The solubility parameter value calculated for liquid n-pentane with NVT MD simulation method at standard condition (0.1 MPa & 298.15 K) was 14.46 MPa$^{1/2}$ in comparison to the value of 14.4 MPa$^{1/2}$. This calculation used a molar volume of 116 cm^{3}mol^{-1} from literature (Reid et al., 1987).

Figure 4-4 shows the parity plots of Giddings and MD versus Allada. In the Giddings expression, the solubility parameter depends on the thermodynamic state of the SCF only through the reduced density (or molar volume), where $\nu = \frac{ZRT}{P}$. Marcus (2006) showed that Allada's correlation is similar to Giddings but with a direct mild dependence on T_r. As Allada correlation is in a more rigorous form, it was selected to calculate the solubility parameters of the supercritical solvents. The solubility parameters calculated are smaller than those from Giddings correlation. Figure 4-4 shows a better agreement between MD and Allada than Giddings and Allada. As MD is a simulation method and more computationally intensive, Allada correlation was selected in this study.

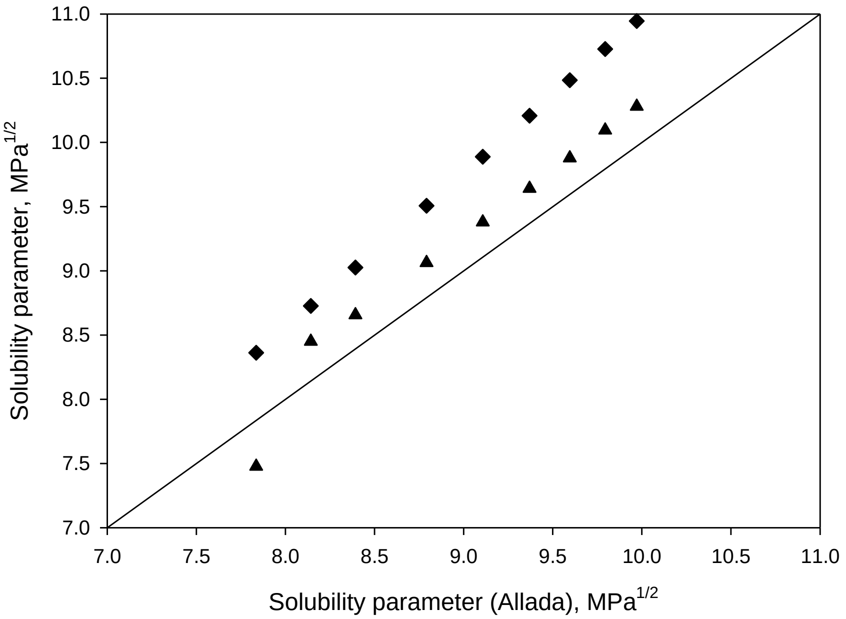

Figure 4-4. **Comparisons between the solubility parameters of the solvents with respect to the Allada estimated values: ♦ Giddings, ▲ MD**

4.2 Solubility parameters of heavy oils and fractions

Figure 4-5 shows the supercritical extraction progress of the vacuum residue with the increasing supercritical n-pentane solubility parameters calculated from the Allada correlation.

The solubility parameters of the extracted fractions of the vacuum residue are shown in this section following the molar volumes and enthalpies/energies of vaporization calculations. The effect of temperature is studied for each of these primary properties and applied to achieve the solubility parameters of the fractions (solutes) at the process condition (473 K).

The individual solubility parameters were also calculated for the Athabasca bitumen from the Marrero-Gani method and its self compatibility was investigated.

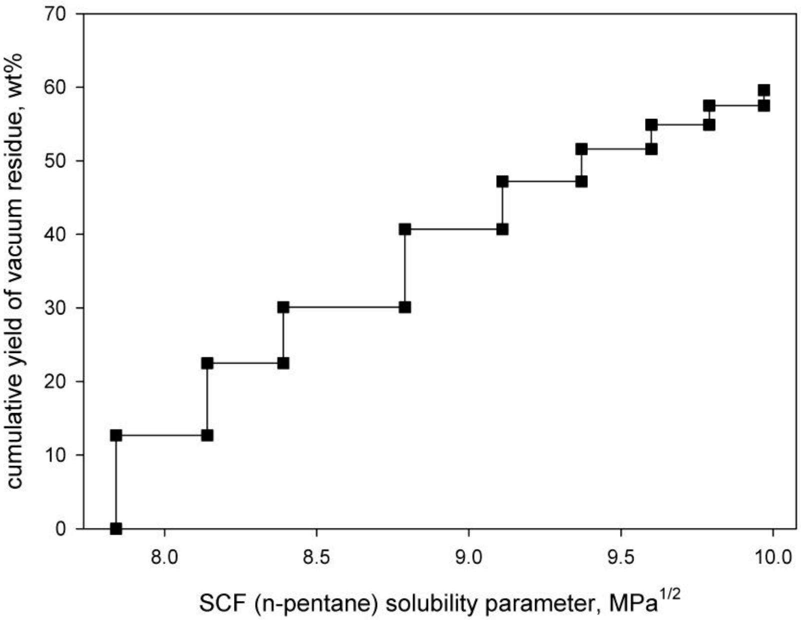

Figure 4-5. **Solubility parameter of the SCF solvent @ 473 K (Allada) versus experimental cumulative wt % recovered**

4.2.1 Molar volume estimates

The molar volumes of the 60 molecules from Fedors' method are compared to the prediction from equation [26] based on elemental analysis. The agreement is quite good, except that equation [26] gives a wider range of density. Given the calibration of equation [26] for heavy asphaltenic materials and bitumens, this equation was used in subsequent calculations.

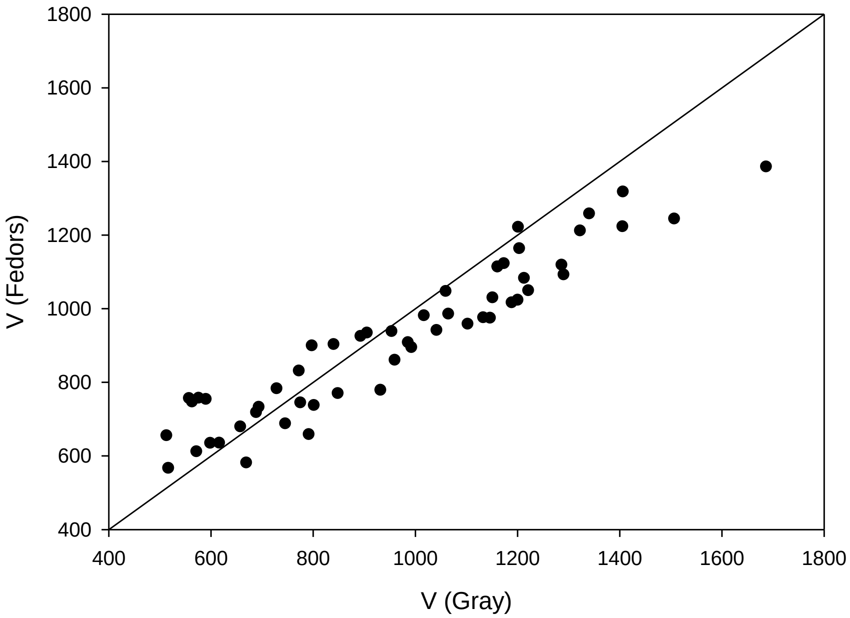

Figure 4-6. **Molar volume from Fedors Group contribution method in comparison with molar volume from the elemental composition correlation (equation [26]) for the 54 molecules of fraction 1 to 9**

Also the average density values from Gray's correlation are compared with the experimental values for the nine fractions in Table 9-7 and Figure 4-7below for justifying the adoption of this correlation.

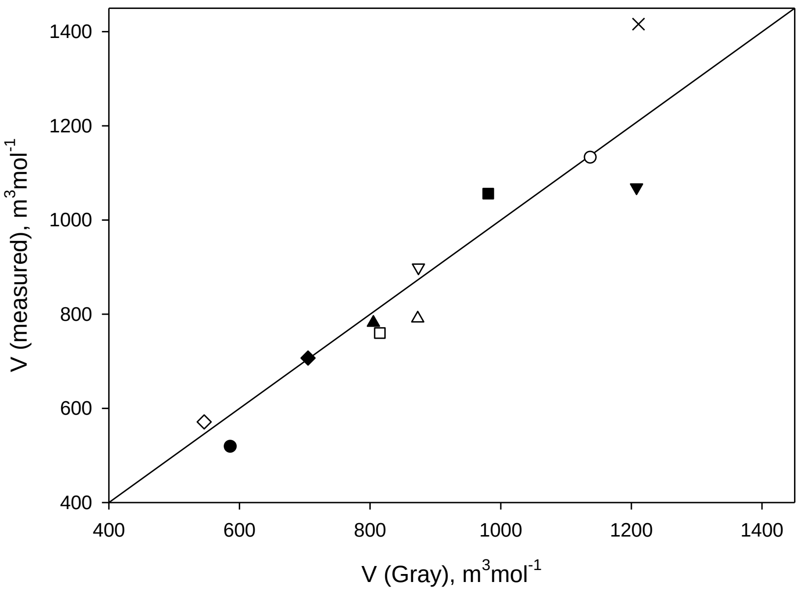

Figure 4-7. **Molar average molar volumes (different symbols) for the nine fractions, ◊ bitumen, ■ AVR from Gray's correlation in comparison with the measured values**

The molar volumes are given for the seventeen representative bitumen molecules (summa) and fifteen Athabasca vacuum residue molecules in Table 4-2 to Table 4-5 and in Table 9-7 to Table 9-15 for the Athabasca vacuum residue fractions.

4.2.2 Molar volume estimates at 473 K and supercritical pressures

The solutes were assumed to be incompressible, i.e. molar volumes did not change with pressure. The effect of temperature on molar volume was estimated as 2% increase in the molar volume of asphaltene for every 30 °C increase in the temperature (communication with Dr. Shaw's group), therefore, a 12% increase in the molar volume was assumed for each fraction (solute) for the change of temperature from 298 K to 473 K (175 K).

4.2.3 Solubility parameters of fractions at 298K (ΔH_i^{298K} and ΔU_i^{298K} from Marrero-Gani and Fedors method respectively)

The individual molecule enthalpy of vaporization calculated from Marrero-Gani method and solubility parameters are given in detail in Table 9-7 to Table 9-15. The individual Fedors' enthalpy of vaporization and molar volume are given in detail in Table 9-16. The MG-enthalpy of vaporization distributions are shown in Figure 4-8. The individual

Marrero-Gani solubility parameters are shown in Figure 4-9 and Figure 4-10 versus H/C ratio.

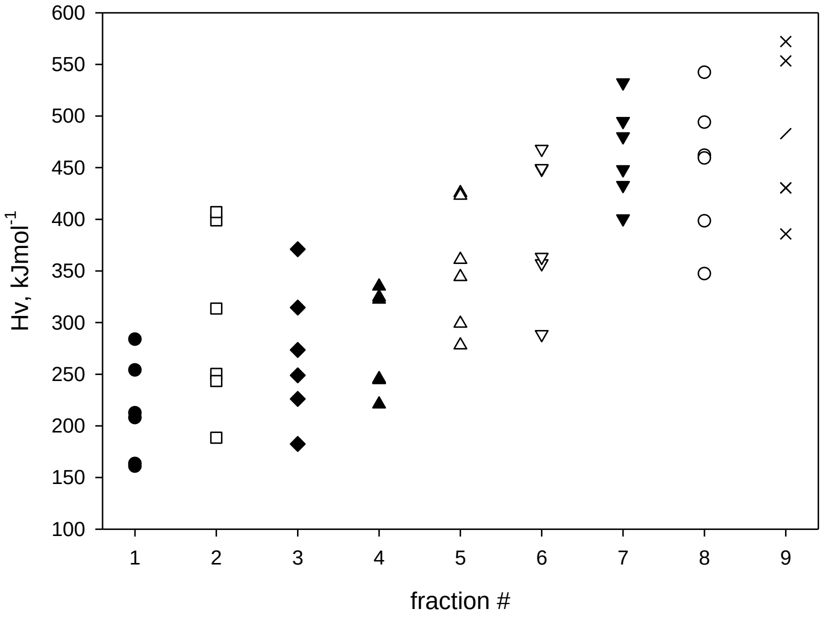

Figure 4-8. **Enthalpy of vaporization distributions calculated from Marrero-Gani group contribution method for the six molecules of each fraction (some points coincide).**

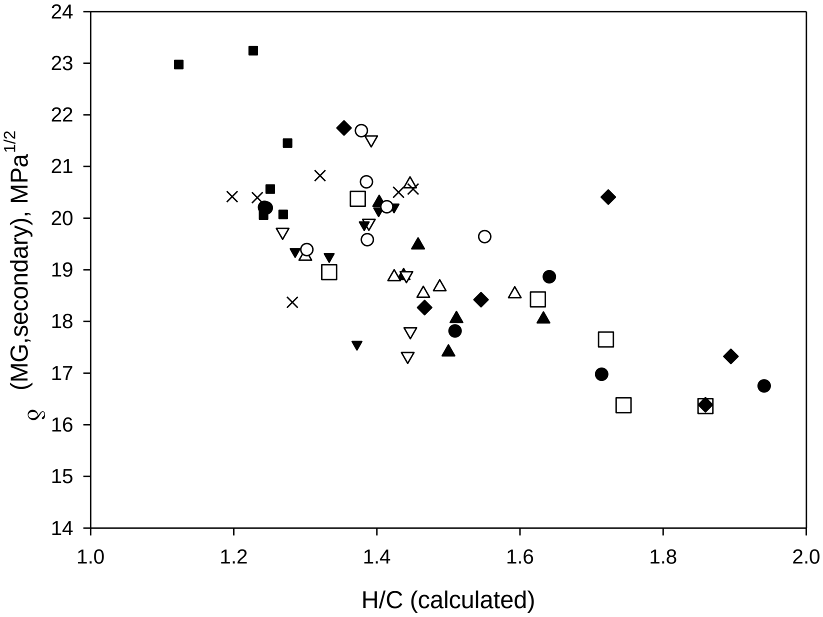

Figure 4-9. **Individual Marrero-Gani solubility parameter versus H/C for sixty molecules**

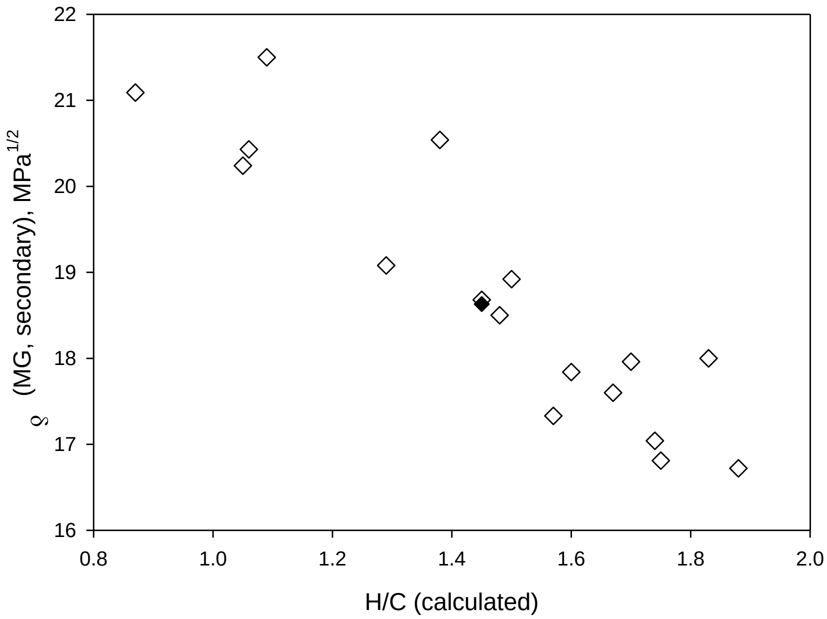

Figure 4-10. ◊ individual Marrero-Gani solubility parameter for 17 bitumen molecules, ♦ average point

The solubility parameters of the majority of the 60 representative molecules were also calculated with Molecular Dynamics and compared with those obtained from the group contribution method.

Figure 4-11 shows the parity plot of the solubility parameters obtained from Marrero-Gani group contribution method and the NVT MD simulation for 40 molecules from the nine fractions. The values are also presented in Table 9-24 in the appendix. The values were not calculated for the last one or two molecules within each fraction (F2M6, F3M6, F5M6, F6M5, F6M6, F7M5, F7M6, F8M5, F8M6, and F9M6) as these molecules are present only in negligible amounts. The molecules of fraction 10, except the first molecule, could not be constructed in Materials Studio as they were large. The first molecule also did not result in an appropriate solubility parameter value. The value could not be obtained for F7M2. The values for F3M2, F6M2, F8M3 and F10M1 were deleted from the regression based on their large studentized residuals.

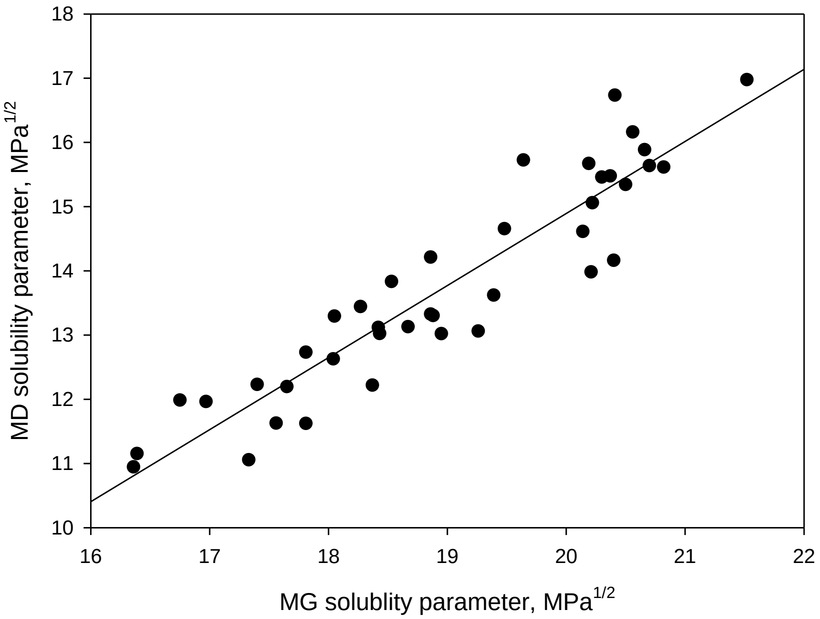

Figure 4-11. **Comparisons of solubility parameters from Marrero-Gani and MD simulation at 298 K**

Marrero-Gani and MD solubility parameter calculations are directionally consistent, though the values from MD simulation are smaller by 4 to 5 units in MPa$^{1/2}$. Considering the extent of the computational work involved in the MD simulation, and the poor results, the results from the group contribution method were used for the rest of this study. The calculated solubility parameters are given in Table 4-1 and Figure 4-12.

Table 4-1. Calculated solubility parameters [$MPa^{1/2}$] of ten fractions at 298 K (MG, Fedors, Rogel)

Fraction	Marrero-Gani, from equations [3] and [26]	Range of values Table 9-7-Table 9-15	Fedors (equation [23])	Rogel (equation [18], H/C from Table 9-1)	MD simulation
F1	18.16	16.75-20.21	18.47	19.00	13.22
F2	18.54	16.36-20.37	18.46	19.21	13.23
F3	18.62	16.39-21.75	18.72	19.53	13.58
F4	19.04	17.40-20.30	19.79	19.94	13.19
F5	19.38	18.53-20.66	19.96	20.47	14.17
F6	19.41	17.33-21.72	20.12	20.89	14.08
F7	19.71	17.56-20.22	20.47	21.31	14.42
F8	19.61	19.39-21.69	20.39	21.31	14.47
F9	19.77	18.37-20.82	20.85	21.52	14.16
F10	20.59	20.06-23.24	21.07	22.98	N/A

In the first three fractions where saturate molecules also exist, the saturate molecules have the minimum solubility parameters in the range of solubility parameters for the molecules in each fraction. Fraction 10 corresponded to the asphaltene fraction in the parent oil and has the molecules with the highest solubility parameters. H/C ratios for Rogel's method were taken from the experimental data (Table 9-1).

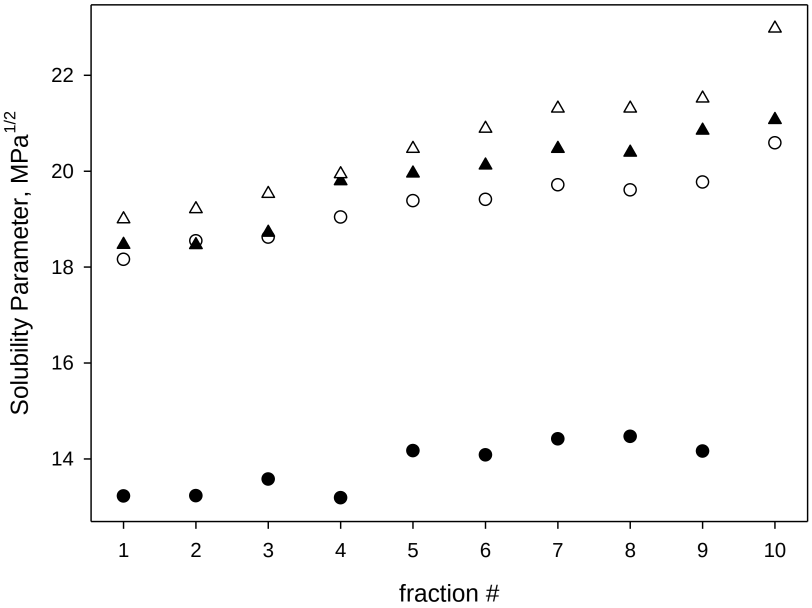

Figure 4-12. **Average solubility parameters @ 298 K calculated for the ten fractions by the different methods: ● MD, ○ Marerro-Gani (secondary), ▲ Fedors, Δ Rogel**

The data of Figure 4-12 show the trends in the predicted solubility parameter for the 10 fractions. Only Rogel's method gives monotonic estimates for the series of fractions. Marrero-Gani is monotonic, except for Fraction 8. The results from Fedors method are erratic. Based on these results, we can also see that the MD simulation method gives lower values and the trend for the average solubility parameter for nine fractions is erratic. Consequently, the Marrero-Gani method gave the most consistent results and is used in the remainder of the thesis.

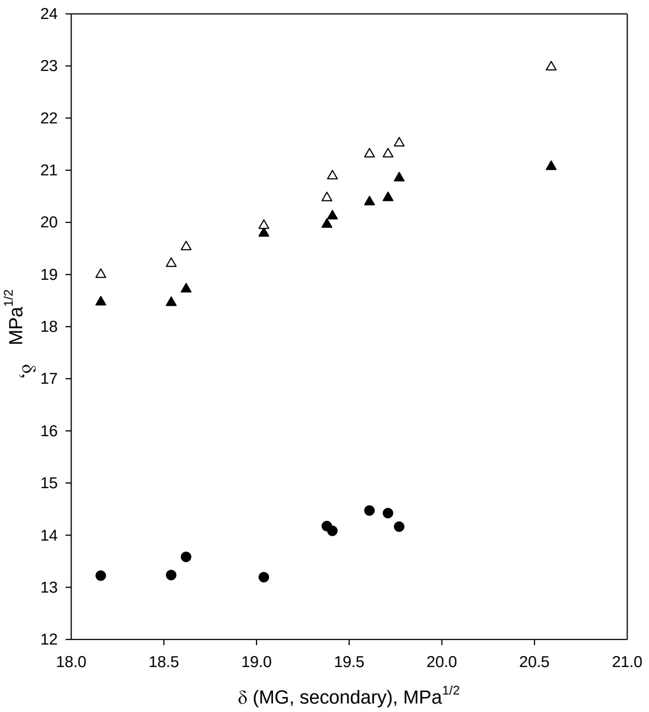

Figure 4-13. **Comparisons between the average solubility parameters of the fractions with respect to the MG estimated values: ▲ Fedors, Δ Rogel, ● MD**

Rogel (1997) suggested that solubility parameters should correlate with H/C ratio (equation [18]), which would also imply a simple correlation with aromaticity. The predicted solubility parameters from Marrero-Gani and Fedors are shown in Figure 4-14 as a function of experimental H/C ratios (Table 9-1). The results from Marrero-Gani give a monotonic series, as expected, while the results of Fedors are highly variable. For such a series of fractions that are linked by a common extraction history, the results from Fedors are unsatisfactory.

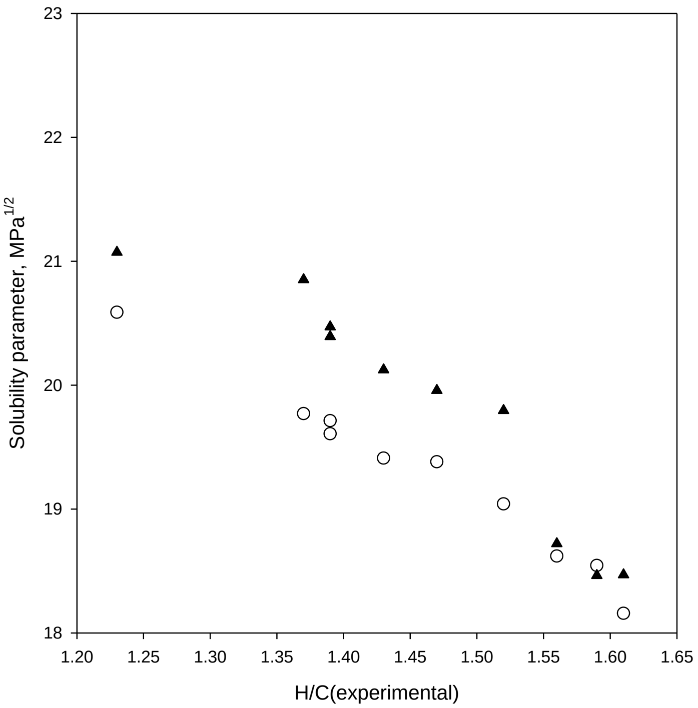

Figure 4-14. **predicted solubility parameters for the ten fractions: ○ Marerro-Gani (secondary), ▲ Fedors, — Rogel**

Figure 4-15 shows a parity plot of the results from Marrero-Gani versus Rogel, to emphasize the systematic differences between the two methods. As illustrated, the solubility parameters predicted by Rogel are systematically higher than the values from Marrero-Gani. Given our interest in molecular representations, and their use for both property prediction and reactions of heavy fractions, we will use the Marrero-Gani method for the rest of this study.

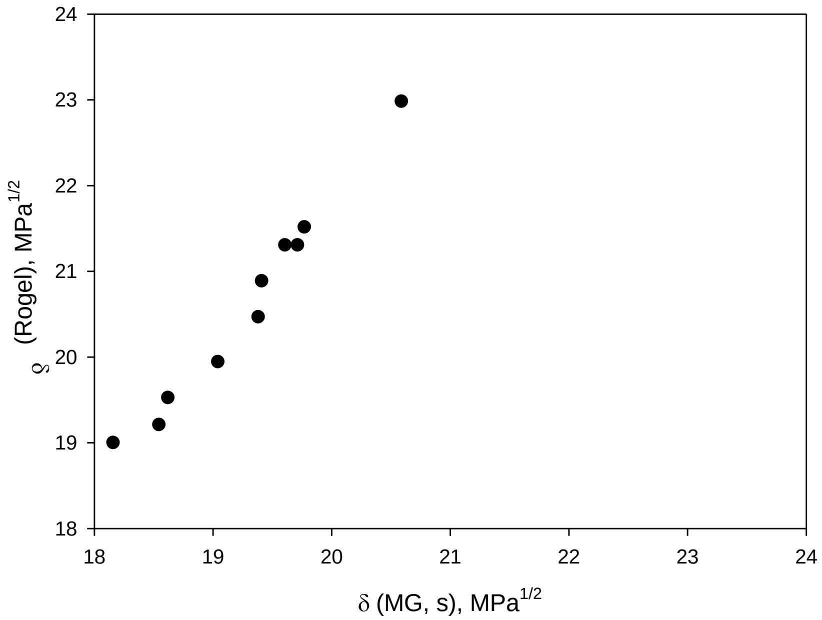

Figure 4-15. **Comparisons between solubility parameters of the ten fractions calculated from Rogel correlation and Marrero-Gani group contribution method**

4.2.4 Sensitivity analysis

The absolute relative errors between the calculated and measured densities are from 0% for fraction 5 to 1.9% for fraction 1 (Table 9-3). Fraction 1, 2 and 3 have the highest errors as saturate molecules exist in the representation of these fractions and as mentioned before, the density correlation with elemental composition is not accurate for saturates. The error for the other fractions is less than 1%. We considered 10% error in the molar volume calculations and 10% error in the enthalpy of vaporization and we calculated the solubility parameter from the MG method with 1.1 ΔH, 0.9 ΔH, 1.1 V and 0.9 V. The results are shown in Figure 4-16. The error bar end values are associated with calculations with 0.9V, 1.1 ΔH, 1.1 V and 0.9 ΔH respectively from top to bottom.

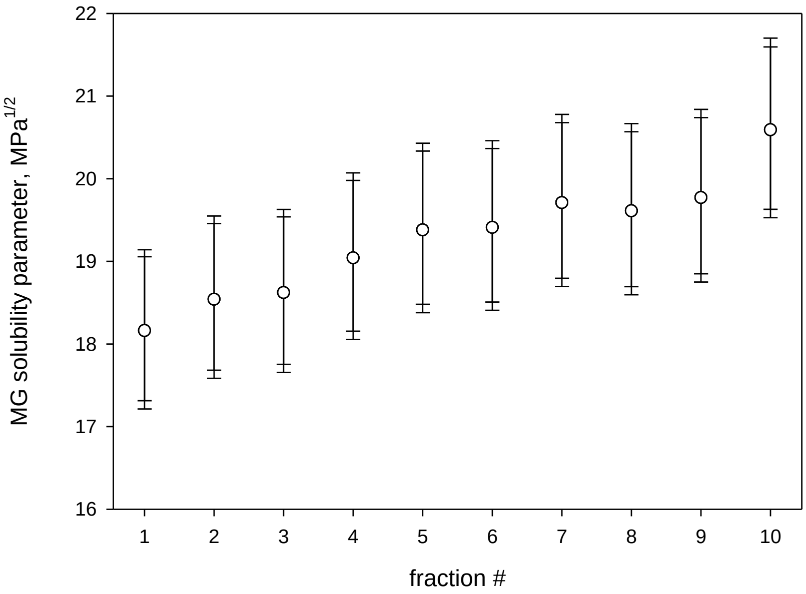

Figure 4-16. Solubility parameter sensitivity analysis (enthalpy of vaporization from MG method and density from Gray's correlation with an uncertainty of ±10%). ○ main series

4.3 Athabasca bitumen and VR solubility parameters

The individual solubility parameters were also calculated for the Athabasca bitumen and its whole vacuum residue from the Marrero-Gani method and their self compatibility were investigated.

Table 4-2. Calculated properties of the seventeen ensemble Athabasca bitumen representative molecules

#	Molecules reference #	Formula	MW, gmol^{-1}	ρ, g/ml	ν, cm^3/mol	H/C	mol%	vol%	δ, MPa$^{0.5}$
1	S5	C16H30	222	0.8469	263	1.88	0.09	0.04	16.72
2	S14	C32H56	441	0.8577	514	1.75	0.12	0.11	16.81
3	S15	C61H106S	872	0.9161	951	1.74	0.06	0.10	17.04
4	S17	C23H36	313	0.8740	358	1.57	0.03	0.02	17.33
5	S2	C48H80S	689	0.9373	735	1.67	0.08	0.10	17.60
6	S12	C65H104S	918	0.9250	992	1.60	0.06	0.11	17.84
7	S7	C92H156S3	1358	0.9726	1397	1.70	0.00	0.00	17.96
8	S6	C24H44S	365	0.9883	369	1.83	0.09	0.06	18.00
9	S13	C31H46S	451	0.9907	455	1.48	0.12	0.09	18.50
10	S11	C11H16	148	0.8841	168	1.45	0.06	0.02	18.68
11	S9	C28H42S	411	1.0000	411	1.50	0.01	0.01	18.92
12	S8	C215H277NS4	3004	1.0188	2948	1.29	0.01	0.03	19.08
13	S10	C129H135NS2	1764	1.0696	1649	1.05	0.01	0.04	20.24
14	S4	C114H121NS3	1601	1.1131	1439	1.06	0.03	0.08	20.43
15	S1	C16H22S	246	1.0900	226	1.38	0.14	0.06	20.54
16	S16	C84H73NS	1129	1.1267	1002	0.87	0.03	0.06	21.09
17	S3	C69H75NS2	982	1.1830	830	1.09	0.06	0.08	21.50
sum/avg			565	0.9842	571	1.45	1	1	18.63

Table 4-3. Athabasca bitumen experimental data (taken from Sheremata, 2008)

	ρ, g/ml	MW, gmol^{-1}	ν, cm^{3}mol^{-1}	H, wt%	C, wt%	H/C	δ_{exp}, MPa$^{0.5}$
	1.0071	550	546	10.3	84.5	1.45	
ARE%	2.3	2.7	4.4	0	0	0.3	N/A

4.3.1 Self compatibility from molecular representation

From Table 4-2, S10, S4, S1, S16 and S3 may be considered as asphaltenes (with overall vol% of 0.31) and the rest twelve molecules as solvent. Then ν_S, δ_S, ν_A, δ_A and ϕ_A^{max} can be calculated as follows:

ν_S, cm^{3}mol^{-1}	600	δ_S, MPa$^{0.5}$	18.82	ν_A, cm^{3}mol^{-1}	653	δ_A, MPa$^{1/2}$	23.81	φ_A^{max}	0.001

From the above analysis the Athabasca bitumen is not self-compatible at room temperature.

Table 4-4. Calculated properties of the fifteen ensembles Athabasca vacuum residue representative molecules

Molecules	Formula	MW, gmol^{-1}	ρ, g/ml	ν, cm^3/mol	H/C	mol%	vol%	δ, MPa$^{0.5}$
R1	C194H272N2S8	2889	1.1383	2538	1.40	0.02	0.06	N/A
R2	C45H64S	637	0.9641	661	1.42	0.13	0.09	17.95
R3	C81H134S2	1172	0.9510	1232	1.65	0.05	0.06	20.58
R4	C37H48S	525	0.9914	529	1.30	0.16	0.08	19.62
R5	C93H109NS3	1337	1.1414	1171	1.17	0.02	0.02	22.53
R6	C83H97NS3	1205	1.1670	1032	1.17	0.11	0.11	22.23
R7	C35H66S	519	0.9431	550	1.89	0.03	0.02	16.67
R8	N/A	1574	1.1665	1350	1.19	0.06	0.09	N/A
R9	C66H116	910	0.8570	1061	1.76	0.12	0.13	18.36
R10	C64H82S	883	0.9552	925	1.28	0.08	0.07	19.6
R11	C171H211NS5	2441	1.0711	2279	1.23	0.04	0.08	N/A
R12	C59H49NS2	836	1.2522	668	0.83	0.05	0.03	21.42
R13	C57H66S	783	0.9734	805	1.16	0.07	0.06	20.84
R14	C118H115NS5	1708	1.1650	1466	0.97	0.03	0.05	N/A
R15	C78H100S3	1134	1.0288	1102	1.28	0.04	0.05	21.00
sum/avg	▨	1016	1.0373	981	1.31	1.00	1.00	19.97

Table 4-5. Athabasca vacuum residue experimental data (taken from Sheremata, 2008)

Property	ρ, g/ml	MW, gmol^{-1}	ν, cm^{3}mol^{-1}	H, wt%	C, wt%	H/C	δ$_{exp}$, MPa$^{0.5}$
Exp. data	1.0528	1112	1056	8.3	84.8	1.17	N/A
ARE%	1.5	8.6	7.1	12.0	1.0	12.0	N/A

4.4 Enthalpies and solubility parameter of the vacuum residue fractions at 473K

4.4.1 SP-derived enthalpy of vaporizations for mixtures and API correlations

The fractions of Athabasca vacuum residue were separated by isothermal supercritical extraction with n-pentane at 473 K; therefore, in order to compare the solubility parameters of the factions with the extracting solvent phase, we need to estimate them at the same temperature of 473 K.

Rather than estimating the solubility parameter for every molecular representation at 473 K, the weighted average values from Marrero-Gani were corrected for temperature. This approach enabled the use of standard correlations for petroleum fractions. The enthalpy of vaporization was calculated at 473 K using the internal energy at 298 K (from equation 27) and correlations for isobaric heat capacity of petroleum fraction liquids and vapors with temperature using Watson characterization factor and specific gravity, following equation [28] (API Technical Data Book, 1997). The integrations were performed using MATLAB. The enthalpies of vaporization of different fractions decreased due to the increase in the temperature. 12% increase in the molar volume was assumed as discussed in section 4.2.1.1 for the temperature change from 298 K to 473 K for different fractions. Table 4-6 shows the resulting solubility parameters at 473K.

Table 4-6. Estimated solubility parameters [MPa$^{1/2}$] for vacuum reside fractions at 473 K (extraction temperature) from the Marrero-Gani solubility parameters at 298 K

Fractions	$\bar{\delta}^{298K}$ MPa$^{1/2}$	$v_{\text{exp.}}^{298K}$ cm^3/mol	$\Delta\bar{H}_V^{298K}$ KJ/mol	$\int C_p dT$ KJ/mol	$\int C_V dT$ KJ/mol	$\Delta\bar{H}_V^{473K}$ KJ/mol	% ΔH_V decrease	δ^{473K} MPa$^{1/2}$	$\Delta\delta^{298\rightarrow473}$
F1	18.16	519.24	174	-65	51	160	8	16.40	-1.75
F2	18.54	760.32	264	-96	79	246	7	16.87	-1.67
F3	18.62	706.69	247	-87	69	230	7	16.90	-1.72
F4	19.04	782.17	286	-97	79	268	6	17.37	-1.67
F5	19.38	791.22	300	-98	81	283	6	17.73	-1.66
F6	19.41	899.17	341	-111	91	322	6	17.77	-1.64
F7	19.71	1068.95	418	-134	112	396	5	18.10	-1.61
F8	19.61	1133.17	438	-140	116	415	5	17.99	-1.62
F9	19.77	1415.67	556	-178	150	528	5	18.18	-1.59
F10	20.59	N/A	1542	N/A	N/A	N/A	N/A	N/A	N/A

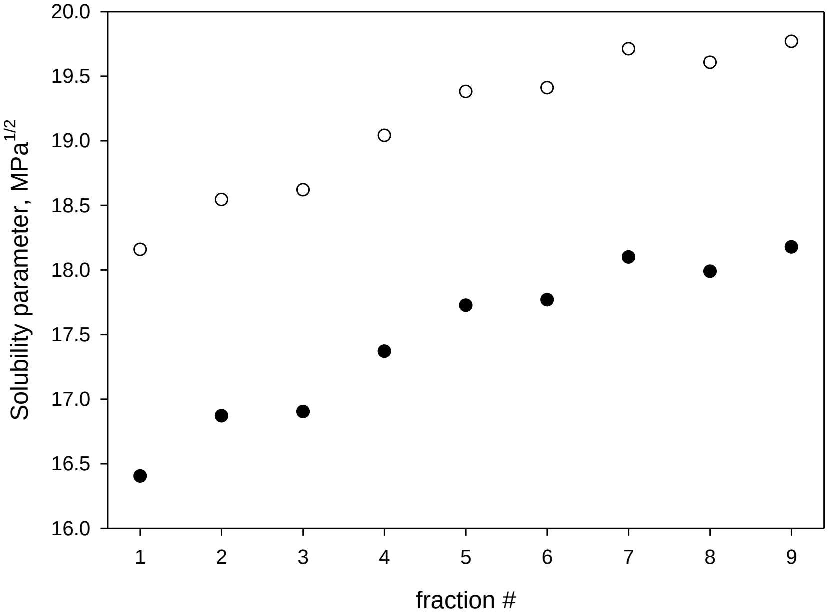

Figure 4-17. **Effect of temperature on solubility parameters of the fractions: ○ @ 298 K (from MG's group contribution method), ● @ 473 K (estimations using API correlations and 298 K values)**

4.4.2 Results from MD simulation at 473 K

The solubility parameters at 473 K were calculated for ten selected molecules (those with larger mole fractions) using the cohesive energy estimated at 473 K. A value of density $\rho^{473K} = 0.89 \times \rho^{298K}$ (equivalent to 12% increase in the molar volume) was used for cell construction and NVT simulation.

Table 4-7. Selected molecules for solubility calculations with MD simulation at 473 K

Name	P, MPa	ρ^{298K}, g/cm^3	ρ^{473K}, g/cm^3	SP^{298K} (NVT), MPa$^{1/2}$	SP^{473K} (NVT), MPa$^{1/2}$	$\Delta\delta^{298\rightarrow473}$
F1M1	5	0.8412	0.7487	11.99	10.0589	-1.93
F2M1	5.5	0.9410	0.8375	13.02	10.8678	-2.1537
F3M1	6	0.9544	0.8494	13.12	10.9951	-2.1222
F4M1	7	1.1314	1.0069	15.46	13.1376	-2.3212
F5M1	8	1.1513	1.0247	15.88	13.5235	-2.361
F6M1	9	1.2336	1.0979	16.98	14.5149	-2.4602
F6M3	9	0.8851	0.7878	11.06	9.2498	-1.8064
F7M1	10	1.1180	0.9950	15.06	13.4427	-1.6218
F8M1	11	1.0158	0.9041	13.62	11.0493	-2.5714
F9M1	12	0.9601	0.8545	12.22	9.5634	-2.6554
F9M3	12	1.1661	1.0378	15.61	13.896	-1.7177

4.5 Comparison of solute and solvent solubility parameters at 473 K (investigation of the compatibility modelling in the supercritical media)

After estimating of the solubility parameters at a higher temperature, the final stage of this study is to compare the solubility parameter of the solutes to the extracting solvents at 473 K. The solubility parameters will also be used in calculation of mol fractions in solution, to check that the solubility models will give reasonable results with the solubility parameters from the Marrero-Gani method.

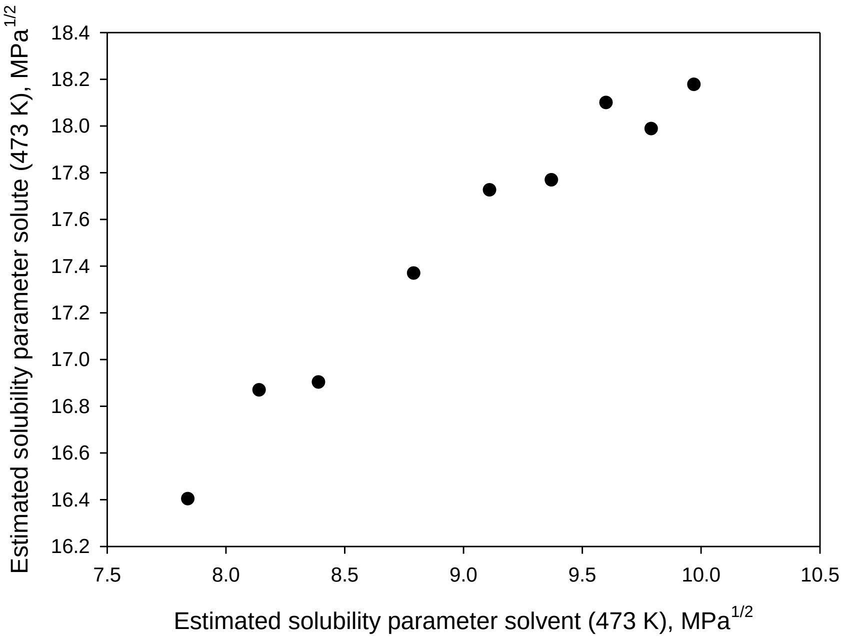

Figure 4-18. Estimated solubility parameters of the solutes (fraction 1 to 9) versus the solvents (Allada), all at process temperature (473 K)

Solubility parameters of the solutes at 473 K in Figure 4-8 were taken from Table 4-6. Figure 4-19 shows the solubility parameters of solvents and solutes at 298 and 473 K. The experiment was one of extraction so each fraction should be reasonably soluble in the solvent that extracted it (solvent pressure where it was removed) and insoluble in the previous solvent in the series. The end-cut is fully insoluble at the remaining solvent condition. This point was considered into the analysis and comparisons to link the correct solvent to the correct solute. Table 4-8 shows the differences in the solubility parameters of the extracting solvent and soluble extracted fraction and their solubilities in terms of mol fraction and g/l calculated from the Flory-Huggins correlation. Table 4-9 shows the differences in the solubility parameters of the previous solvent and insoluble fraction (which remains unextracted and returns to the extraction vessel) and their solubilites.

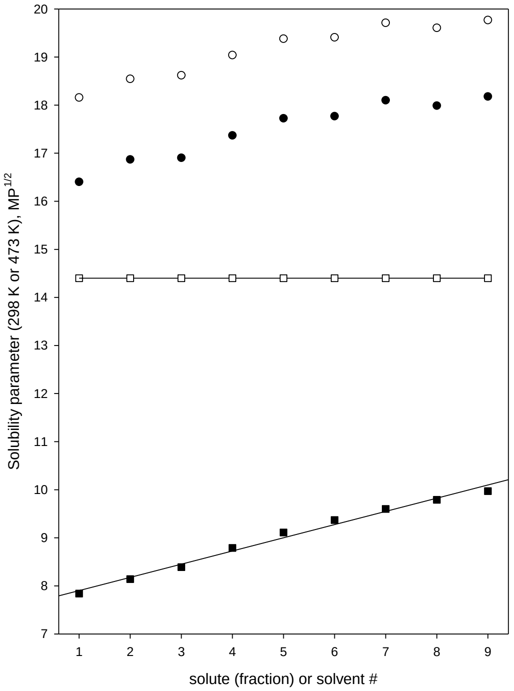

Figure 4-19. **Solubility parameter: ○ solute (298 K), ● solute (473 K), □ liquid solvent (298 K), ■ supercritical solvent (473K)**

Table 4-8. Solubilities of fractions in the supercritical extracting solvents calculated from the F-H theory (eqn. 9) having estimated solubility parameters of fractions and solvents (Table 4-6, Table 9-4)

P, MPa	v_a/v_s	$\ln(v_a/v_s)$	Δδ, MPa$^{1/2}$	$v_a\Delta\delta^2/RT$	sum	solubility (x^*), mol fraction	solubility, g/l
5	2.48	0.91	8.56	9.68	9.11	1.11E-04	0.2676
5.5	3.80	1.33	8.73	14.73	13.27	1.72E-06	0.0065
6	3.65	1.29	8.51	13.02	11.67	8.56E-06	0.0314
7	4.25	1.45	8.58	14.62	12.82	2.70E-06	0.0118
8	4.48	1.50	8.62	14.95	12.97	2.32E-06	0.0109
9	5.25	1.66	8.40	16.13	13.54	1.32E-06	0.0073
10	6.41	1.86	8.50	19.64	16.08	1.03E-07	0.0007
11	6.95	1.94	8.20	19.37	15.35	2.15E-07	0.0016
12	8.87	2.18	8.21	24.25	18.57	8.62E-09	0.0001

From Table 4-8, $\Delta\delta$ is about the same for different pressures with almost a decreasing trend. From Table 4-6, the solubility parameters of the fractions increase from16.4 to 18.18 MPa$^{1/2}$. The solubility parameters of the solvents also increase linearly from 7.84 to 9.97 MPa$^{1/2}$ with a slightly higher slope as shown in Figure 4-19 for supercritical solvent (473 K) and solute (473 K) series. Hence although fraction 9, associated with solvent 9 (P = 12 MPa and δ = 9.97 MPa$^{1/2}$), has the highest solubility parameter its $\Delta\delta$ is slightly smaller.

Although Δδs are similar in magnitude, solubilities (mol fraction) calculated from F-H theory are decreasing from the order of 10^{-4} magnitude to 10^{-8}. The solubility value is very large for fraction 1 in comparison to the other fractions. The results from the F-H theory failed both on an absolute basis (total solubility is too low) and on a relative basis (the problem gets worse with higher solvent density).

Table 4-9. Solubilities of the fractions in the previous supercritical extracting solvents (F2 in S1 to F9 in S8) from the F-H theory

P, MPa	v_a/v_s	$\ln(v_a/v_s)$	Δδ, $MPa^{1/2}$	$v_a\Delta\delta^2/RT$	$\ln(1/x^*)$	solubility (x^*), mol fraction	solubility, g/l
5	3.64	1.29	9.03	15.76	14.42	5.47E-07	0.00209
5.5	3.53	1.26	8.76	13.80	12.53	3.61E-06	0.01256
6	4.03	1.39	8.98	16.02	14.38	5.69E-07	0.00241
7	4.31	1.46	8.94	16.08	14.24	6.56E-07	0.00325
8	5.09	1.63	8.66	17.14	14.68	4.20E-07	0.00217
9	6.24	1.83	8.73	20.72	17.30	3.06E-08	0.00023
10	6.80	1.92	8.39	20.28	16.40	7.58E-08	0.00055
11	8.69	2.16	8.39	25.33	19.80	2.52E-09	0.00002

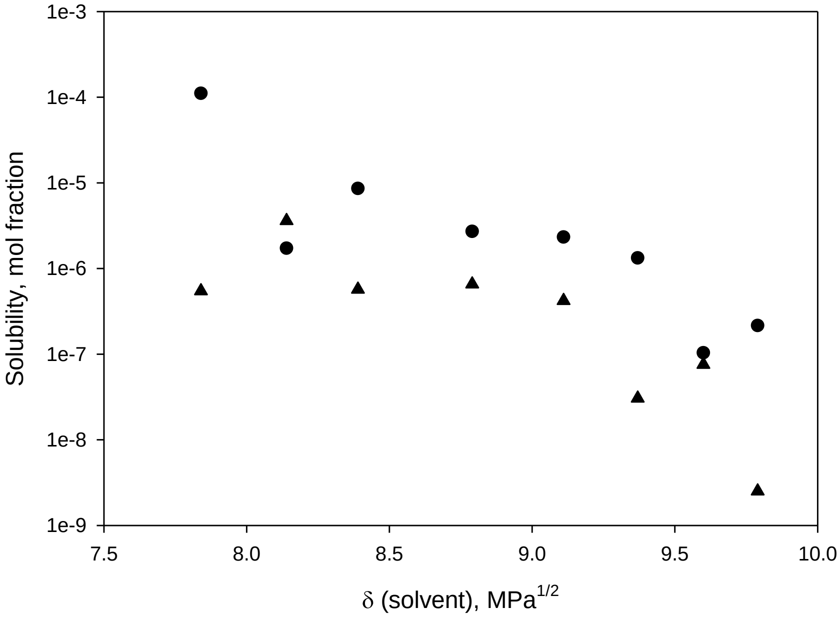

Figure 4-20. **● Solubility of F_i in S_i, ▲ Solubility F_{i+1} in S_i (i = 1 to 8)**

(From Table 4-8 and Table 4-9)

In the calculations given in Table 4-9 and shown in Figure 4-20, the solubility parameters of $F_{(i+1)}$ (i = 1 to 8) were assumed to be the same at $P_{(i+1)}$ and P_i as the fractions were assumed to be incompressible. The solubilities of $F_{(i+1)}$ in S_i (i = 1 to 8), were generally order of magnitude smaller than those of F_i in S_i (i = 1 to 8) as expected for selective dissolving and feasible supercritical-fluid-based extraction process.

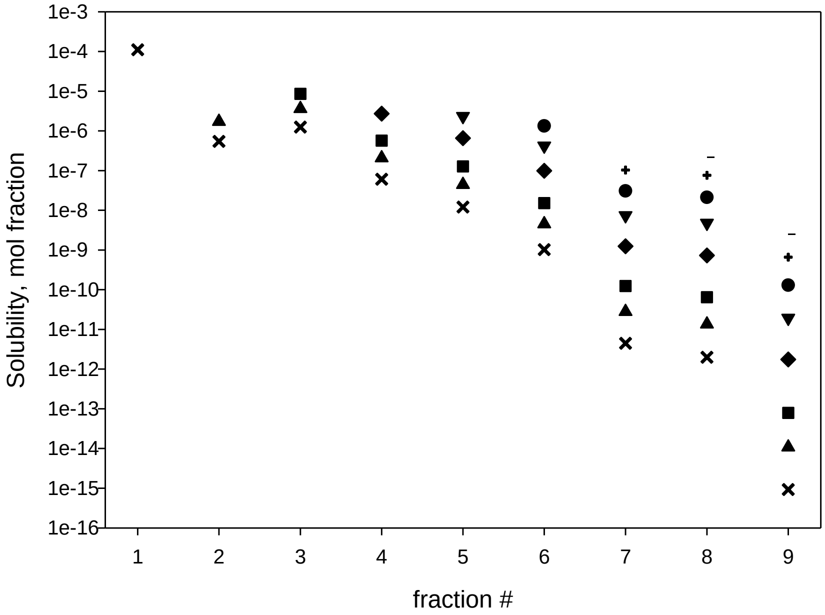

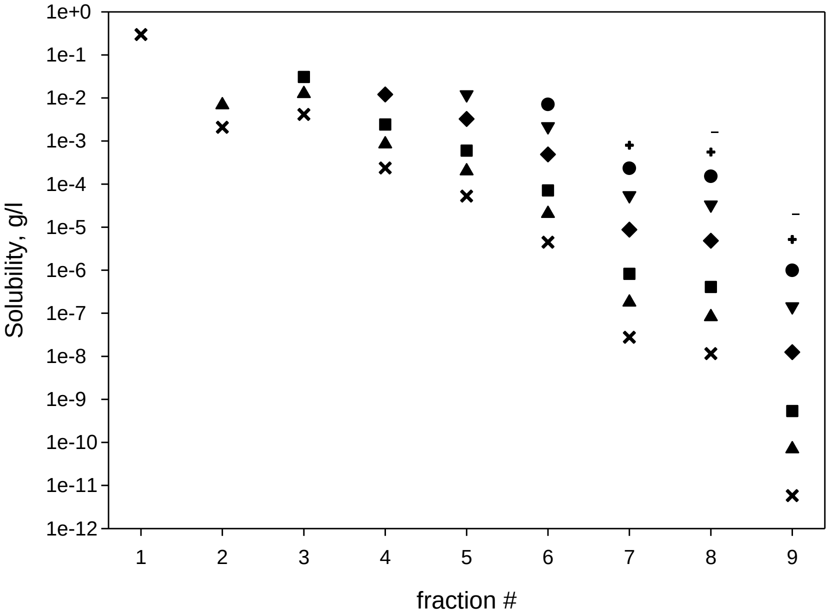

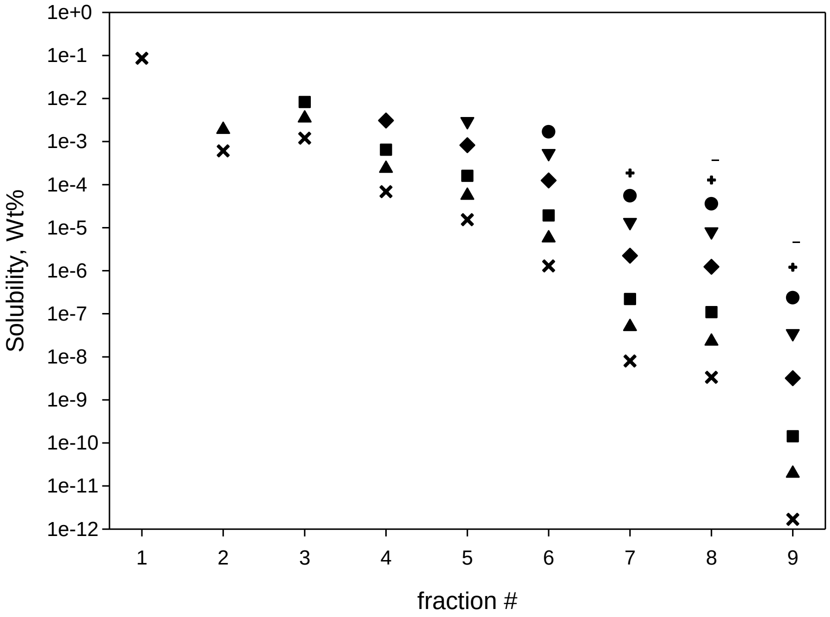

Figure 4-21. **Solubility of different fractions in: × S1, ▲ S2, ■ S3, ♦ S4, ▼ S5, ● S6, + S7, - S8**

As the calculated solubilities from the Flory-Huggins theory were very small, the values were also estimated from the extraction data (%yield, initial amount of vacuum residue and circulating rate of the solvent). The predictions were always much lower than the lowest possible estimate. The estimated solubilities are shown in Table 4-10 and comparison is given in Table 4-11.

Table 4-10. Solubilities of the fractions in the supercritical extracting solvents calculated from the circulating rate of the solvent (100 ml/min) and the extracting process time (8/9 hr); Δδs are then calculated from F-H theory having solubilities

P, MPa	yield	solubility, g/ml	solubility (x), mol fraction	Δδ, $MPa^{1/2}$
5	12.7	0.0357	1.48E-02	5.44
5.5	9.8	0.0276	7.31E-03	5.11
6	7.6	0.0214	5.82E-03	5.38
7	10.6	0.0298	6.86E-03	5.17
8	6.5	0.0183	3.91E-03	5.45
9	4.4	0.0124	2.24E-03	5.53
10	3.3	0.0093	1.36E-03	5.50
11	2.6	0.0073	9.85E-04	5.57
12	2.1	0.0059	6.21E-04	5.48

In Table 4-10, solubility $(g/ml) = \dfrac{\%yield \times 1500g}{100\dfrac{ml}{\min} \times \left(\dfrac{8}{9} \times 60\min\right)}$

Table 4-11. Comparison of the solubilities calculated from F-H theory (x^*) and from the yield and solvent volume (x)

solubility (x^*), mol fraction	ln(1/x^*)	Solubility (x), mol fraction	ln(1/x)	R = ln(1/x) - ln(1/x^*)
1.11E-04	9.11	1.48E-02	4.22	-4.89
1.72E-06	13.27	7.31E-03	4.92	-8.35
8.56E-06	11.67	5.82E-03	5.15	-6.52
2.70E-06	12.82	6.86E-03	4.98	-7.84
2.32E-06	12.97	3.91E-03	5.54	-7.43
1.32E-06	13.54	2.24E-03	6.10	-7.43
1.03E-07	16.08	1.36E-03	6.60	-9.48
2.15E-07	15.35	9.85E-04	6.92	-8.43
8.62E-09	18.57	6.21E-04	7.38	-11.18

R is the difference between the two calculations. In both calculations the solubilities are small in general. Hence good solubility is relative and does not mean x should be near 1.

4.6 Reactions

The solubility parameters of the cracked products from an archipelago (Figure 3-6) and a pericondensed molecule (Figure 3-7) are given at different cracking severities (number of cracks). Figure 4-22 to Figure 4-24 show the distribution of the products with increasing number of cracks from one to three. The solubility parameters are also given in Table 9-20 to Table 9-22. Figure 4-25 shows the overall distribution after different combinations of cracks. Figure 4-26 shows the overall distribution of the cracked products from a pericondensed molecule. The solubility parameters are also given in Table 9-23.

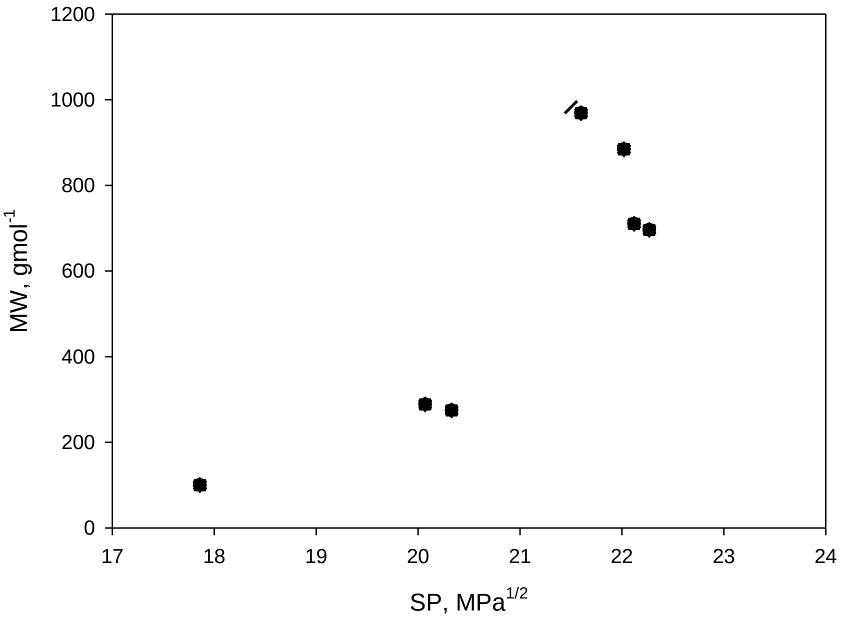

Figure 4-22. **Solubility parameter distribution of the cracked products from an archipelago molecule (×, Figure 3-6) after different single crack. First point (17.86, 100.20) is for n-heptane with experimental SP of 15.3 MPa$^{1/2}$. Data are given in Table 9-20 for the nine products from the five combinations given in Table 3-6.**

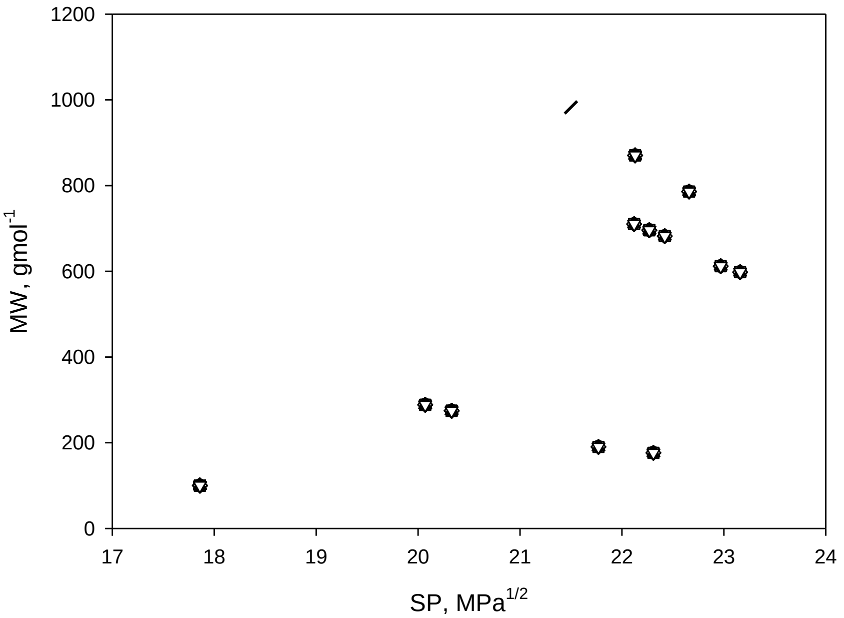

Figure 4-23. **SP distribution of the cracked products from an archipelago molecule (×, Figure 3-6) after different two cracks. Data are given in Table 9-21 and Table 9-22.**

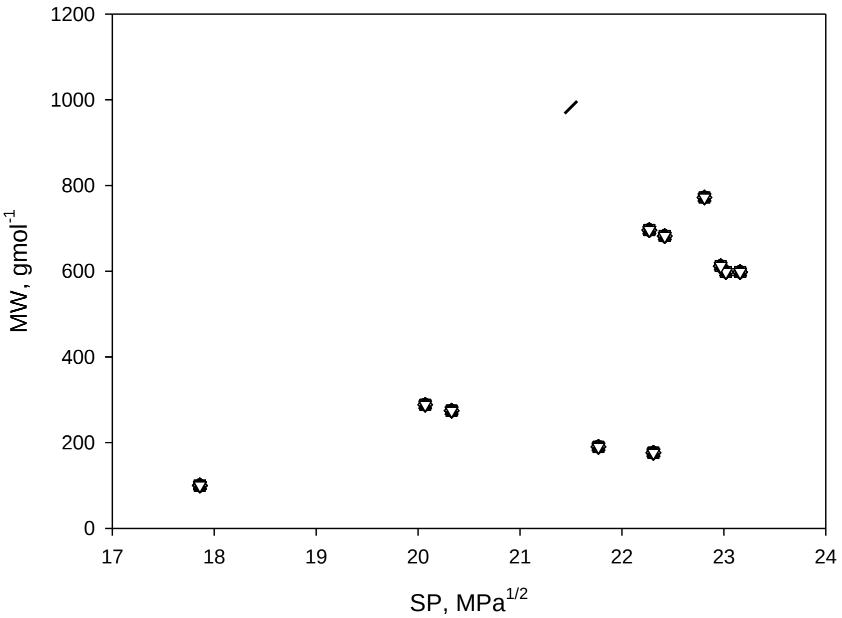

Figure 4-24. SP distribution of the cracked products from an archipelago molecule (×, Figure 3-6) after different three cracks. Data are given in Table 9-21 and Table 9-22.

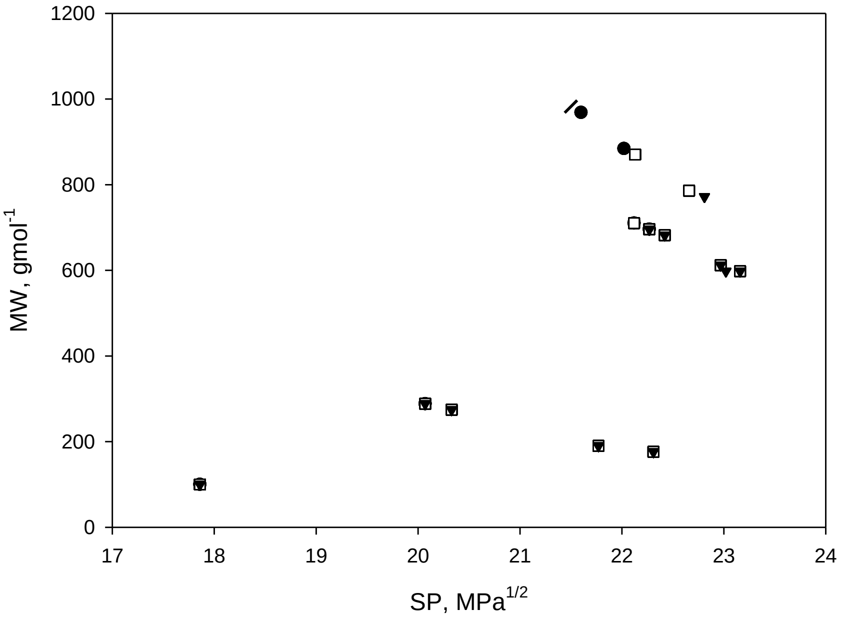

Figure 4-25. Overall SP distribution of the cracked products from an archipelago molecule (×, Figure 3-6) after different combinations of cracks (● one crack, □ two cracks, ▼three cracks; products from different amount of cracking coincide on each other). Data are given in Table 9-22.

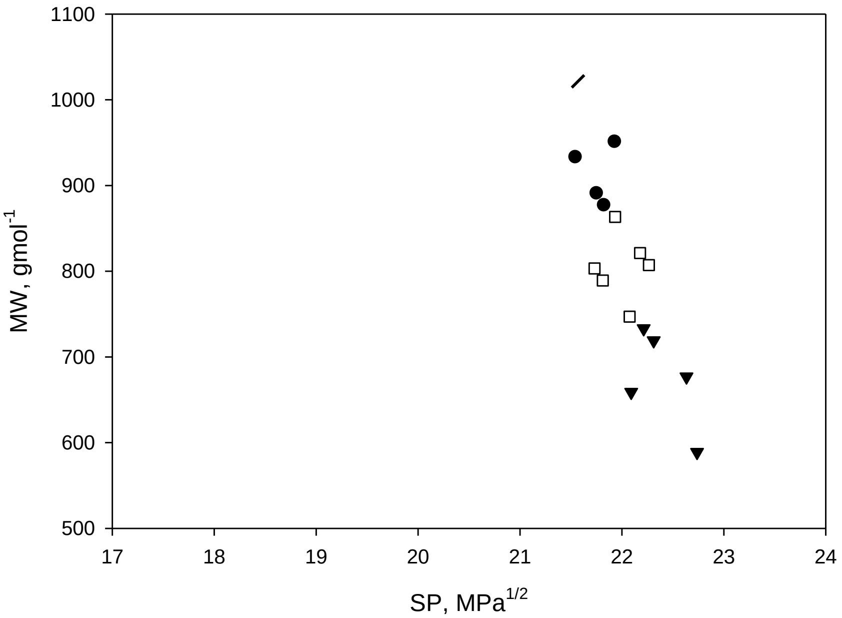

Figure 4-26. **Overall SP distribution of the cracked products from a pericondensed molecule (×, Figure 3-7) after different combinations of cuts (● one crack black, □ two cracks, ▼three cracks; n-pentane (14.4, 72,15) is not presented in this figure). Data are given in Table 9-23.**

The solubility parameter of the main remaining cracked products from the pericondensed molecule, ranges from 21.54 to 22.74 (Δδ = 1.2, Figure 4-26). With an increase in the amount of cracking, the solubility parameters of the products increase incrementally and the molecular weights decrease. This is the result of the dealkylation of the pericondensed structure.

The cracking of the archipelago molecule (even one crack) can produce a relatively low molecular weight product with relatively high solubility parameter i.e. (20.07,288.49), (20.33,274.46), (21.77,190.30) and (22.31,176.28) as seen in Figure 4-25. This is as a result of the existence of the aromatic rings in the low molecular weight products i.e. benzothiophene in $C3_r$ (right product from cut 3), $C4_r$, C3, 5 (middle product from cut 3 and 5) and C4, 5; whereas the low molecular weight products of the pericondensed molecules are aliphatic compounds and the solubility parameter of the products only increases with the cracking severity. The solubility parameter of the cracked products from the archipelago molecule (Figure 4-25) ranges from 20.07 to 22.27 (Δδ = 2.2) for a single cut and 20.07 to 23.16 (Δδ = 3.09) for two or more cuts.

Figure 4-27 shows three of the paths (already shown in Figure 4-25) for solubility parameter changes, of the resulting heavy parts left, with molecular weight as a result of cracking. The centre point represents the sample archipelago molecule (Figure 3-6). The two H2 addition trajectories are for pyrene (+2H2) and dibenzothiphene (+3H2) hydrogenation. The hydrodesulphurization (HDS) is for dipenzothiophene (+H2-S).

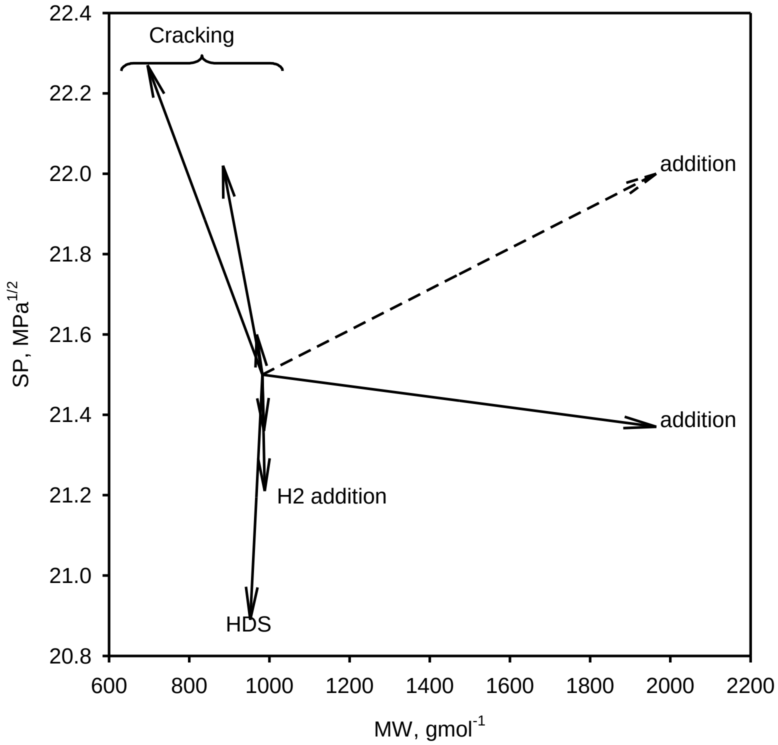

Figure 4-27. **Predicted changes in MW and solubility parameter of the bitumen representative molecule with possible reactions during upgrading (HDS and H2 addition can only happen at the presence of catalyst, other trajectories are associated with mild thermal reactions); - - - Expected trajectory for addition.**

Self-compatibility can be investigated for the cracked products (visbroken vacuum residue) if we have all the cracked products and their solubility parameters. In this work we only studied the cracking of one of the representative molecules of the Athabasca bitumen (archipelago) and asphaltenes (pericondensed).

4.6.1 Compatibility of the reaction products (sample study)

Table 4-12. Solubility modeling of two reaction paths for the archipelago molecule

	δ_i	x_i	ν_i	$x_i\nu_i$	$x_i\nu_i\delta_i$	φ_i
crack 1,5	22.66	0.33	723.92	241.31	5468.01	0.75
	17.86	0.33	123.30	41.10	734.05	0.13
	17.86	0.33	123.30	41.10	734.05	0.13
sum		1		323.51	6936.11	1
crack 1, 3, 5	23.16	0.25	466.7111	116.6778		0.53
	21.77	0.25	163.3689	40.84223	889.1352	0.19
	17.86	0.25	123.3006	30.82515	550.5372	0.14
	17.86	0.25	123.3006	30.82515	550.5372	0.14
sum		1		219.1703	1990.21	1

From Table 4-12, the molecule with the highest solubility parameter may be considered as an asphaltene (with overall vol% of 0.75 and 0.53 respectively) and the remaining molecules as solvent. Then ν_S, δ_S, ν_A, δ_A and ϕ_A^{max} can be calculated as follows:

Table 4-13. Ultimate results of the solubility modeling of the products of the archipelago molecule

	ν_S, cm^{3}mol^{-1}	δ_S, MPa$^{1/2}$	ν_A, cm^{3}mol^{-1}	δ_A, MPa$^{1/2}$	φ_A^{max}
crack 1, 5	123.30	17.76	723.92	22.66	0.16
crack 1, 3, 5	136.66	19.42	466.71	23.16	0.80

From the above analysis the products are compatible if cracking happens at 1, 3 and 5 locations.

5 Discussion

The purpose of this study was to simulate the stability of the hydrocarbons and their products and phase separation during the mild thermal cracking. In order to do that, the first step was to predict the solubility parameters from the molecular representations. The average calculated solubility parameters were then compared with the experimental values and the individual values were used for compatibility or self-compatibility investigation.

The solubility parameter predictions were used in three different applications which are supercritical fluid fractionation, stability and reaction. The vacuum residue fractions extracted with supercritical n-pentane, with a decreasing yield with increasing solubility parameter, were selected in this study for the first application because we thought it is instructive to look at the solubility parameters of the supercritical solvent and the solubilities of the fractions in the solvents. The analytical experimental data and the molecular structures were available for these hydrocarbon fractions from literature (McFarlane, 2007).

The two different correlations (Allada and Giddings) used for calculating the solubility parameters of the solvents were compared with those obtained from MD simulation and Allada was selected. For solutes, the different group contribution methods (Marrero-Gani and Fedors) were compared for solubility parameters in contrast to the values obtained from Rogel correlation and MD simulation for solutes. The solubility and SCF solvent-solute solubility parameter differences are discussed in 5.1.3. The second application is hydrocarbon self-compatibility investigation at room temperature (before reaction) from the solubility parameters of its group of representative molecules. The self-compatibility and the compatibility of blended feed have been discussed in literature from the experimental point of view (Wiehe, 2008). The final application is in studying the phase separation and reaction product stability as a result of different types of reactions and crackings. The solubility parameters of the cracked products are discussed in 5.3.

5.1 Vacuum residue fraction hydrocarbons and super critical solvent

Supercritical fluid-liquid solubility is important in fractionation of food liquids such as vegetable oils or other agricultural materials as well as petroleum liquids. The solubility parameter concept permits conditions to be specified for the optimum extraction by a supercritical fluid. Low vapor pressures of these materials make the enthalpies of vaporization and hence the solubility parameters calculations difficult. If the molecular structure is known, computation of the solubility parameters can be done. To apply this method to the fractionation of heavy oil, both the solubility parameter of the solvent and solutes must be calculated.

5.1.1 Supercritical n-pentane solvent

For simple well characterized solvents, solubility parameter can be calculated using correlations based on equation of state computationally. Three methods (Allada, Giddings and MD simulation) were studied for calculating the solubility parameters of the supercritical solvents. All three methods yielded similar results (Figure 4-3); Allada correlation was selected because of computational simplicity in comparison to MD simulation and its refinement in comparison to the Giddings correlation (Figure 4-4). The SCF solubility parameter calculations show that the cumulative 60 % extraction of the vacuum residue at a set temperature of 473 K based on this SCF method (Chung et al., 1997), happen over around 2 units (in MPa$^{1/2}$) of change in the solubility parameter of the solvent.

5.1.2 Solubility parameter of the heavy oil fractions

A different approach to calculate solubility parameter was needed for the heavy fractions as compared to those of solvents. Critical constants are not available for these large and hard to characterize materials. In this case, different group contribution methods as well as the MD simulation were tested for the enthalpy of vaporization/solubility parameter calculations to find the most robust one. While MD simulation results were satisfactory for solvents, this method did not appear to correlate well for the heavy oil fractions (solutes). Average solubility parameters were calculated for the groups of molecules. The predictions from the group contribution methods were similar while the predictions from MD simulation were considerably lower (Figure 4-12). The MD method was set aside without further comment on the low values obtained; one possible source of this discrepancy may be the large molecular structures themselves. The Marrero-Gani method was selected as the results were consistent from fraction to fraction (Figure 4-12).

The solubility parameters of the fractions calculated from the group contribution method, increased from 18.16 to 19.77 $MPa^{1/2}$ at room temperature (or 16.40 to 18.18 $MPa^{1/2}$ at 473 K) (without the end cut) as expected with increasing aromaticity and were generally consistent with the data from literature on petroleum materials. The range of solubility parameters in the representation for each of the fractions was quite broad (Table 4-1), given that these fractions were separated based on extraction by supercritical n-pentane. These results suggest that the molecular representations could be improved by adding solubility parameter as a constraint to the selection of candidate molecules for optimization.

Calculated solubility parameters for asphaltenes range from 21 (Akbarzadeh et al., 2004) to 25.8 (Rogel, 1997), and the experimental values are in agreement with the lower end of this range. Akbarzadeh et al. (2004) developed a correlation for asphaltenes solubility parameter with density $\delta = (0.366\rho)^{1/2}$ which gives the value of 21 $MPa^{1/2}$ for Athabasca asphaltenes using the density of 1192 gcm^{-3}. The max calculated values for asphaltenes were 25.8 for asphalt asphaltenes and 24.3 for Cold Lake asphaltenes from Rogel (1997). Wiehe & Liang (1996) obtained the solubility parameter of 10.8 $cal^{1/2}cm^{-3/2}$ or 22.1 $MP^{1/2}$ experimentally for Cold Lake asphaltenes; studying the solubility of the asphaltenes in different solvents with known solubility parameters at a fixed concentration. Correra et al. (2005) developed a correlation of solubility parameter with density, similar to Akbarzadeh et al. (2004), for the oil. Correra's correlation $\delta = (13.181\rho^{15.5°C} + 6.3583)$ gives the value of 19.8 $MPa^{1/2}$ for Athabasca bitumen using the density of 1.0217 gcm^{-3} (°API = 7.0) (Syncrude Canada Ltd.).

(Zhao et al., 2005, Wang et al., 2009) performed experimental solubility parameter measurements on the similar supercritically extracted vacuum residue fractions studying the phase equilibrea in the sub-critical high pressure propane system (50°C, 4-6 MPa). The correlation that was obtained with the key properties, estimated solubility parameter of 19.16 $^{\mathrm{MPa1/2}}$ for the end-cut from the Athabasca residue in good agreement with the actual measured data of 18.9 MPa$^{1/2}$ (Zhao et al., 2005). For other fractions the experimental solubility parameters were from 14.6 to 16.8.

To use the solubility parameters of the solvents and solutes to predict solubility, they must be calculated on the same basis. The solubility parameters of the solvents were calculated at the actual separation conditions while the solubility parameters of the solutes were calculated at room temperature. There are two ways of calculating the solubility parameter changes with temperature. The first one is to estimate the enthalpy of vaporization and molar volume at elevated temperature (used in this study) and the second way is using the given correlations from literature. These computations must be viewed with caution when extrapolated to supercritical conditions.

The solubility parameters decreased 1.59 to 1.75 MPa$^{1/2}$ for different fractions as a result of 8-5% decrease in the enthalpy of vaporizations and 12% increase in the molar volumes as the temperature changes from 298 K to 473 K (Table 4-6).

Correra et al. (2005) mentioned a correlation for the temperature dependence of δ_{oil} as follows

$$\delta = \delta_{ref} \exp\left[-K\left(T - T_{ref}\right)\right] \qquad [32]$$

Hirschberg et al. (1984) proposed a value of $K = -\ 0.0009\ \mathrm{K}^{-1}$ for asphaltenes from the fit to the experimental solubility parameters obtained from titration at different temperatures. Correra et al. (2005) obtained similar K for crude oil by minimizing the deviation of the solubility parameters from the above correlation from the values calculated with the viscosity correlations. The above equation results in the average $\Delta\delta$ of 2.8 MPa$^{1/2}$ for the nine fractions, with a small deviation, when temperature changes from 298 K to 473 K. Zhao et al (2008) got the solubility parameter decrease of 0.5 MPa$^{1/2}$ for a supercritically extracted fraction with change of temperature from 30 to 50 °C. Hence for a temperature difference of 175 °C ($25\rightarrow200$), a larger decrease of solubility parameter, around 4 MPa$^{1/2}$, is expected if Zhao's results can be generalized. Even if a larger decrease in the solubility parameter be considered, the solubilities calculated in section 5.1.3 will not change in the order of magnitude. The values calculated using the first method, were hence selected for solubility calculations.

5.1.3 Solubility and SCF solvent-solute solubility parameter differences (Δδ)

Cumulative yield of the extraction of the components of the residue versus the solubility parameters of the SCF n-pentane from Allada (corresponding to the supercritical pressures) are shown in Figure 4-5. The horizontal lines show the step changes in the pressure. The results are in agreement with the amount of asphaltene precipitated from bitumen (parent oil) with n-pentane at room temperature (Mitchell & Speight, 1973). The 40% left in this extraction (end-cut) is consisting primarily of asphaltenes (Zhao et al., 2005).

The difference between the solubility parameter of the associated solvent and solute were similar for different fractions and large. Similar differences may have been arisen as a result of possible errors in the estimated solubility parameters and the trends (slopes shown in Figure 4-9). Large differences in the solubility parameters have also been given in literature for the supercritical media.

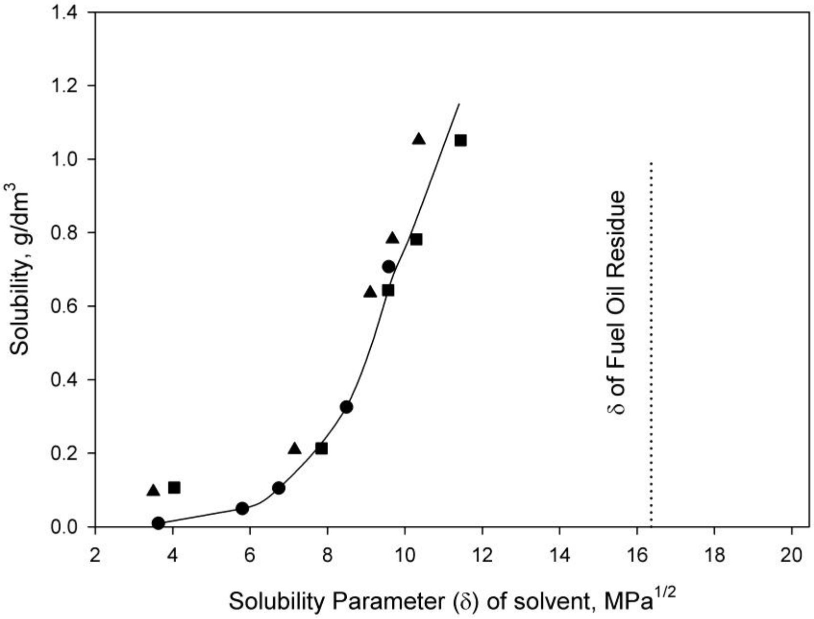

Figure 5-1. **Effect of solubility parameters of ● C2H4 (20-50 MPa), ▲C3H6 (5-15 MPa), ■ C3H8 (5-15 MPa) @378 K on solubility of fuel-oil residue**

Allada showed the effect of solubility parameters of supercritical C2H4 at 20 to 50 MPa and C3H8 and C3H6 at 5 to 15 MPa, all at 378 K, on the solubility of Russian fuel-oil residue, assuming n-hexadecane with solubility parameter of 8 $(cal/cc)^{1/2}$ or 16.4 $MPa^{1/2}$ as the average composition of the fuel-oil residue. The solute and solvents were chemically compatible. Allada explained that a significant increase in solubility took place when solubility parameter of the solvents exceeded about 4 $(cal/cc)^{1/2}$ or 8.2 $MPa^{1/2}$, which is approximately 4 units $(cal/cc)^{1/2}$ below that of the solute. The minimum difference between the solubility parameter of the solute and the solvent which causes phase separation was considered to be about 4 $MPa^{1/2}$ (Andersen, 1999) in general not in a supercritical media. According to the solution theories, to the first approximation, $\Delta\delta$ is corresponding to the solubility of a solute (in term of mol fraction or molarity) in the solution. Wiehe (2009) explained, in his development of the two dimensional solubility parameter, that the exact matching of the solubility parameter components only assures solubility if the material is a liquid and that a material may still be insoluble in a liquid of identical solubility parameter components if the material is a crystalline solid with a high heat of fusion and the temperature is well below the melting point.

F-H theory does not only incorporate $\Delta\delta$ for calculating solubility but also the ν_a/ν_s ratio. The first term ($v_a \Delta\delta^2 / RT$) were increasing with increasing molar volumes of the fractions. Also the molar volumes of the solvents were decreasing in such a way that ν_a/ν_s were increasing (table 4-8).

The supercritical extraction process happens over a time frame at constant pressure and temperature for each fraction and the yield is cumulative with higher extractions in the beginning. This is because vacuum residue and its fractions are amorphous mixture of compounds with different molecular weights, molar volumes, enthalpies of vaporization, solubility parameters, etc. The solubility parameters calculated for fractions from group contribution method are the lumped values, with experimental molar volumes calculated from experimental molecular weights and densities, and calculated lumped enthalpies of vaporization. The solubility distribution of each of these fractions could be investigated separately in a PVT cell with a solvent such as propane. The lumped solubilities are decreasing as those calculated from F-H theory, but they have orders of magnitude larger values than those given in Table 4-8. F-H theory gives the equilibrium solubility, so even if solubilities in Table 4-10 are not the equilibrium one, they should be the minimum values.

Excess volume of mixing is assumed to be zero in the Flory-Huggins theory. This assumption is not valid in the supercritical media. The refinement factor (R) shown in Table 4-11, may be the V^E/RT term which is in the enthalpy. Also all the errors in the solubility parameter calculations are lumped into this factor. More over the Flory-Huggins theory does not consider the polar and hydrogen bonding effects, hence it fails for calculating the solubility of heavy oil fractions (with pi bonds) in the supercritical media (with large negative partial molar volumes).

Pure compounds like phenanthrene, pyrene or any model compound have specific solubility parameters and solubilities in a solvent at a specific pressure and temperature. In order to increase the solubility, one has to decrease the difference between the solubility parameter of the solute and solvent by increasing the solubility parameter of the solvent. This can be done using a supercritical solvent or a mixture of solvents (for example toluene and heptane or dichlorometane and heptane instead of heptane).

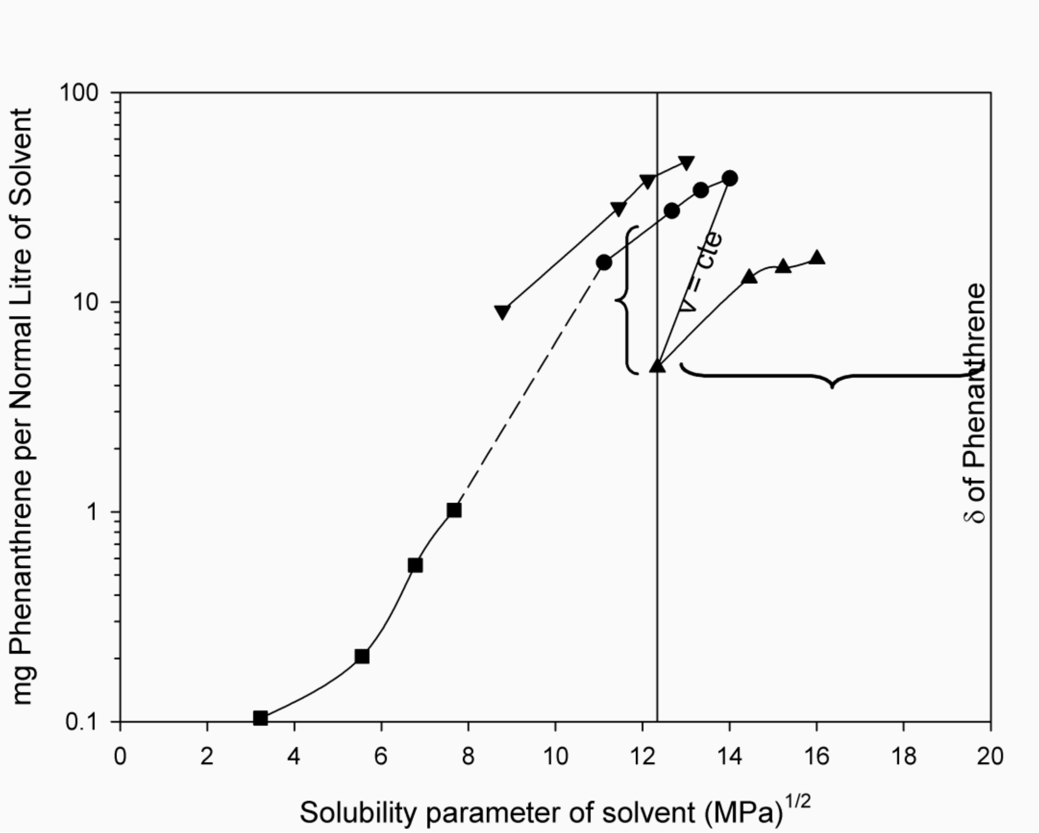

Figure 5-2. **■ CH4, ● C2H6, ▲ CO2, ▼ C2H4**

Allada (1984) showed the effect of the solubility parameters of supercritical solvents on the solubility of phenanthrene. Solubility parameter of phenanthrene is 20.3 MPa$^{1/2}$ (the temperature in not given but should be above the critical temperature of the solvents and the solubility parameter of the solute at supercritical condition is assumed the same as the one in 298 K). When pressure changes from 15 to 55 MPa, the solubility parameter changes from 3 to 8 MPa$^{1/2}$ for supercritical CH4, 10.2 to 14 for C2H6 and 12.3 to 16 for CO2. The solubility of phenanthrene changes from 0.1 to 1 mg/l in CH4, 15 to 40 mg/l in C2H6 and 5 to 15 mg/l in CO2. The solubility was smaller in CH4 because the differences in the solubility parameters of the supercritical CH4 and solubility parameter of phenanthrene were larger. At the same solubility parameter of the solvents, for example 12.3 MPa$^{1/2}$, the solubility was larger in C2H6 than CO2 because of the nature of the solvent and different solvent-solute interaction. Even the molar volume of C2H6 is larger than CO2 and ln(va/vs)+(1-va/vs) is a smaller negative number and hence x should be smaller so this is not because of the difference in the molar volumes of the solvents (va/vs). Allada paper shows the solubility (mg/l) of phenanthrene (with fixed SP) in three different SCF solvents with the same SP (hence same deltaSP) is different because of the nature of the solvents. Even if we draw the constant molar volume line, there is not a considerable difference between the solubility parameter differences, which confirms the difference in solubilities is not because of densities.

We are dealing with the solubility of different solutes (with increasing SPs or aromaticity and different natures) in n-pentane (same nature with increasing SPs). As solubility parameter differences are almost the same, the differences can come from molar volumes of the solutes and solvents as well as non-idealities.

As we used the F-H theory and even that theory failed, we cannot make any judgment about solubiltiy immediately based on the differences in the solubility parameters of the solvent and solutes at supercritical conditions.

5.2 Solubility parameter and stability of the vacuum residue

Although there were some discrepancies between the solubility parameter of the solvent and vacuum residue fractions discussed in the first application, but the reason is that it is a comparison between the liquid and the supercritical phase. The solubility parameter calculations should work well for the liquid-liquid phase. The solubility parameter of the representative molecules can be used for calculating the average solubility parameter and comparison with the experimental value. Further they may be used for investigating the self compatibility by dividing them into two groups as heavy and light liquids. The average solubility parameter of the bitumen looked good in comparison with the experimental value. The distributions of the solubility parameters were too wide and the sample was not self compatible from the computations. The solubility parameter data are useful to be included in the molecular representation generation to satisfy the stability status of the sample.

5.3 Reactions

Properties such as solubility parameters are related to structures. With chemical reaction as structures change, the solubility parameters change. The solubility parameter is a function of enthalpy of vaporization and molar volume. Enthalpy of vaporization was determined from the group contribution method and density was determined from a correlation with the elemental compositions (H, S, and N). We took a representative molecule and reacted. During hydro desulfurization when H2 is added to Dibenzothiophene and S is removed as H2S, the number of aCH groups change. During H2 addition, the number of CH2, aCH, aC, CH2(cyc) and CH(cyc) groups may change. During addition the enthalpy of vaporization almost doubles because the numbers of existing groups double. and the molar volume doubles because the MW doubles while the density is constant (N%, S% and H% are constant). Hence the solubility parameter does not change significantly when investigated computationally. Phase separation can happen during mild thermal reactions as a result of cracking or addition (condensation, coagulation). Cracking can produce products with larger solubility parameters.

The prediction for addition reaction does not show the phase sepperation as a result of condensation. The applicability of the density corollation in case of addition is questionable as density is not correlated with Molecular weight.

The predictions at room temperature are conservative to be applied at higher temperatures. Asphaltene solubility in oils always increase with increasing temperature as long as no major fraction of a gas or other component at temperature near its critical point is in the oil.

6 Conclusions

In this work, the appropriateness of the group contribution method for calculation the solubility parameter of the heavy oil fractions was investigated. The solubility parameters calculated at room temperature cannot accurately be converted to the higher process conditions. The solubility calculations based on the solubility parameter calculations were not reasonable for the supercritical system as the solution theories fail because of non-idealities in these systems. The solubility parameters of the representative molecules were used to predict its self compatibility and the incompatibility result showed that the solubility parameter should have been incorporated into molecular representation generation. Limited study on a sample heavy molecule showed that the solubility parameters can be used for predicting the phase separation during the mild thermal cracking computationally (two cases were investigated which resulted in compatible or incompatible products). Calculations are not expected to have limitations for a liquid-liquid system unlike the supercritical fluid-liquid system.

7 Recommendations

The Hildebrand solubility parameter is a valuable property to be considered during molecular representation generations itself, in addition to other physical properties such as boiling point. It can also be used to refine molecular representations if not incorporated into the generation step. A more complete study can be done on combinations of representative molecules for one sample, when all representative molecules crack at favoured cracking locations and different compatibility and incompatibility scenarios can be studied (the study was limited to one of the representative molecules in this work).

8 References

Akbarzadeh K., A. Dhillon, W. Y. Svrcek, and H. W. Yarranton. 2004. Methodology for the characterization and modeling of asphaltene from heavy oils diluted with n-alkanes. Energy & Fuels 18: 1434-1441.

Akbarzadeh K., H. Alboudwarej, W. Y. Svrcek, H. W. Yarranton. 2005. A generalized regular solution model for asphaltene precipitation from *n*-alkane diluted heavy oils and bitumens. Fluid Phase Equilibria 232: 159-170.

Alboudwarej H., K. akbarzadeh, J. Beck, W. Y. Svrcek, and H. W. Yarranton. 2003. Regular solution model for asphaltene precipitation from bitumens and solvents. AICHE Journal 49: 2948-2956.

Allada S.R. 1984. Solubility parameters of supercritical fluids. Ind. Eng. Chem. Process Des. Dev. 23: 344-348.

Andersen, S.I. 1999. Flocculation Onset Titration of Petroleum Asphaltenes. Energy & Fuels 13: 315-322.

API technical data book: petroleum refining. 1997.

Barton, Allan F.M. 1983. CRC handbook of solubility parameters and other cohesion parameters.

Boek E.S., D.S. Yakovlev, T. F. Headen. 2009. Quantitative molecular representation of Asphaltenes and molecular dynamics simulation of their aggregation. Energy & Fuels 23: 1209-1219.

Chung K. H., C. Xu, Y. Hu, and R. Wang. 1997. Supercritical fluid extraction reveals resid properties. Oil & Gas Journal 95:66-69.

Chung K. H., C. Xu, M.R. Gray,Y. Zhao, L.S. Kotlyar, and B. D. Sparks. 1998. The chemistry, reactivity, and processability of Athabasca bitumen pitch. Reviews in Process Chemistry and Engineering 1: 41.79.

Correra S., M. Merlini, A. DiLullo, and D. Merino-Garcia 2005. Estimation of the solvent power of crude oil from density and viscosity measurments. Ind. Eng. Chem. Res. 44:9307-9315.

Dechaine G. P., Y. Maham, X. Tan, and M.R. Gray. 2009. Solubility of model porphyrins and model asphaltenes. 8th world congress of chemical engineering.

Fedors R. F. 1974. A method for estimating both the solubility parameters and molar volumes of liquids. Polymer engineering and science 14:147-154.

Flory P. J. 1953. Principles of polymer chemistry. Ithaca, NY. Cornell University press: 495-594.

Gray M.R., Y. Zhao, G. M. Mcknight, D. A. Komar, and J. D. Carruthers. 1999. Coking of hydroprocessing catalyst by residue fractions of bitumen. Energy & fuels 13:1037-1045.

Gray M.R. 2002. New technique defines the limit of upgrading heavy oils, bitumens. Oil & Gas Journal 100:50-54.

Gray M.R. 2008. Oil Sands Extraction and Upgrading Course Notes. University of Alberta.

Hansen C.M. 2000. Hansen solubility parameters: a user's handbook. Boca Raton: CRC Press.

Hildebrand J. H. and R. L. Scott. 1964. The solubility of nonelectrolytes, 3rd ed. New York. Dover Publication: page 134.

Hirschberg A., L.N.J. Dejong, B.A. Schipper, J.G. Meijer. 1984. Influence of temperature and pressure on asphaltene flocculation. SPE Journal: 283-293.

Klein M.T. 2006. Molecular modeling in heavy hydrocarbon conversions. Boca Raton: CRC.

Konstogeorgis G. M. and R. Gani. 2004. Computer aided property estimation for process and product design. Elsevier. page 51.

Marcus Y. 2006. Are solubility parameters relevant to supercritical fluids? The journal of supercritical fluids 38:7-12

Marrero J., R. Gani. 2001. Group-contribution based estimation of pure component properties. Fluid Phase Equilibria 183-184:183-208.

McFarlane R.A. 2007. Evaluation of new co-volume mixing rules for the Peng-Robinson equation of state. PhD dissertation, University of Alberta.

Reid. R.C., J. M. Prauznitz, B. E. Poling. 1987. The properties of gases and liquids. McGraw-Hill. New York. Page 286.

Rogel E. 1997. Theoretical estimation of the solubility parameter distributions of asphaltenes, resins, and oils from crude oils and related materials. Energy & Fuel 11:920-925.

Rogel E. 1998. Theoretical approach to the stability of visbreaken residues. Energy & Fuel 12:875-880.

Sheremata J. M. 2008. Residue Molecules: Molecular representations and thermal reactivity. PhD dissertation, University of Alberta.

Sheremata J.M., M.R. Gray, H. D. Dettman, and W. C. McCaffrey. 2004. Quantitative molecular representation and sequential optimization of Athabasca asphaltenes. Energy & Fuels 18:1377-1384.

Smith J. M., H. C. Van Ness, A. M. Abbott. 2005. 7th ed. Introduction to chemical engineering thermodynamics. McGraw-Hill.

Yang G. and R.A. Wang. 1999. The supercritical fluid extractive fraction and the characterization of heavy oils and petroleum residua. Journal of petroleum science & engineering 22:47-52.

Wang X., Z. Xu, S. Zhao, C. Xu, and K.H. Chung 2009. Solubility parameters of bitumen-derived narrow vacuum resid fractions. Energy & Fuels 23: 386-391.

Wiehe I.A. and K. S. Liang. 1996. asphaltenes, resins, and other petroleum macromolecules. Fluid Phase Equilibria 117:201-210.

Wiehe I.A., H.W. Yarranton, K. Akbarzadeh, P. M. Rahimi, and A. Teclemariam. 2005. The paradox of asphaltene precipitation with normal paraffins. Energy & Fuels 19: 1261-1267.

Wiehe I.A. 2008. Process chemistry of petroleum macromolecules. Boca Raton : CRC.

Yan T.Y. 1990. Characterization of visbreaker feeds. Fuel 69:1062-1064.

Zhao S., Z. Xu, C. Xu, K. H. Chung, R. Wang. 2005. Systematic characterization of petroleum residua based on SFEF. Fuel 84: 635-645.

Zhao S., B. D. Sparks, L. S. Kotlyar, and K. H. Chung. 2007. Correlation of processibility and reactivity data for residua from bitumen, heavy oils and conventional crudes: characterization of fractions from supercritical pentane separation as a guide to process selection. Calalysis Today 125:122-136.

9 Appendix

Most of the experimental properties of fractionated Athabasca vacuum residue are available in the literature as shown Table 9-1.

Table 9-1. Experimental properties of fractionated Athabasca vacuum residue (Sheremata, 2008, Gray et al., 1999)

Fractions	Yield, wt%	Density, g/cm^3	MW	ν, cm^3/mol	H/C	% aromaticity	% saturate	% aromatic S	MCR, wt%
1	12.7	0.9745	506	519.24	1.61	27.5	26.9	64.7	5.6
2	9.8	0.9930	755	760.32	1.59	29.7	16.4	67.0	7.9
3	7.6	1.0061	711	706.69	1.56	28	9.68	69.2	10.8
4	10.6	1.0228	800	782.17	1.52	34	-	71.4	14.3
5	6.5	1.0427	825	791.22	1.47	36	-	73.7	18.2
6	4.4	1.0543	948	899.17	1.43	40	-	73.5	21.5
7	3.3	1.0646	1138	1068.95	1.39	40	-	73.3	26.3
8	2.6	1.0678	1210	1133.17	1.39	42	-	73.1	
9	2.1	1.0737	1520	1415.67	1.37	46	-	71.7	
10	40.4	N/A	4190	N/A	1.23	50	-	70.4	48.9
Error (%)	-	-	10	10	-	3.0	6.0	5.0	-

H/C is the atomic ratio

$$H/C = (H/C)_{EA}(12.011/1.008)$$

where H_{EA} and C_{EA} are the elemental compositions in wt%.

F1M1 (first molecule of fraction 1), F2M5, F2M6, F3M3 and F3M6 are the saturate molecules (table A2).

Table 9-2. Calculated properties of the structural representations of fractionated Athabasca vacuum residue

Molecules	Formula	Mol% (x_i)	Vol% (φ_i)	MW, g/mol	ρ_i, g/ml
F1M1	C34H66	30.44	0.29	474.89	0.8412
F1M2	C39H64S2	20.03	0.20	597.06	1.0338
F1M3	C35H60	19.80	0.19	480.85	0.8608
F1M4	C37H46S2	12.51	0.11	554.89	1.0787
F1M5	C57H71N	12.34	0.15	770.18	1.1162
F1M6	C53H80S	4.88	0.07	749.27	0.9449
F2M1	C48H78S	37.10	0.33	687.20	0.9410
F2M2	C75H103NS2	23.42	0.27	1082.76	1.1334
F2M3	C50H86S	17.18	0.16	719.29	0.9298
F2M4	C36H48S	11.22	0.07	512.83	0.9904
F2M5	C71H132	11.10	0.16	985.82	0.8482
F2M6	C94H164	0.01	0.00	1294.32	0.8581
F3M1	C44H68S	64.80	0.61	629.08	0.9544
F3M2	C48H65NS2	13.71	0.11	720.17	1.2568
F3M3	C71H132	8.40	0.14	985.82	0.8482
F3M4	C47H81NS	7.69	0.06	692.22	1.1698
F3M5	C75H110S2	4.70	0.07	1075.81	0.9745
F3M6	C38H72S	0.75	0.01	561.05	0.9351
F4M1	C62H87NS	29.70	0.29	878.43	1.1314
F4M2	C64H92S2	24.99	0.29	925.55	0.9918
F4M3	C49H80S	16.92	0.16	701.23	0.9389
F4M4	C45H68S	13.12	0.11	641.09	0.9559
F4M5	C59H86S3	9.49	0.10	891.51	1.0493
F4M6	C52H78	5.77	0.06	703.18	0.8799
F5M1	C56H81NS	40.03	0.32	800.32	1.1513
F5M2	C54H86S2	22.40	0.21	799.40	0.9957
F5M3	C82H122S2	14.20	0.20	1171.98	0.9651
F5M4	C66H94S2	12.99	0.14	951.59	0.9900
F5M5	C80H104S3	10.37	0.13	1161.88	1.0241

F5M6	C71H104S2	0.01	0.00	1021.72	0.9795
F6M1	C51H71NS2	44.15	0.31	762.25	1.2336
F6M2	C68H98S2	38.00	0.43	979.64	0.9856
F6M3	C79H114	11.16	0.15	1063.76	0.8851
F6M4	C94H136S	4.81	0.08	1298.16	0.9226
F6M5	C82H104S4	1.59	0.02	1217.97	1.0610
F6M6	C90H125NS2	0.29	0.00	1285.10	1.0940
F7M1	C92H131NS3	63.77	0.64	1347.23	1.1180
F7M2	C84H108S3	19.08	0.19	1213.96	1.0200
F7M3	C86H118	11.33	0.12	1151.86	0.8916
F7M4	C82H115NS2	3.97	0.03	1178.93	1.1112
F7M5	C90H120S3	1.58	0.02	1298.12	1.0081
F7M6	C102H141NS3	0.27	0.00	1477.42	1.1012
F8M1	C86H112S3	38.09	0.41	1242.01	1.0158
F8M2	C69H107NS2	33.09	0.26	1014.73	1.1347
F8M3	C106H147NS2	20.88	0.26	1499.45	1.0650
F8M4	C83H115NS4	5.74	0.05	1255.07	1.1772
F8M5	C74H102N2S	1.82	0.01	1051.69	1.2496
F8M6	C99H140N2	0.38	0.00	1358.19	1.1294
F9M1	C117H150S2	26.09	0.36	1620.58	0.9601
F9M2	C79H113NS3	21.11	0.18	1172.95	1.1518
F9M3	C78H103NS3	19.78	0.16	1150.86	1.1661
F9M4	C71H103NS3	17.56	0.13	1066.79	1.1766
F9M5	C103H127NS3	13.29	0.15	1475.32	1.1144
F9M6	C91H109NS2	2.17	0.02	1280.98	1.1114
F10M1	C231H289N3OS7	51.93	0.47	3348.26	1.1519
F10M2	C273H339NO5S13	30.28	0.35	4131.48	1.0987
F10M3	C287H366N6OS8	14.54	0.15	4172.56	1.2301
F10M4	C276H310N12O7S4V2	3.22	0.03	4035.77	1.4529
F10M5	C286H351N3O2S8	0.01	0.00	4119.41	1.1197
F10M6	C275H349N3O3S9	0.01	0.00	4033.34	1.1332

$$\phi_i = \frac{x_i V_i}{\sum_{i=1}^{6} x_i V_i}$$

$$V_i = MW_i / \rho_i$$

Table 9-3. Calculated properties of fractionated Athabasca vacuum residue (ensemble of six molecules for each fraction) and the absolute errors

fraction	H/C	%error	MW	%error	density	%error	%saturate	%error
1	1.61	0.20	560.38	10.75	0.9558	1.9	30.44	13.16
2	1.68	5.83	799.20	5.85	0.9808	1.2	11.11	32.26
3	1.80	15.65	697.19	1.94	0.9887	1.7	9.15	5.47
4	1.48	2.33	820.13	2.64	1.0189	0.4	0	-
5	1.47	0.09	910.05	10.31	1.0423	0.0	0	-
6	1.39	2.46	913.05	3.69	1.0447	0.9	0	-
7	1.38	0.66	1292.56	13.58	1.0700	0.5	0	-
8	1.40	1.05	1218.28	0.68	1.0718	0.4	0	-
9	1.26	7.98	1309.25	13.86	1.0814	0.7	0	-
10	1.26	2.70	3727.22	11.04	1.1535	-	0	-

$$\frac{H}{C} = \frac{\sum_{i=1}^{6} x_i H_i}{\sum_{i=1}^{6} x_i C_i}$$

$$MW = \sum_{i=1}^{6} x_i MW_i$$

Table 9-4. Details of supercritical n-pentane SP calculations from Allada and Giddings (n-pentane at 473 K and supercritical pressure 5 to 12 MPa)

P, MPa	H^{ig} - H, $Jmol^{-1}$ (PR EOS)	Z (PR EOS)	ν_S, cm^3mol^{-1} (PR EOS)	δ_{Allada}, $MPa^{1/2}$	$\delta_{Giddings}$, $MPa^{1/2}$
5	15724.050	0.266	209.030	7.84	8.36
5.5	16111.719	0.280	200.303	8.14	8.73
6	16412.397	0.295	193.659	8.39	9.03
7	16859.323	0.327	183.871	8.79	9.51
8	17181.453	0.359	176.765	9.11	9.89
9	17426.342	0.392	171.230	9.37	10.21
10	17618.386	0.424	166.726	9.60	10.48
11	17771.868	0.456	162.947	9.79	10.73
12	17895.908	0.487	159.705	9.97	10.95

Table 9-5. Solubility parameters of n-pentane computed with different methods at 473 K

P, MPa	δ_G, $MPa^{1/2}$	δ_A, $MPa^{1/2}$	δ_{MD}, $MPa^{1/2}$
5	8.36	7.84	7.48
5.5	8.73	8.14	8.45
6	9.03	8.39	8.66
7	9.51	8.79	9.06
8	9.89	9.11	9.38
9	10.21	9.37	9.64
10	10.48	9.60	9.88
11	10.73	9.79	10.10
12	10.95	9.97	10.28

Table 9-6. Measured and calculated densities and molar volumes for the ten fractions, Athabasca bitumen and AVR

fraction	ρ measured g/ml	$\bar{\rho}$ (Gray), g/ml ($\bar{\rho} = \sum_{i=1}^{6} \phi_i \rho_i$) (ρ_i from Table 9-2, Table 4-2 & Table 4-4	ARE (%) $\frac{\rho - \bar{\rho}}{\rho} \times 100$	ν measured m^3/mol	$\bar{v}$ (Gray) ($\bar{v} = \sum_{i=1}^{6} x_i v_i$) m^3/mol
F1	0.9745	0.9558	1.9	519	586
F2	0.9930	0.9808	1.2	760	815
F3	1.0061	0.9887	1.7	707	705
F4	1.0228	1.0189	0.4	782	805
F5	1.0427	1.0423	0.0	791	873
F6	1.0543	1.0447	0.9	899	874
F7	1.0646	1.0700	0.5	1069	1208
F8	1.0678	1.0718	0.4	1133	1137
F9	1.0737	1.0814	0.7	1416	1211
F10	N/A	1.1535	N/A	N/A	3231
Athabasca bitumen	1.0071	0.9842	2.3	571	546
AVR	1.0528	1.0373	1.5	1056	981

Table 9-7. Details of SP calculations of the molecules of fraction 1

		F1M1	F1M2	F1M3	F1M4	F1M5	F1M6
groups	Hvi	C34H66	C39H64S2	C35H60	C37H46S2	C57H71N	C53H80S
CH3	2.8768	5	6	6	6	7	3
CH2	4.8674	16	9	7	5	6	10
CH	4.4937	3	3	3	1	1	2
aCH	4.5216	0	2	3	5	11	5
aC	6.07	0	2	0	6	2	4
aC	6.2214	0	0	0	2	4	2
aC	4.1803	0	0	0	0	6	0
aC-CH3	8.5968	0	0	0	1	1	1
aC-CH2	9.441	0	2	3	4	4	2
aC-CH=CH	22.7017	0	0	0	0	0	0
CH2S	15.6689	0	1	0	0	0	1
CH2(cyc)	4.2419	6	6	6	0	5	11
CH(cyc)	4.1375	4	4	4	0	3	7
CH=CH(cyc)	8.2613	0	0	0	0	0	0
CH=C(cyc)	8.7037	0	1	0	1	1	0
NH(cyc)	14.8713	0	0	0	0	1	0
S(cyc)	13.4267	0	1	0	2	0	0
(CHn=C)cyc-CH3	1.2994	0	0	0	1	0	0
(CHn=C)cyc-CH2	1.7743	0	1	0	0	1	0
CH(CH3)CH(CH3)	1.3663	2	1	2	0	0	0
CHcyc-CH3	0.1038	0	0	0	0	0	0
CHcyc-CH2	-0.6827	2	2	2	0	1	3
AROMRINGs1s3s5	1.601	0	0	1	0	0	0
AROMRINGs1s2s4	1.8085	0	0	0	0	1	0
Hv, kJmol^{-1} (eqn. #)	▨	160.8451	207.9226	163.4041	212.5126	283.8716	254.0786
MW, gmol^{-1}	▨	474.89	597.06	480.85	554.89	770.18	749.27
V, cm^{3}mol^{-1} (eqn. #)	▨	564.5304	577.5147	558.6045	514.4239	690.0047	792.9367
δ, MPa$^{1/2}$	▨	16.75	18.86	16.97	20.21	20.19	17.81

AROMRING is a single aromatic ring with its indicated carbons connected to the adjacent carbons as a chain/branch or to the carbon(s) in the other neighboring aromatic ring(s) by a bridge (not fused).

Table 9-8. Details of SP calculations of the molecules of fraction 2

		F2M1	F2M2	F2M3	F2M4	F2M5	F2M6
groups	Hvi	C48H78S	C75H103NS2	C50H86S	C36H48S	C71H132	C94H164
CH3	2.8768	7	7	11	6	7	4
CH2	4.8674	17	13	10	6	25	22
CH	4.4937	4	2	8	1	5	2
aCH	4.5216	5	7	1	5	0	0
aC	6.07	4	0	2	2	0	0
aC	6.2214	0	10	0	2	0	0
aC	4.1803	0	0	0	2	0	0
aC-CH3	8.5968	2	1	1	1	0	0
aC-CH2	9.441	3	6	2	4	0	0
aC-CH=CH	22.7017	1	0	0	0	0	0
CH2S	15.6689	0	0	0	0	0	0
CH2(cyc)	4.2419	0	11	6	0	22	40
CH(cyc)	4.1375	0	7	4	0	12	26
CH=C(cyc)	8.7037	0	2	1	1	0	0
NH(cyc)	14.8713	0	1	0	0	0	0
S(cyc)	13.4267	0	2	1	1	0	0
(CHn=C)cyc-CH3	1.2994	0	1	0	0	0	0
(CHn=C)cyc-CH2	1.7743	0	1	1	1	0	0
CH(CH3)CH(CH3)	1.3663	2	0	5	0	1	0
CHcyc-CH3	0.1038	0	0	0	0	0	0
CHcyc-CH2	-0.6827	0	3	2	0	10	14
Hv, kJmol^{-1}	▨	250.4301	399.0233	243.5140	188.50888	313.5352	407.0036
MW, gmol^{-1}	▨	687.20	1082.76	719.29	512.83	985.82	1294.32
V, cm^{3}mol^{-1}	▨	730.2937	955.2973	773.6352	517.7857	1162.21	1508.266
δ, MPa$^{1/2}$	▨	18.43	20.37	17.65	18.95	16.36	16.38

Table 9-9. Details of SP calculations of the molecules of fraction 3

		F3M1	F3M2	F3M3	F3M4	F3M5	F3M6
groups	Hvi	C44H68S	C48H65NS2	C71H132	C47H81NS	C75H110S2	C38H72S
CH3	2.8768	8	6	6	7	7	3
CH2	4.8674	10	5	27	15	13	15
CH	4.4937	4	3	4	4	2	2
aCH	4.5216	4	5	0	2	9	0
aC	6.07	0	0	0	0	6	0
aC	6.2214	6	8	0	2	2	0
aC	4.1803	0	0	0	0	0	0
aC-CH3	8.5968	0	1	0	0	1	0
aC-CH2	9.441	2	4	0	2	6	0
CH2S	15.6689	0	1	0	1	2	1
CH2(cyc)	4.2419	4	5	22	6	13	10
CH(cyc)	4.1375	4	3	12	4	7	6
CH=CH(cyc)	8.2613	0	1	0	0	0	0
CH=C(cyc)	8.7037	0	0	0	1	0	0
NH(cyc)	14.8713	0	1	0	1	0	0
S(cyc)	13.4267	1	1	0	0	0	0
(CHn=C)cyc-CH3	1.2994	0	0	0	0	0	0
(CHn=C)cyc-CH2	1.7743	0	0	0	1	0	0
CH(CH3)CH(CH3)	1.3663	3	2	0	3	0	0
CHcyc-CH3	0.1038	1	0	0	0	0	0
CHcyc-CH2	-0.6827	1	1	10	2	5	4
Hv, kJmol^{-1}		226.1573	273.452	314.5332	248.9775	370.9657	182.5439
MW, gmol^{-1}		629.08	720.17	985.82	692.22	1075.81	561.05
V, cm^{3}mol^{-1}		659.1156	573.0149	1162.21	591.7478	1104.005	600.0096
δ, MPa$^{1/2}$		18.42	21.75	16.39	20.41	18.27	17.32

Table 9-10. Details of SP calculations of the molecules of fraction 4

		F4M1	F4M2	F4M3	F4M4	F4M5	F4M6
groups	Hvi	C62H87NS	C64H92S2	C48H80S	C45H68S	C59H86S3	C52H78
CH3	2.8768	5	7	8	6	7	5
CH2	4.8674	12	15	18	6	19	10
CH	4.4937	2	3	3	2	2	2
aCH	4.5216	5	5	5	6	6	7
aC	6.07	0	0	4	0	0	2
aC	6.2214	10	10	0	4	8	2
aC	4.1803	2	0	0	0	2	0
aC-CH3	8.5968	0	0	0	0	0	1
aC-CH2	9.441	1	3	5	2	2	4
CH2S	15.6689	14	9	1	1	1	0
CH2(cyc)	4.2419	8	7	0	8	4	9
CH(cyc)	4.1375	1	1	0	8	4	5
CH=C(cyc)	8.7037	1	0	0	0	1	0
NH(cyc)	14.8713	1	2	0	0	0	0
S(cyc)	13.4267	0	0	0	0	2	0
(CHn=C)cyc-CH3	1.2994	0	0	0	0	0	0
(CHn=C)cyc-CH2	1.7743	0	0	0	0	1	0
CH(CH3)CH(CH3)	1.3663	0	2	0	1	1	1
CHcyc-CH3	0.1038	0	1	0	2	1	0
CHcyc-CH2	-0.6827	4	2	0	2	1	3
Hv, kJmol^{-1}	▨	322.4519	335.233	245.6036	220.9954	324.7873	244.556
MW, gmol^{-1}	▨	878.43	925.55	701.23	641.09	891.51	703.18
V, cm^{3}mol^{-1}	▨	776.4310	933.206	746.8631	670.6654	849.6072	799.1328
δ, MPa$^{1/2}$	▨	20.30	18.88	18.04	18.05	19.48	17.40

Table 9-11. Details of SP calculations of the molecules of fraction 5

		F5M1	F5M2	F5M3	F5M4	F5M5	F5M6
groups	Hvi	C56h81NS	C54H86S2	C82H122S2	C66H94S2	C80H104S3	C71H104S2
CH3	2.8768	10	8	6	9	4	10
CH2	4.8674	8	14	32	18	15	17
CH	4.4937	7	3	1	3	1	4
aCH	4.5216	7	9	9	8	12	8
aC	6.07	0	0	0	0	0	0
aC	6.2214	8	0	12	10	12	8
aC	4.1803	0	0	0	2	2	2
aC-CH3	8.5968	0	0	0	0	1	0
aC-CH2	9.441	3	9	3	4	3	6
CH2S	15.6689	0	2	0	0	0	0
CH2(cyc)	4.2419	5	0	8	4	15	6
CH(cyc)	4.1375	3	0	8	4	9	4
CH=C(cyc)	8.7037	1	0	0	0	1	0
NH(cyc)	14.8713	1	0	0	0	0	0
S(cyc)	13.4267	1	0	2	2	3	2
(CHn=C)cyc-CH3	1.2994	0	0	0	0	0	0
(CHn=C)cyc-CH2	1.7743	1	0	0	0	1	0
CH(CH3)CH(CH3)	1.3663	5	0	0	1	0	1
CHcyc-CH3	0.1038	0	0	2	1	0	0
CHcyc-CH2	-0.6827	1	0	2	1	5	2
AROMRINGs1s3s5	1.601	0	3	0	0	0	0
Hv, kJmol^{-1}	▨	299.1883	278.1763	425.6493	344.3883	423.1519	361.0279
MW, gmol^{-1}	▨	800.32	799.40	1171.98	951.59	1161.88	1021.72
V, cm^{3}mol^{-1}	▨	695.1333	802.8867	1214.3180	961.1769	1134.487	1043.14
δ, MPa$^{1/2}$	▨	20.66	18.53	18.67	18.86	19.26	18.54

Table 9-12. Details of SP calculations of the molecules of fraction 6

		F6M1	F6M2	F6M3	F6M4	F6M5	F6M6
groups	Hvi	C51H71NS2	C58H98S2	C79H114	C94H136S	C82H104S4	C90H125NS2
CH3	2.8768	6	9	7	12	7	9
CH2	4.8674	11	18	14	20	12	22
CH	4.4937	2	4	3	8	4	4
aCH	4.5216	7	9	13	15	12	12
aC	6.07	0	0	2	6	0	6
aC	6.2214	8	10	2	2	16	6
aC	4.1803	0	0	4	4	2	2
aC-CH3	8.5968	0	0	2	4	2	2
aC-CH2	9.441	3	5	5	5	4	6
CH2S	15.6689	1	0	0	1	1	1
CH2(cyc)	4.2419	4	4	13	5	11	6
CH(cyc)	4.1375	4	4	7	3	5	4
CH=C(cyc)	8.7037	1	0	0	0	0	1
NH(cyc)	14.8713	1	0	0	0	0	1
S(cyc)	13.4267	1	2	0	0	3	1
(CHn=C)cyc-CH3	1.2994	0	0	0	0	0	0
(CHn=C)cyc-CH2	1.7743	1	0	0	0	0	1
CH(CH3)CH(CH3)	1.3663	0	3	1	4	1	0
CHcyc-CH3	0.1038	1	1	1	0	0	0
CHcyc-CH2	-0.6827	1	1	4	1	1	2
AROMRINGs1s2s3	1.3007	0	0	1	0	0	0
AROMRINGs1s2	-0.0452	0	0	0	1	0	0
Hv, kJmol^{-1}	▨	288.6516	357.2166	363.4266	448.5806	449.3550	467.9705
MW, gmol^{-1}	▨	762.25	979.64	1063.76	1298.16	1217.97	1285.10
V, cm^{3}mol^{-1}	▨	617.9115	993.9342	1201.83	1407.003	1147.925	1174.6860
δ, MPa$^{1/2}$	▨	21.52	18.89	17.33	17.81	19.73	19.91

Table 9-13. Details of SP calculations of the molecules of fraction 7

		F7M1	F7M2	F7M3	F7M4	F7M5	F7M6
groups	Hvi	C92H131NS3	C84H108S3	C86H118	C82H115NS2	C90H120S3	C102H141NS3
CH3	2.8768	9	6	9	9	9	8
CH2	4.8674	21	15	19	21	15	19
CH	4.4937	6	1	4	2	2	3
aCH	4.5216	11	12	18	10	12	13
aC	6.07	0	0	4	0	0	0
aC	6.2214	14	16	2	10	14	12
aC	4.1803	0	0	6	2	0	4
aC-CH3	8.5968	1	1	2	0	0	1
aC-CH2	9.441	4	7	6	8	11	6
CH2S	15.6689	1	0	0	0	0	1
CH2(cyc)	4.2419	12	12	5	6	11	18
CH(cyc)	4.1375	6	6	3	4	7	8
CH=C(cyc)	8.7037	1	0	0	1	0	1
NH(cyc)	14.8713	1	0	0	1	0	1
S(cyc)	13.4267	2	3	0	2	3	2
(CHn=C)cyc-CH3	1.2994	0	0	0	0	0	0
(CHn=C)cyc-CH2	1.7743	1	0	0	1	0	1
CH(CH3)CH(CH3)	1.3663	3	0	1	0	1	1
CHcyc-CH3	0.1038	0	0	0	0	0	0
CHcyc-CH2	-0.6827	4	4	1	2	3	6
AROMRINGs1s3s5	1.601	0	0	0	0	0	1
AROMRINGs1s2s3	1.3007	0	0	1	0	0	0
AROMRINGs1s2	-0.0452	0	0	1	0	0	0
Hv, kJmol^{-1}	▨	494.9673	448.2610	400.6737	432.9843	480.0541	532.3076
MW, gmol^{-1}	▨	1347.23	1213.96	1151.86	1178.93	1298.12	1477.42
V, cm^{3}mol^{-1}	▨	1205.04	1190.177	1291.858	1060.9640	1287.7280	1341.6840
δ, MPa$^{1/2}$	▨	20.22	19.35	17.56	20.14	19.26	19.87

Table 9-14. Details of SP calculations of the molecules of fraction 8

		F8M1	F8M2	F8M3	F8M4	F8M5	F8M6
groups	Hvi	C86H112S3	C69H107NS2	C106H147NS2	C83H115NS4	C74H102N2S	C99H140N2
CH3	2.8768	8	9	8	8	6	9
CH2	4.8674	17	18	26	18	17	27
CH	4.4937	5	5	3	2	1	5
aCH	4.5216	12	6	16	9	8	14
aC	6.07	0	0	2	0	0	2
aC	6.2214	18	6	10	12	10	8
aC	4.1803	2	0	4	2	2	6
aC-CH3	8.5968	1	1	2	0	0	1
aC-CH2	9.441	3	5	6	7	4	3
CH2S	15.6689	0	0	1	2	0	0
CH2(cyc)	4.2419	12	6	12	9	11	10
CH(cyc)	4.1375	4	4	6	5	7	6
CH=CH(cyc)	8.2613	0	0	0	1	0	1
CH=C(cyc)	8.7037	0	1	1	0	2	1
NH(cyc)	14.8713	0	1	1	1	2	2
S(cyc)	13.4267	3	1	1	2	1	0
(CHn=C)cyc-CH3	1.2994	0	0	0	0	0	0
(CHn=C)cyc-CH2	1.7743	0	1	1	0	2	1
CH(CH3)CH(CH3)	1.3663	3	0	2	0	0	1
CHcyc-CH3	0.1038	0	0	0	0	0	1
CHcyc-CH2	-0.6827	2	2	4	3	3	1
AROMRINGs1s2	-0.0452	0	0	1	0	0	0
AROMRINGs1s3	-1.2584	0	0	0	0	0	1
Hv, kJmol^{-1}	▨	461.9529	347.3777	542.1706	459.2871	398.4453	493.9826
MW, gmol^{-1}	▨	1242.01	1014.73	1499.45	1255.07	1051.69	1358.19
V, cm^{3}mol^{-1}	▨	1222.6560	894.2534	1407.8940	1066.1370	841.6345	1202.5850
δ, MPa$^{1/2}$	▨	19.39	19.64	19.58	20.70	21.69	20.22

Table 9-15. Details of SP calculations of the molecules of fraction 9

		F9M1	F9M2	F9M3	F9M4	F9M5	F9M6
groups	Hvi	C117H150S2	C79H113NS3	C78H103NS3	C71H103NS3	C103H127NS3	C91H109NS2
CH3	2.8768	11	7	6	7	9	6
CH2	4.8674	16	21	13	25	16	12
CH	4.4937	5	3	3	2	2	1
aCH	4.5216	19	7	9	8	16	14
aC	6.07	4	0	0	0	2	6
aC	6.2214	10	10	14	8	16	12
aC	4.1803	8	2	2	0	2	2
aC-CH3	8.5968	3	1	1	1	1	1
aC-CH2	9.441	6	4	4	7	9	5
CH2S	15.6689	0	1	1	0	0	0
CH2(cyc)	4.2419	15	9	13	0	10	14
CH(cyc)	4.1375	7	5	5	0	6	8
CH=CH(cyc)	8.2613	1	1	1	0	0	0
CH=C(cyc)	8.7037	1	1	0	2	2	2
NH(cyc)	14.8713	0	1	1	1	1	1
S(cyc)	13.4267	2	2	2	2	3	2
(CHn=C)cyc-CH3	1.2994	0	0	0	0	1	0
(CHn=C)cyc-CH2	1.7743	1	1	0	2	1	2
CH(CH3)CH(CH3)	1.3663	3	1	2	0	1	0
CHcyc-CH3	0.1038	0	0	0	0	0	0
CHcyc-CH2	-0.6827	5	3	3	0	2	4
AROMRINGs1s2s3	1.3007	1	0	0	0	0	0
Hv, kJmol^{-1}	▨	572.1777	430.4694	430.4381	385.8515	553.3218	482.8744
MW, gmol^{-1}	▨	1620.58	1172.95	1150.86	1066.79	1475.32	1280.98
V, cm^{3}mol^{-1}	▨	1687.965	1018.359	986.9509	906.6952	1323.9150	1152.5570
δ, MPa$^{1/2}$	▨	18.37	20.50	20.82	20.56	20.40	20.42

Table 9-16. Details of SP calculations of the molecules from Fedors

	U_i, kJmol^{-1}	Vi, cm^{3}mol^{-1}	F1M1	F1M2	F1M3	F1M4	F1M5	F1M6
CH3	4.71	33.5	5	6	6	8	8	4
CH2	4.94	16.1	28	25	25	13	15	32
CH	3.43	-1.0	11	11	11	1	4	9
-NH-	8.4	4.5	0	0	0	0	1	0
-S-	14.15	12.0	0	1	0	2	0	0
-CH=	4.31	13.5	0	3	3	6	12	5
>C=	4.31	-5.5	0	5	3	12	17	8
ring	1.05	16	10	10	10	10	10	10
conjugation	1.67	-2.2	10	10	10	10	10	10
U, kJmol^{-1}	▨	▨	226.80	265.32	242.55	238.41	286.09	246.56
V, cm^{3}mol^{-1}	▨	▨	745.30	755.50	754.50	653.30	716.50	656.80
δ, MPa$^{1/2}$	▨	▨	17.44	18.74	17.93	19.10	19.98	19.38

	U_i, kJmol^{-1}	Vi, cm^{3}mol^{-1}	F2M1	F2M2	F2M3	F2M4	F2M5	F2M6
CH3	4.71	33.5	9	8	12	7	7	4
CH2	4.94	16.1	20	30	18	10	47	62
CH	3.43	-1.0	4	9	12	1	17	28
-NH-	8.4	4.5	0	1	0	0	0	0
-S-	14.15	12.0	0	2	1	1	0	0
-CH=	4.31	13.5	5	9	2	6	0	0
>C=	4.31	-5.5	8	17	5	11	0	0
ring	1.05	16	10	10	10	10	10	10
conjugation	1.67	-2.2	10	10	10	10	10	10
U, kJmol^{-1}	▨	▨	238.14	392.71	258.12	200.42	350.66	448.36
V, cm^{3}mol^{-1}	▨	▨	781.00	936.50	829.30	565.00	1112.20	1242.20
δ, MPa$^{1/2}$	▨	▨	17.46	20.48	17.64	18.83	17.76	19.00

	U_i, kJmol^{-1}	Vi, cm^{3}mol^{-1}	F3M1	F3M2	F3M3	F3M4	F3M5	F3M6
CH3	4.71	33.5	8	7	6	7	8	3
CH2	4.94	16.1	16	14	49	23	32	25
CH	3.43	-1.0	8	6	16	8	9	8
-NH-	8.4	4.5	0	1	0	1	0	0
-S-	14.15	12.0	1	1	0	0	0	0
-CH=	4.31	13.5	4	5	0	3	9	0
>C=	4.31	-5.5	8	12	0	5	14	0
ring	1.05	16	10	10	10	10	10	10
conjugation	1.67	-2.2	10	10	10	10	10	10
U, kJmol^{-1}	▨	▨	237.23	245.73	352.4	244.11	352.96	192.27
V, cm^{3}mol^{-1}	▨	▨	677.6	609.9	1111.9	752.3	956.7	633.0
δ, MPa$^{1/2}$	▨	▨	18.71	20.07	17.80	18.01	19.21	17.43

	U_i, kJmol^{-1}	Vi, cm^{3}mol^{-1}	F4M1	F4M2	F4M3	F4M4	F4M5	F4M6
CH3	4.71	33.5	5	7	8	6	7	6
CH2	4.94	16.1	27	27	23	16	25	36
CH	3.43	-1.0	10	10	3	10	6	12
-NH-	8.4	4.5	1	0	0	0	0	0
-S-	14.15	12.0	1	0	0	0	2	0
-CH=	4.31	13.5	5	5	5	6	7	7
>C=	4.31	-5.5	13	13	9	6	13	8
ring	1.05	16	10	9	3	6	7	6
conjugation	1.67	-2.2	10	10	7	6	10	8
U, kJmol^{-1}	▨	▨	318.56	304.38	236.77	209.64	315.60	331.57
V, cm^{3}mol^{-1}	▨	▨	742.7	777.2	685.9	579.4	768.0	897.5
δ, MPa$^{1/2}$	▨	▨	20.71	19.79	18.58	19.02	20.27	19.22

	U_i, kJmol^{-1}	Vi, cm^{3}mol^{-1}	F5M1	F5M2	F5M3	F5M4	F5M5	F5M6
CH3	4.71	33.5	10	8	6	9	5	10
CH2	4.94	16.1	16	23	43	26	33	29
CH	3.43	-1.0	10	3	9	7	10	8
-NH-	8.4	4.5	1	0	0	0	0	0
-S-	14.15	12.0	1	0	2	2	3	2
-CH=	4.31	13.5	8	9	9	8	13	8
>C=	4.31	-5.5	12	9	15	16	18	16
ring	1.05	16	7	3	10	8	13	8
conjugation	1.67	-2.2	10	9	12	12	16	12
U, kJmol^{-1}	▨	▨	293.24	257.35	433.83	355.02	437.3	377.98
V, cm^{3}mol^{-1}	▨	▨	731.1	735.5	1080.9	858.7	974.1	939.5
δ, MPa$^{1/2}$	▨	▨	20.03	18.71	20.03	20.33	21.19	20.06

	U_i, kJmol^{-1}	Vi, cm^{3}mol^{-1}	F6M1	F6M2	F6M3	F6M4	F6M5	F6M6
CH3	4.71	33.5	6	9	9	16	9	11
CH2	4.94	16.1	18	27	32	30	27	34
CH	3.43	-1.0	6	8	10	11	9	8
-NH-	8.4	4.5	1	0	0	0	0	1
-S-	14.15	12.0	1	2	0	0	3	1
-CH=	4.31	13.5	8	9	13	15	12	13
>C=	4.31	-5.5	12	15	13	17	22	21
ring	1.05	16	7	8	9	9	13	11
conjugation	1.67	-2.2	10	12	15	18	18	18
U, kJmol^{-1}	▨	▨	270.56	363.39	381.33	438.72	439.34	457.91
V, cm^{3}mol^{-1}	▨	▨	633.3	892.8	1021.7	1221.4	972.6	1120.8
δ, MPa$^{1/2}$	▨	▨	20.67	20.17	19.32	18.95	21.25	20.21

	U_i, kJmol^{-1}	Vi, cm^{3}mol^{-1}	F7M1	F7M2	F7M3	F7M4	F7M5	F7M6
CH3	4.71	33.5	10	7	11	9	9	9
CH2	4.94	16.1	37	34	30	35	37	43
CH	3.43	-1.0	12	7	7	6	9	11
-NH-	8.4	4.5	1	0	0	1	0	1
-S-	14.15	12.0	2	3	0	2	3	2
-CH=	4.31	13.5	12	12	18	11	12	14
>C=	4.31	-5.5	19	23	18	21	25	23
ring	1.05	16	12	13	9	10	13	14
conjugation	1.67	-2.2	16	18	19	16	18	19
U, kJmol^{-1}			480.67	461.95	420.36	447.71	501.67	535.14
V, cm^{3}mol^{-1}			1161.5	1014.8	1090.7	1045.3	1117.1	1256.0
δ, MPa$^{1/2}$			20.34	21.34	19.63	20.70	21.19	20.64

	U_i, kJmol^{-1}	Vi, cm^{3}mol^{-1}	F8M1	F8M2	F8M3	F8M4	F8M5	F8M6
CH3	4.71	33.5	9	10	10	8	6	10
CH2	4.94	16.1	32	29	44	34	32	40
CH	3.43	-1.0	9	9	9	7	8	11
-NH-	8.4	4.5	0	0	1	1	0	2
-S-	14.15	12.0	3	1	1	2	1	0
-CH=	4.31	13.5	12	7	17	9	10	15
>C=	4.31	-5.5	23	12	23	21	18	20
ring	1.05	16	13	7	13	11	11	12
conjugation	1.67	-2.2	18	10	21	16	14	19
U, kJmol^{-1}			468.35	341.32	539.00	433.92	383.54	494.41
V, cm^{3}mol^{-1}			1047.6	923.4	1315.7	983.7	901.4	1219.7
δ, MPa$^{1/2}$			21.14	19.23	20.24	21.00	20.63	20.13

	U_i, kJmol^{-1}	Vi, cm^{3}mol^{-1}	F9M1	F9M2	F9M3	F9M4	F9M5	F9M6
CH3	4.71	33.5	14	8	7	8	10	7
CH2	4.94	16.1	37	34	30	32	35	31
CH	3.43	-1.0	12	8	8	2	8	9
-NH-	8.4	4.5	0	1	1	1	1	1
-S-	14.15	12.0	2	2	2	2	3	2
-CH=	4.31	13.5	20	8	9	10	18	16
>C=	4.31	-5.5	29	17	20	17	30	27
ring	1.05	16	16	10	12	7	16	16
conjugation	1.67	-2.2	27	14	16	14	25	22
U, kJmol^{-1}			591.26	411.41	409.62	386.42	563.72	492.55
V, cm^{3}mol^{-1}			1383.8	979.6	906.3	932.4	1210.0	1028.2
δ, MPa$^{1/2}$			20.67	20.49	21.26	20.36	21.58	21.89

Table 9-17. Calculated solubility parameters [$MPa^{1/2}$] of ten fractions at 298 K (MG, Fedors, Rogel)

Fraction	Marrero-Gani, from equations [3] and [26]	Range of values Table 9-7-Table 9-15	Fedors (equation [23])	Rogel (equation [18], H/C Table 9-1)	MD simulation
F1	18.16	16.75-20.21	18.47	19.00	13.22
F2	18.54	16.36-20.37	18.46	19.21	13.23
F3	18.62	16.39-21.75	18.72	19.53	13.58
F4	19.04	17.40-20.30	19.79	19.94	13.19
F5	19.38	18.53-20.66	19.96	20.47	14.17
F6	19.41	17.33-21.72	20.12	20.89	14.08
F7	19.71	17.56-20.22	20.47	21.31	14.42
F8	19.61	19.39-21.69	20.39	21.31	14.47
F9	19.77	18.37-20.82	20.85	21.52	14.16
F10	20.59	20.06-23.24	21.07	22.98	N/A

Table 9-18. Details of SP calculations of molecules of Athabasca bitumen

		S1	S2	S3	S4	S5	S6	S7	S8
groups	Hvi	C16H22S	C48H80S	C69H75NS2	C114H121NS3	C16H30	C22H44S	C92H156S3	C215H277NS4
CH3	2.8768	3	8	3	9	3	2	5	8
CH2	4.8674	2	11	13	4	2	5	28	37
CH	4.4937	1	3	0	2	1	0	2	0
aCH	4.5216	2	2	14	24	0	0	1	27
aC fused with aro	6.0700	0	0	6	12	0	0	0	12
aC fused with nonaro	6.2214	2	2	8	10	0	0	4	22
aC	4.1803	0	0	3	7	0	0	0	6
aC-CH3	8.5968	1	0	3	1	0	0	0	0
aC-CH2	9.441	1	2	6	9	0	0	1	7
aC-CH=CH	22.7017	0	0	0	1	0	0	0	0
CH2S	15.6689	0	0	0	1	0	1	2	0
CH2(cyc)	4.2419	0	8	0	12	6	10	29	52
CH(cyc)	4.1375	0	8	0	6	4	6	17	32
CH=CH(cyc)	8.2613	0	0	2	2	0	0	0	2
CH=C(cyc)	8.7037	1	1	0	0	0	0	1	1
NH(cyc)	14.8713	0	0	1	1	0	0	0	1
S(cyc)	13.4267	1	1	2	2	0	0	1	4
(CHn=C)cyc-CH3	1.2994	0	0	0	0	0	0	1	1
(CHn=C)cyc-CH2	1.7743	1	1	0	0	0	0	0	0
(CH3)2CH	-0.1315	1	3	0	2	1	0	1	0
CH2-CHm=CHn	-0.2899	0	0	0	1	0	0	0	0
CHcyc-CH3	0.1038	0	2	0	0	1	0	2	1
CHcyc-CH2	-	0	4	0	2	1	4	9	15

	0.6827								
aC-(CHn=CHm)cyc(fused rings) (n,m in 0..1)	-2.1142	1	1	2	2	0	0	1	3
aC-aC(different rings)	-0.1492	0	0	2	3	0	0	0	4
aC-CHncyc (fused rings) (n in 0..1)	1.4617	0	0	0	2	0	0	2	8
CH multi-ring	-0.2147	0	2	0	4	2	2	6	16
aC-Scyc (fused rings)	N/A	1	1	3	3	0	0	1	6
aC-CHm-aC (diff. rings)	0.2013	0	0	1	3	0	0	0	2
aC-NHncyc (fused rings)	N/A	0	0	1	1	0	0	0	1
AROM.FUSED[2]	-2.2739	0	0	0	1	0	0	0	0
AROM.FUSED[2]s1	4.8774	0	0	0	2	0	0	0	2
AROM.FUSED[2]s1s2	N/A	1	1	0	0	0	0	0	3
AROM.FUSED[2]s2	0.0798	0	0	1	1	0	0	0	0
AROM.FUSED[2]s2s3	N/A	0	0	1	1	0	0	0	0
AROM.FUSED[2]s1s3	-4.5728	0	0	1	2	0	0	0	0
Hv, kJmol^{-1}	▨	97.8889	230.1601	386.3578	602.9089	75.8829	122.0057	452.7667	1075.7500
MW, gmol^{-1}	▨	246.41	689.22	982.48	1601.39	222.41	364.67	1358.43	3003.78
V, cm^{3}mol^{-1}	▨	226.062	735.355	830.487	1438.641	262.629	368.998	1396.69	2948.253
δ, MPa$^{1/2}$ (secondary property)	▨	20.54	17.60	21.50	20.43	16.72	18.00	17.96	19.08
δ, MPa$^{1/2}$ (primary property, Propred)	▨	19.15	18.36	20.97	23.51	16.75	17.29	21.52	N/A

Table 9-19. Details of SP calculations of molecules of Athabasca bitumen

	S9	S10	S11	S12	S13	S14	S15	S16	S17
groups	C28H42S	C129H135NS2	C11H16	C65H104S	C31H46S	C32H65	C61H106S	C84H73NS	C23H36
CH3	2	8	1	7	5	0	2	4	3
CH2	5	19	1	24	2	6	15	2	1
CH	1	1	0	2	1	0	0	0	0
aCH	2	30	3	5	1	0	0	26	3
aC fused with aro	0	18	0	6	0	0	0	16	0
aC fused with nonaro	2	8	0	0	4	0	0	6	0
aC	0	8	0	0	0	0	0	4	0
aC-CH3	2	5	2	1	0	0	0	4	1
aC-CH2	0	10	1	4	0	0	0	8	1
aC-CH	0	0	0	0	1	0	0	0	1
aC-CH=CH	0	1	0	0	0	0	0	0	0
CH2S	0	0	0	1	0	0	1	0	0
CH2(cyc)	6	0	0	5	8	18	28	0	6
CH(cyc)	4	0	0	5	6	8	18	0	4
CH=CH(cyc)	0	2	0	0	1	0	0	1	0
CH=C(cyc)	1	0	0	0	0	0	0	0	0
NH(cyc)	0	1	0	0	0	0	0	1	0
S(cyc)	1	2	0	0	1	0	0	1	0
(CHn=C)cyc-CH3	0	0	0	0	0	0	0	0	0
(CHn=C)cyc-CH2	1	0	0	0	0	0	0	0	0
(CH3)2CH	0	0	0	2	1	0	0	0	0
CH2-CHm=CHn	0	1	0	0	0	0	0	0	0
CH(CH3)CH(CH3)	0	0	0		1	0	0	0	0
CHcyc-CH3	0	0	0	0	1	0	1	0	1
CHcyc-CH2	2	0	0	3	3	4	9	0	0
CHcyc-CH	0	0	0	0	0	0	0	0	1
AROMRINGs1s2s3	0	0	1	0	0	0	0	0	1
aC-(CHn=CHm)cyc (fused rings) (n,m in 0..1)	1	2	0	0	1	0	0	1	0
aC-aC(different rings)	0	3	0	0	0	0	0	2	0
aC-CHncyc	0		0	0	2	0	0	0	0

(fused rings) (n in 0..1)									
CH multi-ring	2		0	2	2	4	8	0	2
aC-Scyc (fused rings)	1	3	0	0	1	0	0	2	0
aC-CHm-aC (diff. rings)	0	2	0	0	0	0	0	2	0
aC-NHncyc (fused rings)	0	1	0	0	0	0	0	1	0
AROM.FUSED [2]	0	2	0	0	0	0	0	0	0
AROM.FUSED [2]s1	0	0	0	0	0	0	0	2	0
AROM.FUSED [2]s1s2	1	1	0	0	0	0	0	0	0
AROM.FUSED [2]s2	0	1	0	0	0	0	0	2	0
AROM.FUSED [2]s2s3	0		0	0	0	0	0	0	0
AROM.FUSED [2]s1s3	0	2	0	0	0	0	0	0	0
Hv, kJmol^{-1}	149.5376	677.8964	60.9773	318.3192	158.2555	147.6608	278.7720	448.1807	109.8095
MW, gmol^{-1}	410.70	1763.60	148.25	917.59	450.76	440.79	871.57	1128.55	312.53
V, cm^{3}mol^{-1}	410.695	1648.806	167.687	991.998	454.997	513.931	951.362	1001.657	357.571
δ, MPa$^{1/2}$ (secondary property)	18.92	20.24	18.68	17.84	18.50	16.81	17.04	21.09	17.33
δ, MPa$^{1/2}$ (primary property, Propred)	18.85	N/A	18.29	19.11	17.26	17.55	18.73	20.99	17.84

Table 9-20. Details of SP calculations of the liquid cracked products from an archipelago molecule (one crack, Figure 3-6)

		no crack	$C1_l/C5_r$	$C1_r/C5_l$	$C2_r$	$C3_l$	$C3_r$	$C4_l$	$C4_r$
groups	Hvi	C69H75NS2	C7H16	C62H61NS2	C68H73NS2	C50H49NS	C19H28S	C51H51NS	C18H26S
CH3	2.8768	3	2	2	2	2	2	3	1
CH2	4.8674	13	5	7	13	6	6	6	6
aCH	4.5216	14		14	14	13	1	13	1
aC	6.0700	6		6	6	6	0	6	0
aC	6.2214	8		8	8	6	2	6	2
aC	4.1803	3		3	3	3	0	3	0
aC-CH3	8.5968	3		4	4	3	1	2	2
aC-CH2	9.4410	6		5	5	3	2	4	1
CH=CH (cyc)	8.2613	2		2	2	1	1	1	1
NH (cyc)	14.8713	1		1	1	1	0	1	0
S (cyc)	13.4267	2		2	2	1	1	1	1
Hv, kJmol^{-1}	▨	386.3578	41.8236	353.4324	382.6368	282.4338	112.8222	286.1548	109.1012
MW	▨	982.48	100.20	884.28	968.44	695.99	288.49	710.02	274.46
V, cm^{3}mol^{-1}	▨	830.4874	123.3006	723.9204	815.1619	564.6978	273.9682	579.7640	257.9308
δ, MPa$^{1/2}$	▨	21.50	17.86	22.02	21.60	22.27	20.07	22.12	20.33

Table 9-21. Details of SP calculations of the middle liquid cracked products from an archipelago molecule (two or three cracks, Figure 3-6)

	C1, 2/ C2, 5	C1, 3	C1, 4	C1, 5	C2, 3	C2, 4	C3, 5	C4, 5	C1, 2, 3	C1, 2, 5
groups	C61H59NS2	C43H35NS	C44H37NS	C55H47NS2	C49H47NS	C50H49NS	C12H14S	C11H12S	C43H33NS	C54H45NS2
CH3	1	1	2	1	1	2	1	0	0	0
CH2	7	0	0	1	6	6	0	0	0	1
aCH	14	13	13	14	13	13	1	1	13	14
aC	6	6	6	6	6	6	0	0	6	6
aC	8	6	6	8	6	6	2	2	6	8
aC	3	3	3	3	3	3	0	0	3	3
aC-CH3	5	4	3	5	4	3	2	3	5	6
aC-CH2	4	2	3	4	2	3	1	0	1	3
CH=CH (cyc)	2	1	1	2	1	1	1	1	1	2
NH (cyc)	1	1	1	1	1	1	0	0	1	1
S (cyc)	2	1	1	2	1	1	1	1	1	2
Hv, kJmol^{-1}	349.7114	249.5084	253.2294	320.5070	278.7128	282.4338	79.8968	76.1758	245.7874	316.786
MW	870.26	597.81	611.83	786.10	681.97	695.99	190.30	176.28	597.81	772.07
V, cm^{3}mol^{-1}	708.8402	460.7111	475.3897	619.1537	549.6885	564.6978	163.3689	148.0112	459.0777	604.3548
δ, MPa$^{1/2}$	22.13	23.16	22.97	22.66	22.42	22.27	21.77	22.31	23.02	22.81

Table 9-22. Solubility parameters of the cracked products from an archipelago molecule (Figure 3-6)

crack #	Product 1	Product 2	Product 3	Product 4	Product 5
1	17.86	22.02			
2	21.60	δ CH4			
3	22.27	20.07			
4	22.12	20.33			
5	22.02	17.86			
1, 2	17.86	22.13	δ CH4		
1, 3	17.86	23.16	20.07		
1, 4	17.86	22.97	20.33		
1, 5	17.86	22.66	17.86		
2, 3	22.42	20.07	δ CH4		
2, 4	22.27	20.33	δ CH4		
2, 5	22.13	17.86	δ CH4		
3, 4	22.27	20.33	δ CH4		
3, 5	22.27	21.77	17.86		
4, 5	22.12	22.31	17.86		
1, 2, 3	17.86	23.02	20.07	CH4	
1, 2, 4	17.86	22.27	20.33	CH4	
1, 2, 5	17.86	22.81	17.86	CH4	
1, 3, 4	17.86	23.16	20.33	CH4	
1, 3, 5	17.86	23.16	21.77	17.86	
1, 4, 5	17.86	22.97	22.31	17.86	
2, 3, 4	22.42	20.33	CH4	CH4	
2, 3, 5	22.42	21.77	17.86	CH4	
2, 4, 5	22.27	22.31	17.86	CH4	
3, 4, 5	22.27	22.31	17.86	CH4	
1, 2, 3, 4	17.86	23.02	22.31	17.86	2 CH4
1, 2, 3, 5	17.86	23.02	21.77	17.86	CH4
2, 3, 4, 5	22.42	22.31	17.86	CH4	CH4
1, 2, 4, 5	17.86	22.27	22.31	17.86	CH4
1, 3, 4, 5	17.86	23.16	22.31	17.86	2 CH4

Table 9-23. Details of SP calculations of the main cracked products from a pericondensed molecule (Figure 3-7). The SP of the smaller fragments C1-C5 and H2S are not presented; the experimental SP of n-pentane is 14.4 MPa$^{1/2}$.

cracks		**no crack**	**- C1**	**- C2**	**- C3**	**- C4**
groups	Hvi	C69H82NS3	C65H74NS2	C62H68NS2	C64H72NS3	C61H66NS2
CH3	2.8768	5	4	4	4	4
CH2	4.8674	17	15	12	13	11
aCH	4.5216	14	14	14	14	14
aC	6.07	18	18	18	18	18
aN	10.6417	1	1	1	1	1
aC-CH3	8.5968	1	2	2	2	2
aC-CH2	9.441	5	4	4	4	4
CH2S	15.6689	3	2	2	3	2
Hv, kJ/mol	▨	394.8754	365.7507	351.1485	371.6848	346.2811
MW	▨	1021.59	933.42	891.34	951.46	877.31
V, cm^3/mol	▨	843.3954	782.8261	737.1411	767.9712	721.9776
δ, MPa$^{1/2}$	▨	21.57	21.54	21.75	21.93	21.82

cracks	**- C1, 2**	**- C1, 3**	**- C1, 4**	**- C2, 3**	**- C2, 4**	**- C3, 4**
groups	C58H60NS	C60H64NS2	C57H58NS	C57H58NS2	C54H52NS	C56H56NS2
CH3	3	3	3	3	3	3
CH2	10	11	9	8	6	7
aCH	14	14	14	14	14	14
aC	18	18	18	18	18	18
aN	1	1	1	1	1	1
aC-CH3	3	3	3	3	3	3
aC-CH2	3	3	3	3	3	3
CH2S	1	2	1	2	1	2
Hv, kJ/mol	322.0238	342.5601	317.1564	327.9579	302.5542	323.0905
MW	803.17	863.28	789.14	821.20	747.06	807.18
V, cm^3/mol	676.6512	706.8500	661.3573	661.7044	615.7154	646.7425
δ, MPa$^{1/2}$	21.73	21.93	21.81	22.18	22.08	22.27

cracks		**- C1, 2, 3**	**- C1, 2, 4**	**- C1, 3, 4**	**- C2, 3, 4**	**- C1, 2, 3, 4**
groups	Hvi	C53H50NS	C50H44N	C52H48NS	C49H42NS	C45H34N
CH3	2.8768	2	2	2	2	1
CH2	4.8674	6	4	5	2	0
aCH	4.5216	14	14	14	14	14
aC	6.07	18	18	18	18	18
aN	10.6417	1	1	1	1	1
aC-CH3	8.5968	4	4	4	4	5
aC-CH2	9.441	2	2	2	2	1
CH2S	15.6689	1	0	1	1	0
Hv, kJ/mol	▨	298.8332	273.4295	293.9658	279.3636	250.2389
MW	▨	733.03	658.89	719.01	676.93	588.76
V, cm^3/mol	▨	600.5801	555.1803	585.4978	540.5119	479.2269
δ, MPa$^{1/2}$	▨	22.21	22.09	22.31	22.63	22.74

Table 9-24. Solubility parameter at 298 K from NVT MD simulation (the values for the last one or two molecules in each fraction were not calculated as the amount of these molecules are negligible)

Name	Mol%	Density, g/cm3	δ_{GC}	δ_{MD}	No. Molecule	Cell parameter, Angstrom
F1M1	30.44	0.8412	16.75	11.9866	15	22.95
F1M2	20.03	1.0338	18.86	14.2132	15	23.41
F1M3	19.8	0.8608	16.97	11.9641	15	22.99
F1M4	12.51	1.0787	20.21	13.9821	15	22.72
F1M5	12.34	1.1162	20.19	15.6708	15	24.98
F1M6	4.88	0.9449	17.81	12.7304	10	22.73
F2M1	37.1	0.9410	18.43	13.0215	10	22.06
F2M2	23.42	1.1334	20.37	15.4764	10	24.29
F2M3	17.18	0.9298	17.65	12.1948	10	22.44
F2M4	11.22	0.9904	18.95	13.0202	15	22.69
F2M5	11.1	0.8482	16.36	10.9443	15	25.56
F2M6	0.01	0.8581	16.38	N/C		
F3M1	64.8	0.9544	18.42	13.1173	15	24.45
F3M2	13.71	1.2568	21.75	13.1982	13	22.4
F3M3	8.4	0.8482	16.39	11.1532	10	25.56
F3M4	7.69	1.1698	20.41	16.7334	15	23.51
F3M5	4.7	0.9745	18.27	13.4424	10	25.43
F3M6	0.75	0.9351	17.32	N/C		
F4M1	29.7	1.1314	20.30	15.4588	10	22.64
F4M2	24.99	0.9918	18.88	13.3013	10	24.07
F4M3	16.92	0.9389	18.04	12.6266	10	22.22
F4M4	13.12	0.9559	18.05	13.2927	10	21.5
F4M5	9.49	1.0493	19.48	14.6556	10	23.35
F4M6	5.77	0.8799	17.40	12.2293	10	22.76
F5M1	40.03	1.1513	20.66	15.8845	15	24.96
F5M2	22.40	0.9957	18.53	13.8339	10	22.82
F5M3	14.20	0.9651	18.67	13.1284	10	26.23
F5M4	12.99	0.9900	18.86	13.3249	10	24.31

F5M5	10.37	1.0241	19.26	13.0607	10	25.78
F5M6	0.01	0.9795	18.54	N/C		
F6M1	44.15	1.2336	21.52	16.9751	12	22.34
F6M2	38.00	0.9856	18.89	7.0878	10	24.57
F6M3	11.16	0.8851	17.33	11.0562	10	26.11
F6M4	4.81	0.9226	17.81	11.6222	8	25.57
F6M5	1.59	1.0610	19.73	N/C		
F6M6	0.29	1.0940	19.91	N/C		
F7M1	63.77	1.1180	20.22	15.06	6	22.12
F7M2	19.08	1.0200	19.35	error		
F7M3	11.33	0.8916	17.56	11.6275	6	22.61
F7M4	3.97	1.1112	20.14	14.6118	10	25.14
F7M5	1.58	1.0081	19.26	N/C		
F7M6	0.27	1.1012	19.87	N/C		
F8M1	38.09	1.0158	19.39	13.6207	10	26.42
F8M2	33.09	1.1347	19.64	15.7243	10	23.67
F8M3	20.88	1.0650	19.58	11.3494	10	27.62
F8M4	5.74	1.1772	20.70	15.6366	10	25.23
F8M5	1.82	1.2496	21.69	N/C		
F8M6	0.38	1.1294	20.22	N/C		
F9M1	26.09	0.9601	18.37	12.2188	5	23.33
F9M2	21.11	1.1518	20.50	15.3430	8	23.03
F9M3	19.78	1.1661	20.82	15.6137	10	24.61
F9M4	17.56	1.1766	20.56	16.1617	10	23.86
F9M5	13.29	1.1144	20.40	14.1631	8	25.23
F9M6	2.17	1.1114	20.42	N/C		
F10M1	51.93	1.1519	20.56	10.447	4	26.02
F10M2	30.28	1.0987	20.06	erorr		
F10M3	14.54	1.2301	21.45	error		
F10M4	3.22	1.4529	22.98	N/C		
F10M5	0.01	1.1197	23.24	error		
F10M6	0.01	1.1332	20.07	error		

FRACTION 1

Molecule # 1

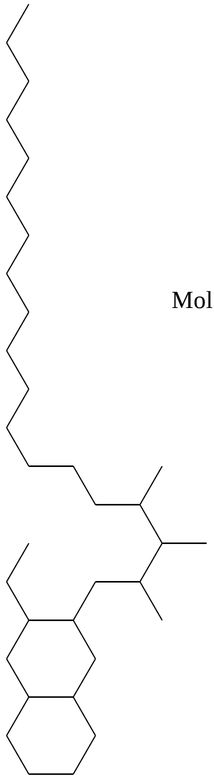

$C_{34}H_{66}$
Mol. Wt.: 474.89

Molecule # 2

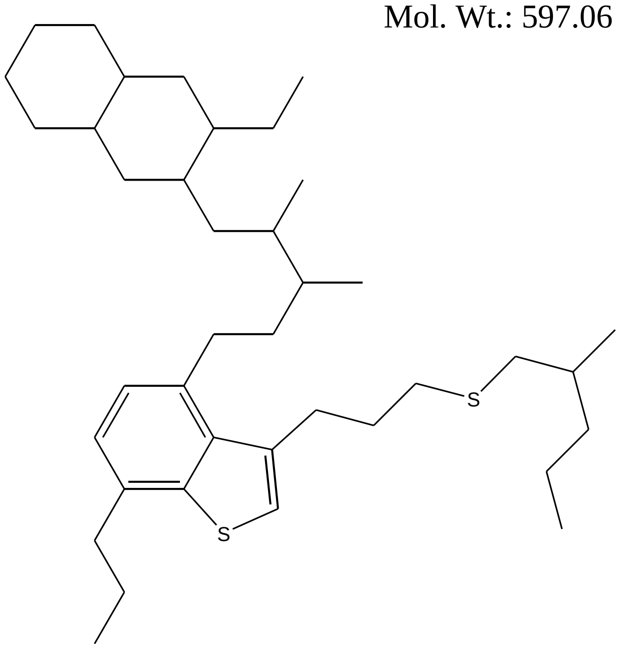

$C_{39}H_{64}S_2$
Mol. Wt.: 597.06

Molecule # 3

$C_{35}H_{60}$
Mol. Wt.: 480.85

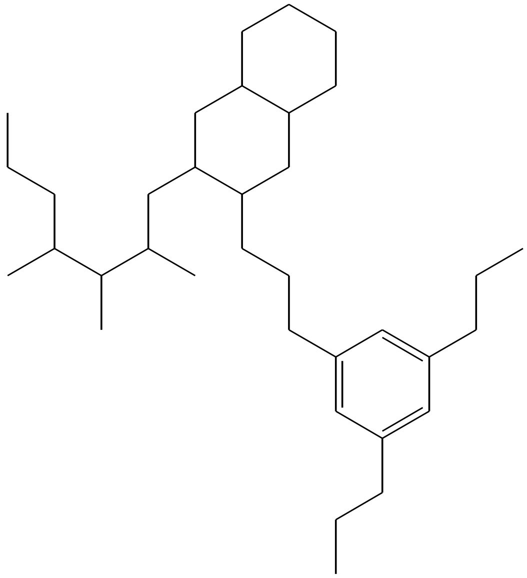

Molecule # 4

$C_{37}H_{46}S_2$
Mol. Wt.: 554.89

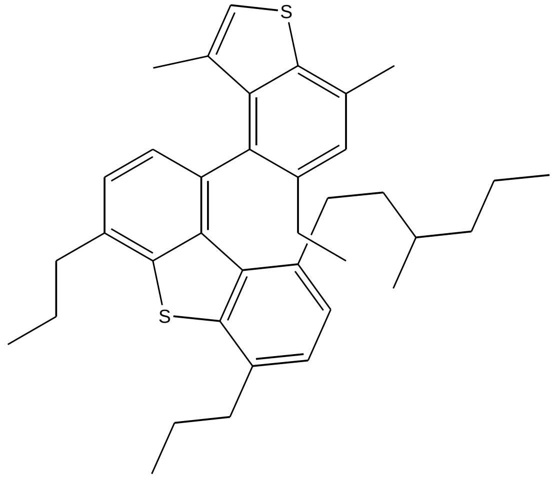

Molecule # 5

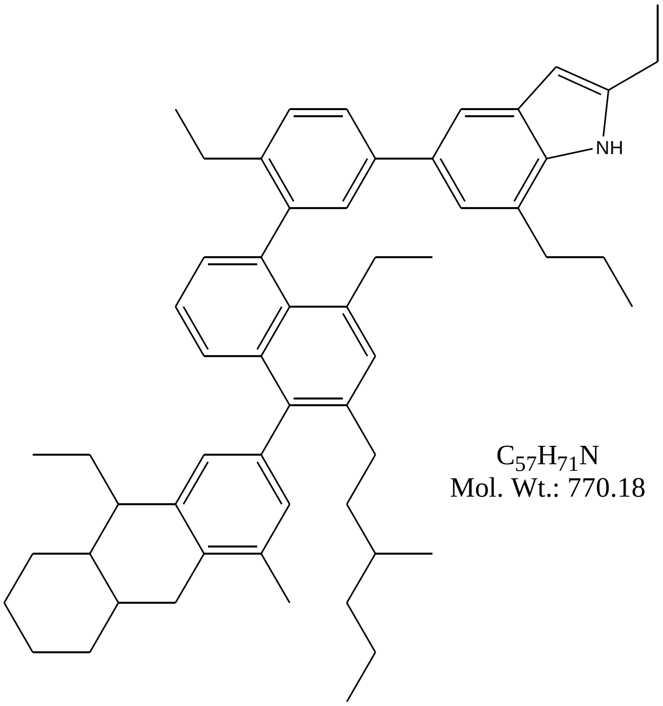

$C_{57}H_{71}N$
Mol. Wt.: 770.18

Molecule # 6

$C_{53}H_{80}S$
Mol. Wt.: 749.27

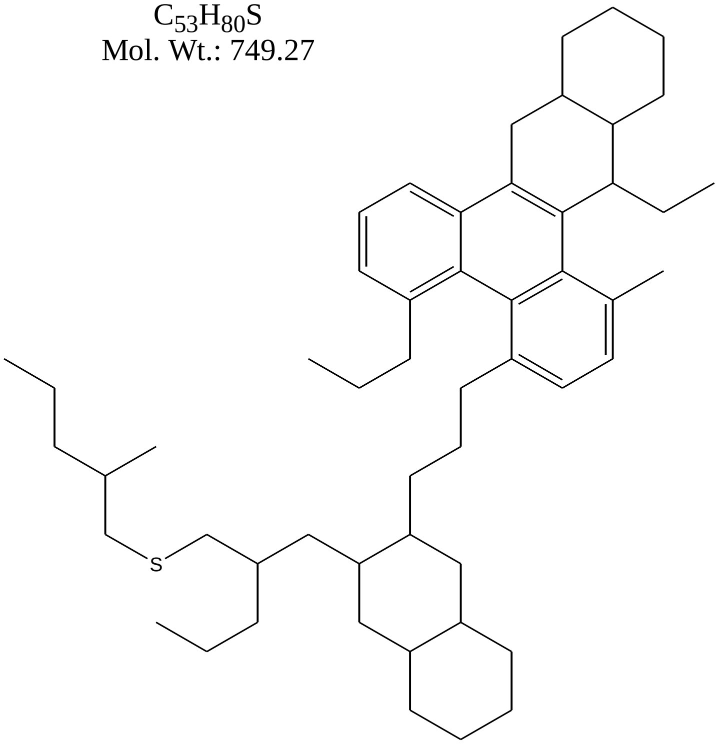

FRACTION 2

Molecule # 1

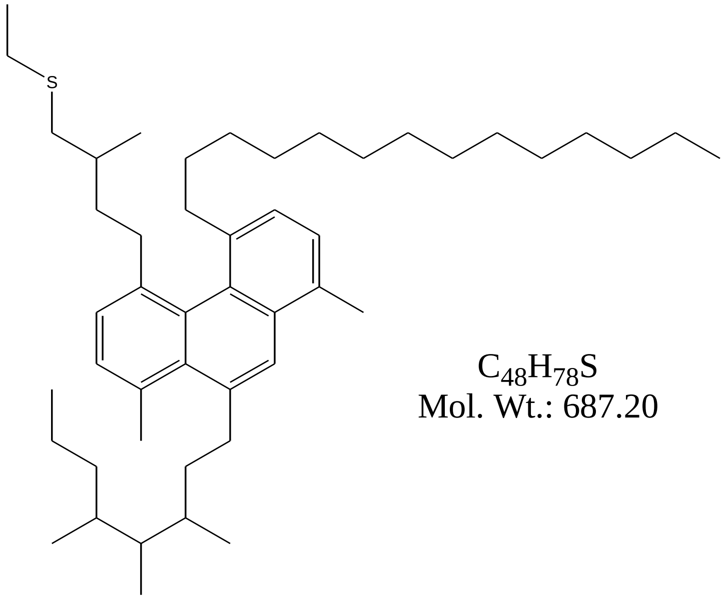

$C_{48}H_{78}S$
Mol. Wt.: 687.20

Molecule # 2

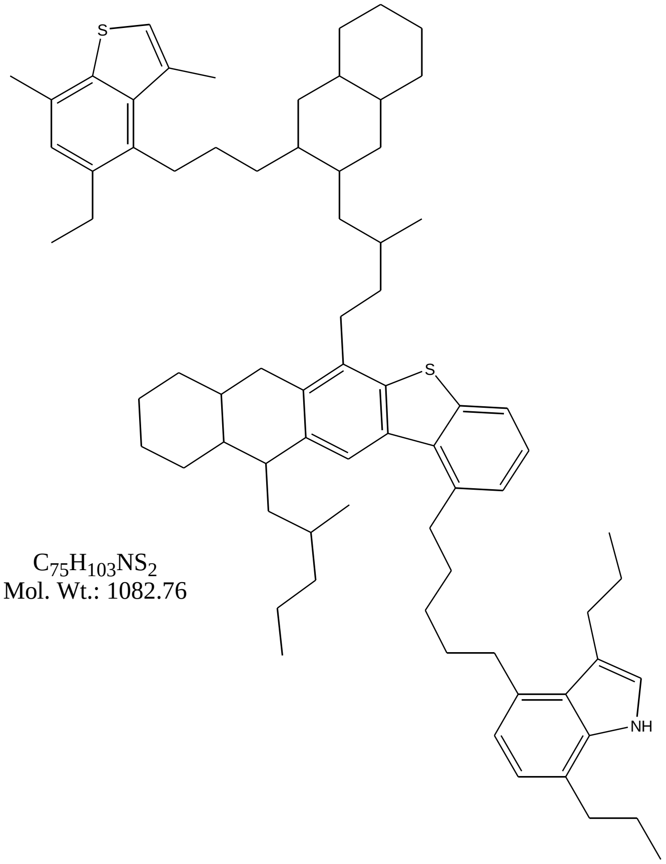

$C_{75}H_{103}NS_2$
Mol. Wt.: 1082.76

Molecule # 3

$C_{50}H_{86}S$
Mol. Wt.: 719.28

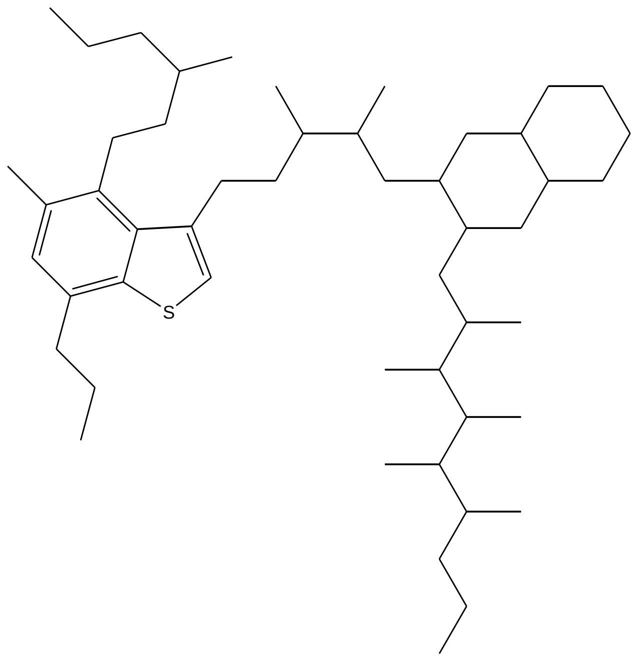

Molecule # 4

$C_{36}H_{48}S$
Mol. Wt.: 512.83

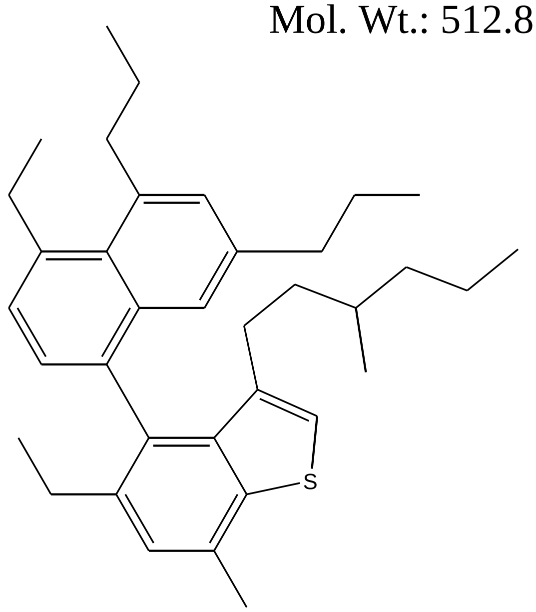

Molecule # 5

$C_{71}H_{132}$
Mol. Wt.: 985.81

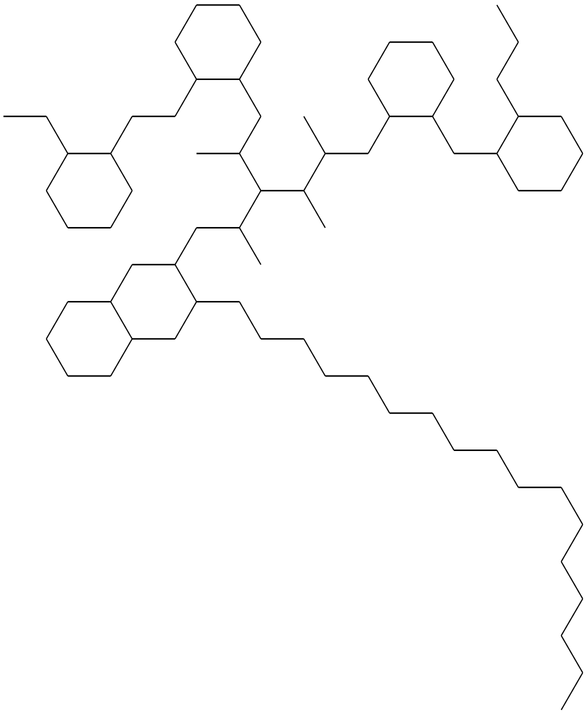

Molecule # 6

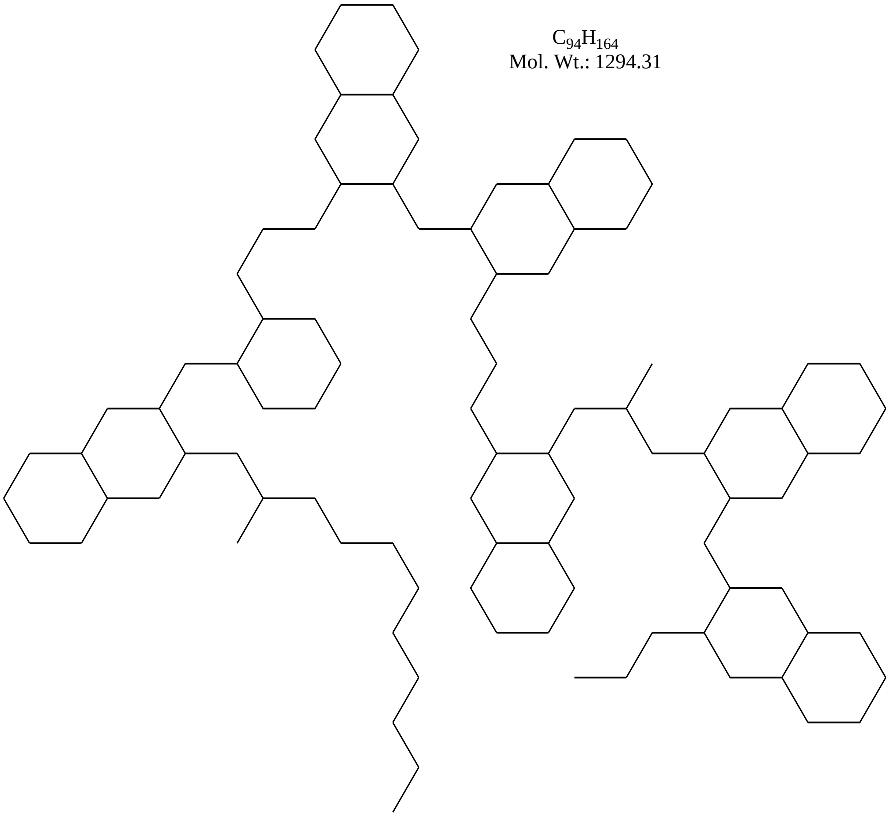

$C_{94}H_{164}$
Mol. Wt.: 1294.31

FRACTION 3

Molecule #1

$C_{44}H_{68}S$
Mol. Wt.: 629.08

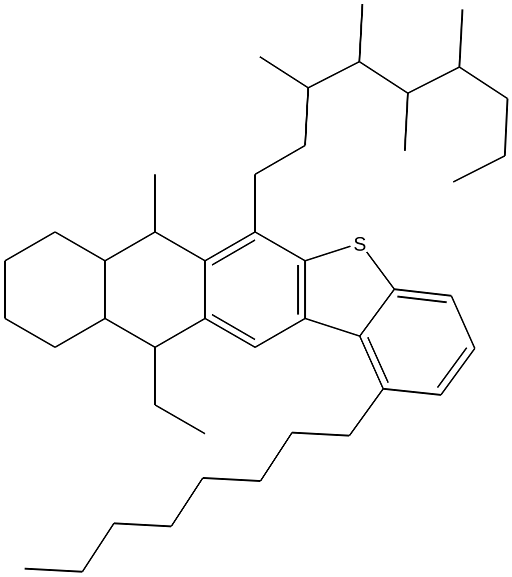

Molecule # 2

$C_{48}H_{65}NS_2$
Mol. Wt.: 720.17

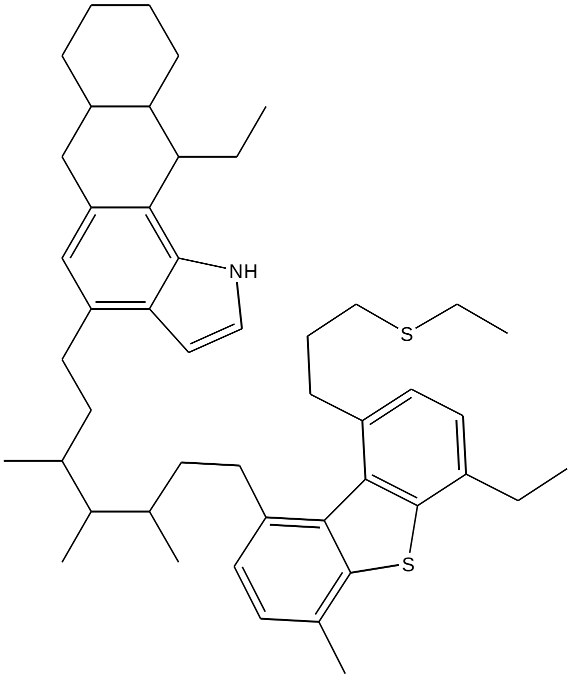

Molecule #3

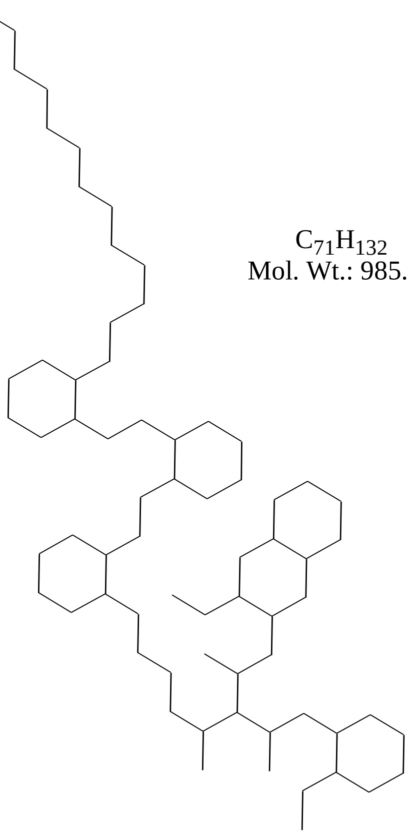

$C_{71}H_{132}$
Mol. Wt.: 985.81

Molecule #4

$C_{47}H_{81}NS$
Mol. Wt.: 692.22

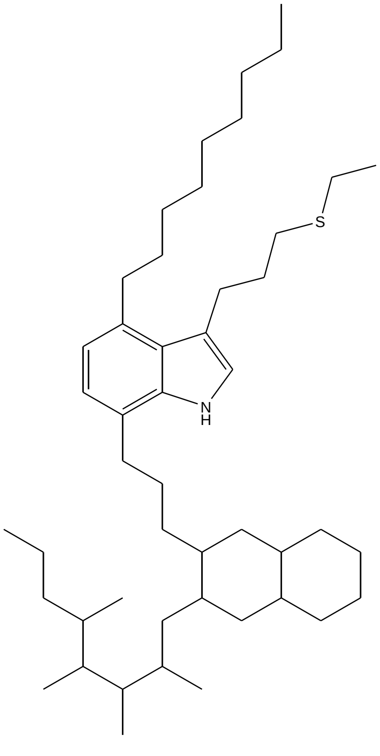

Molecule #5

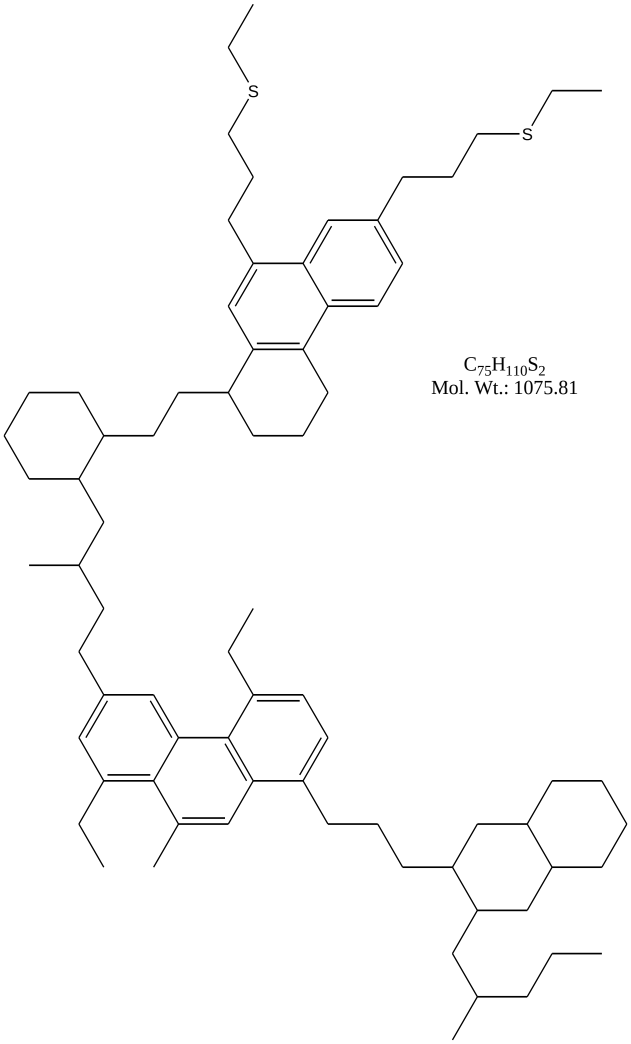

$C_{75}H_{110}S_2$
Mol. Wt.: 1075.81

Molecule # 6

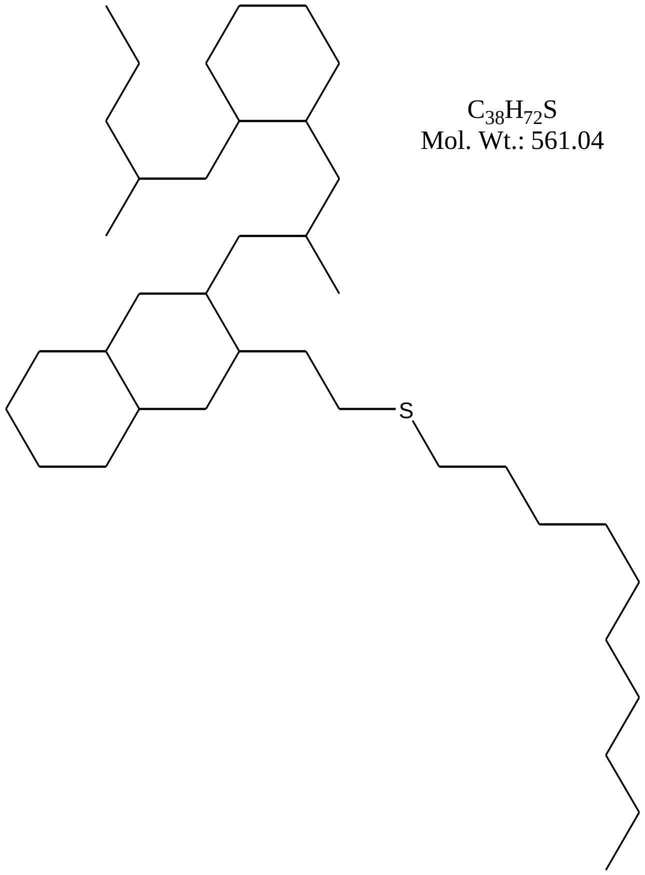

$C_{38}H_{72}S$
Mol. Wt.: 561.04

FRACTION 4

Molecule #1

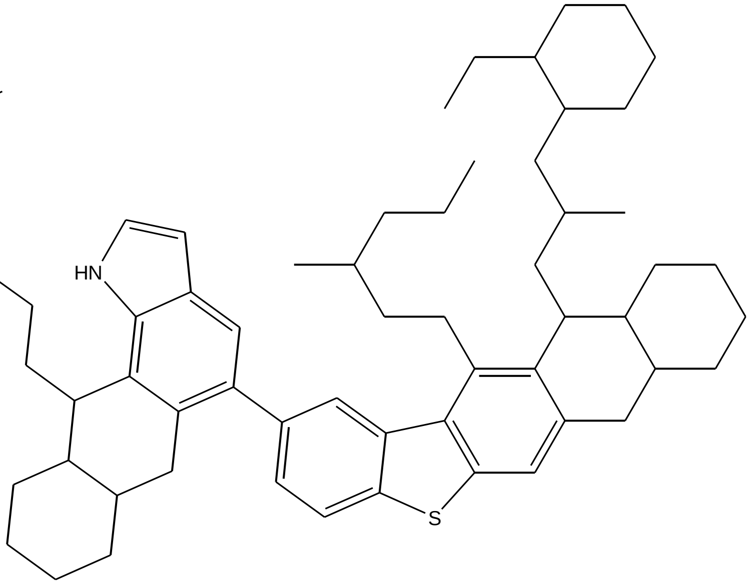

$C_{62}H_{87}NS$
Mol. Wt.: 878.43

Molecule # 2

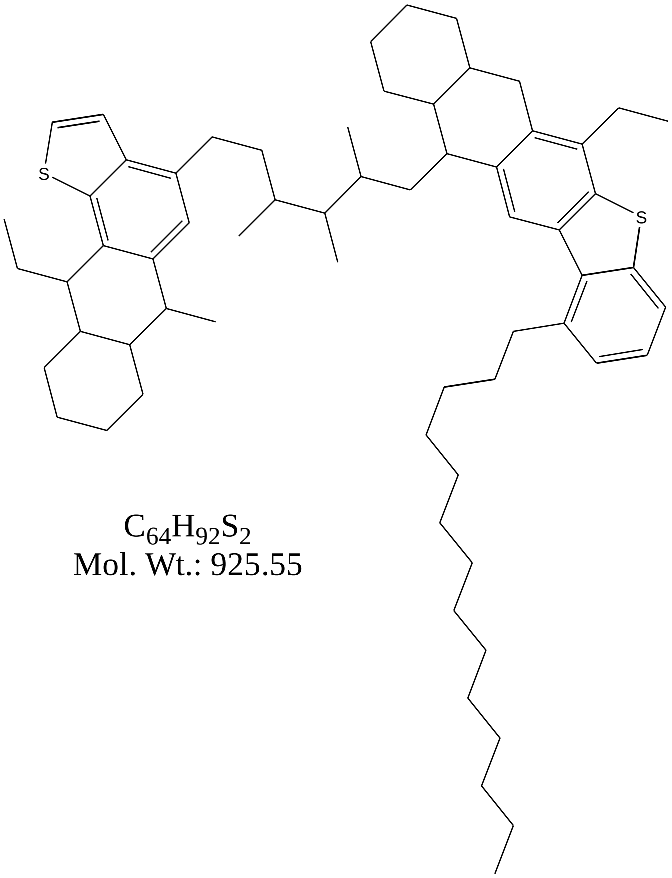

$C_{64}H_{92}S_2$
Mol. Wt.: 925.55

Molecule # 3

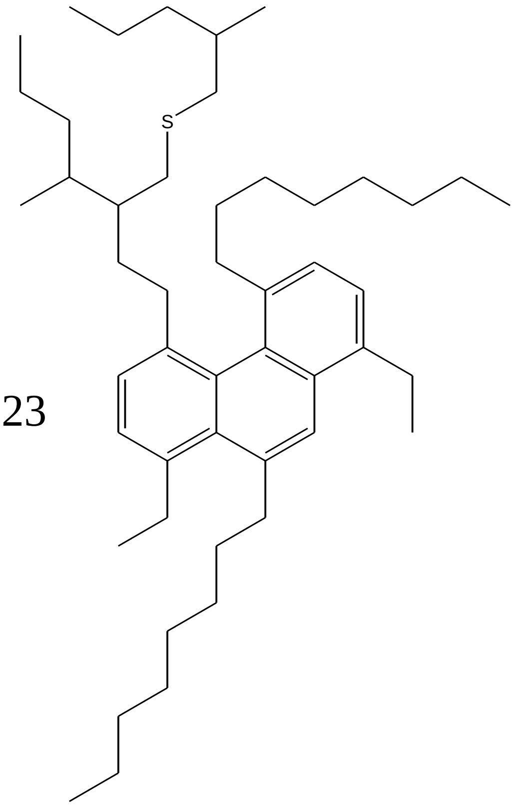

$C_{49}H_{80}S$
Mol. Wt.: 701.23

Molecule #4

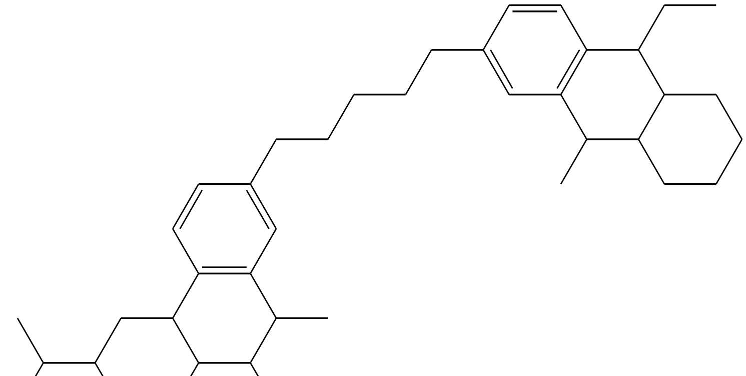

$C_{45}H_{68}S$
Mol. Wt.: 641.09

Molecule #5

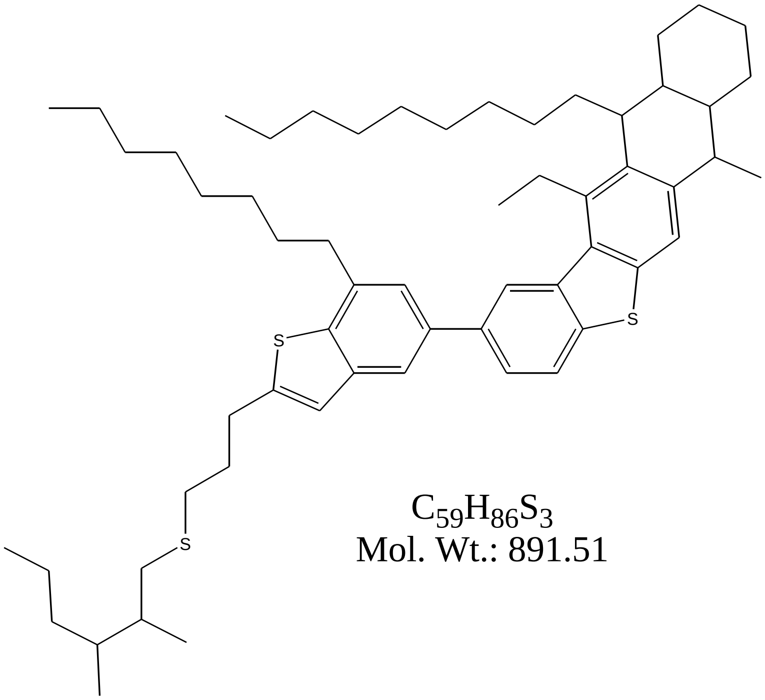

$C_{59}H_{86}S_3$
Mol. Wt.: 891.51

Molecule #6

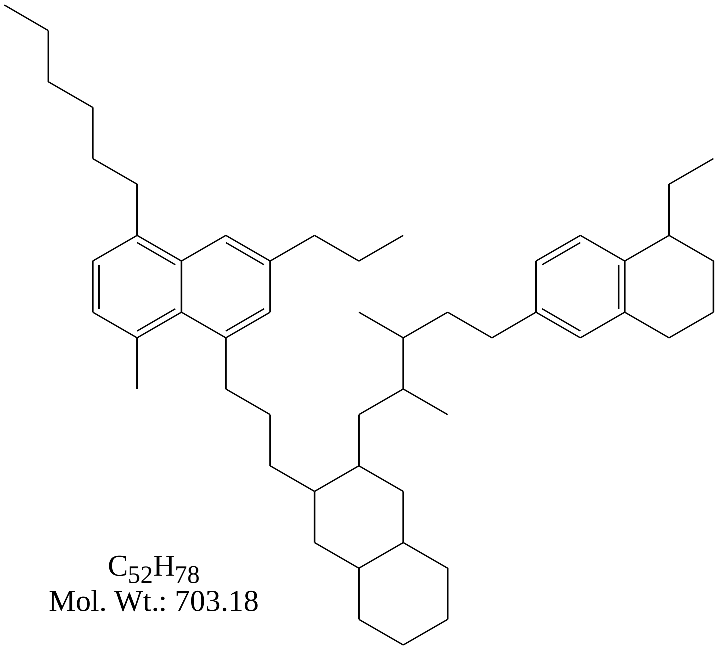

$C_{52}H_{78}$
Mol. Wt.: 703.18

FRACTION 5

Molecule # 1

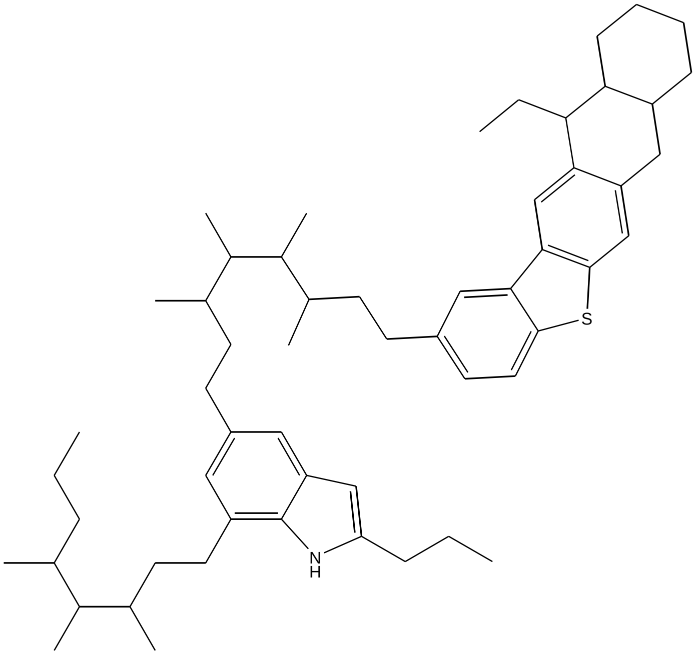

$C_{56}H_{81}NS$
Mol. Wt.: 800.32

Molecule #2

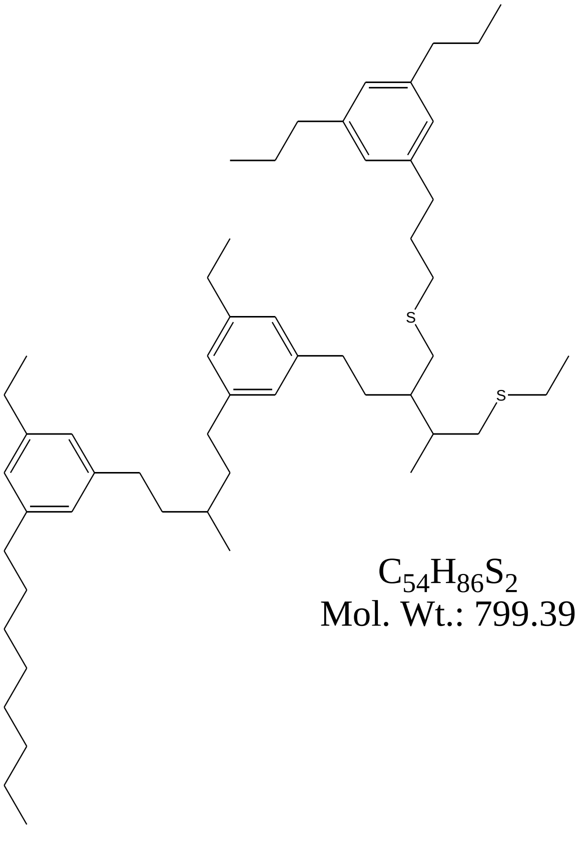

$C_{54}H_{86}S_2$
Mol. Wt.: 799.39

Molecule #3

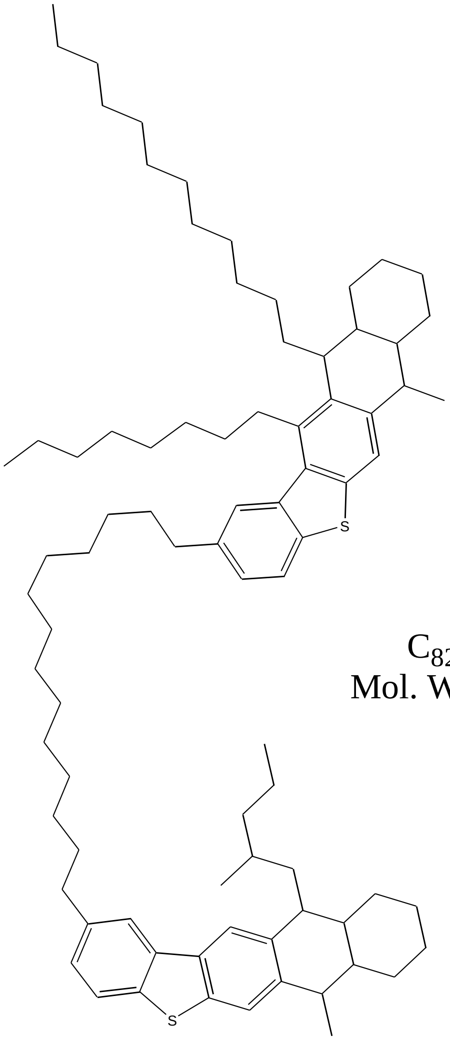

$C_{82}H_{122}S_2$
Mol. Wt.: 1171.98

Molecule # 4

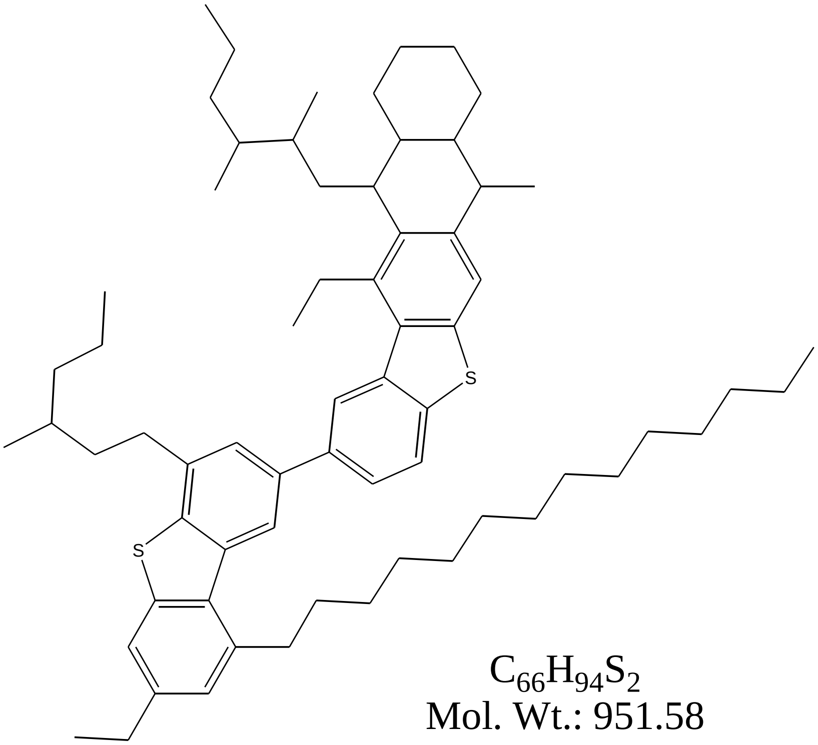

$C_{66}H_{94}S_2$
Mol. Wt.: 951.58

Molecule # 5

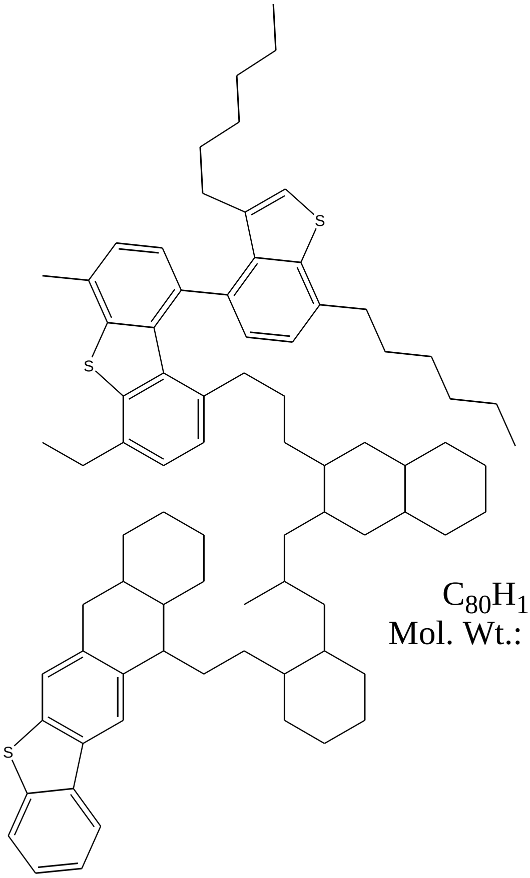

$C_{80}H_{104}S_3$
Mol. Wt.: 1161.88

Molecule # 6

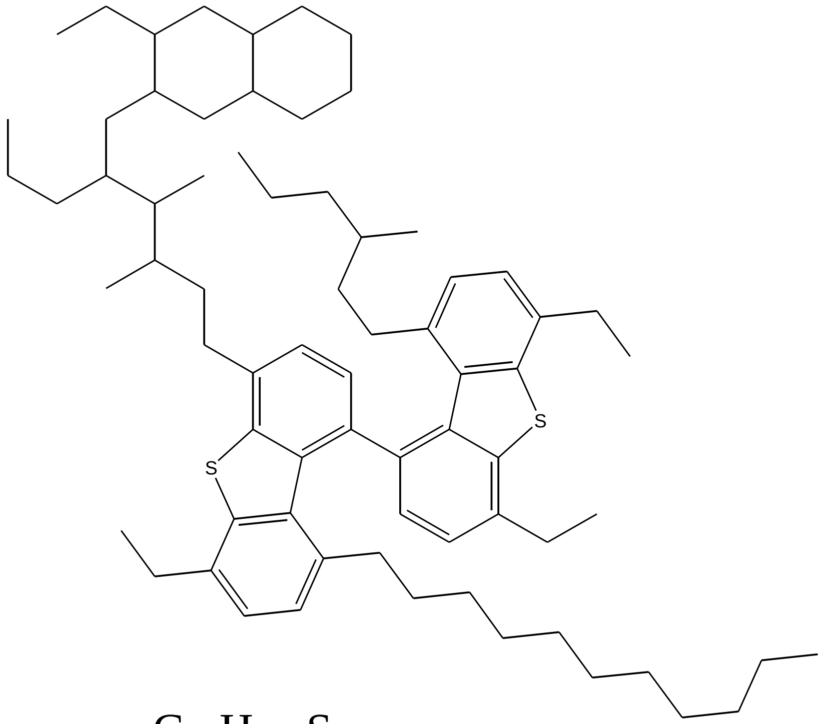

$C_{71}H_{104}S_2$
Mol. Wt.: 1021.72

FRACTION 6

Molecule # 1

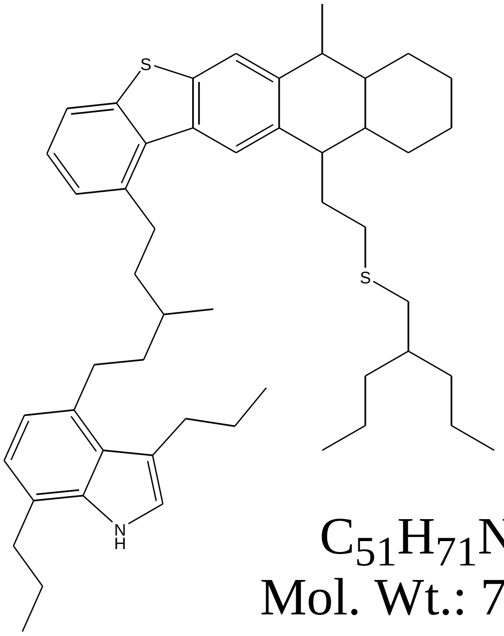

$C_{51}H_{71}NS_2$
Mol. Wt.: 762.25

Molecule # 2

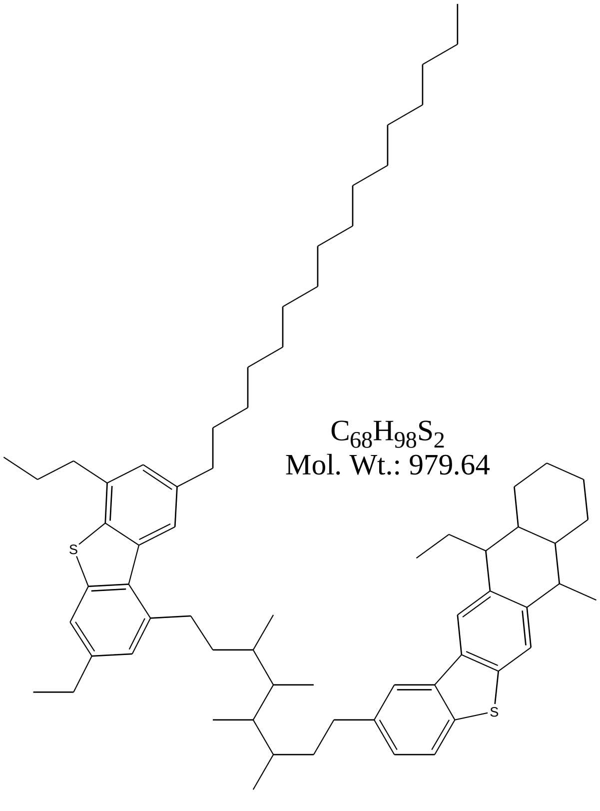

$C_{68}H_{98}S_2$
Mol. Wt.: 979.64

Molecule # 3

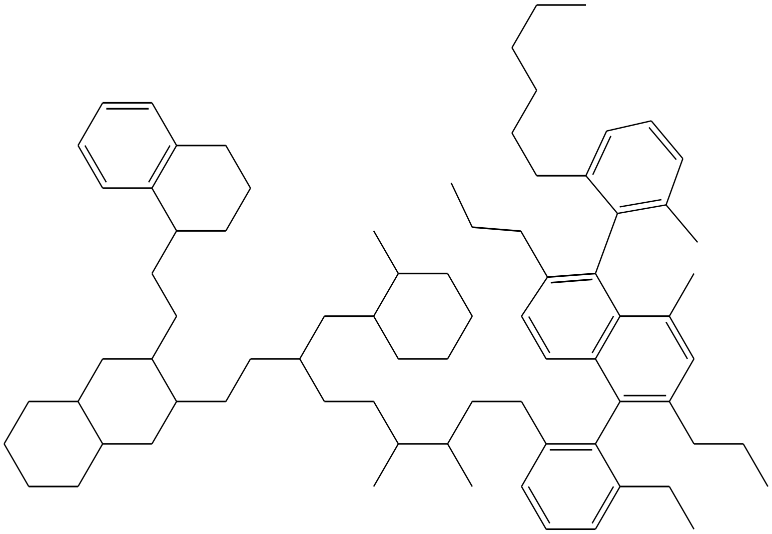

$C_{79}H_{114}$
Mol. Wt.: 1063.75

Molecule # 4

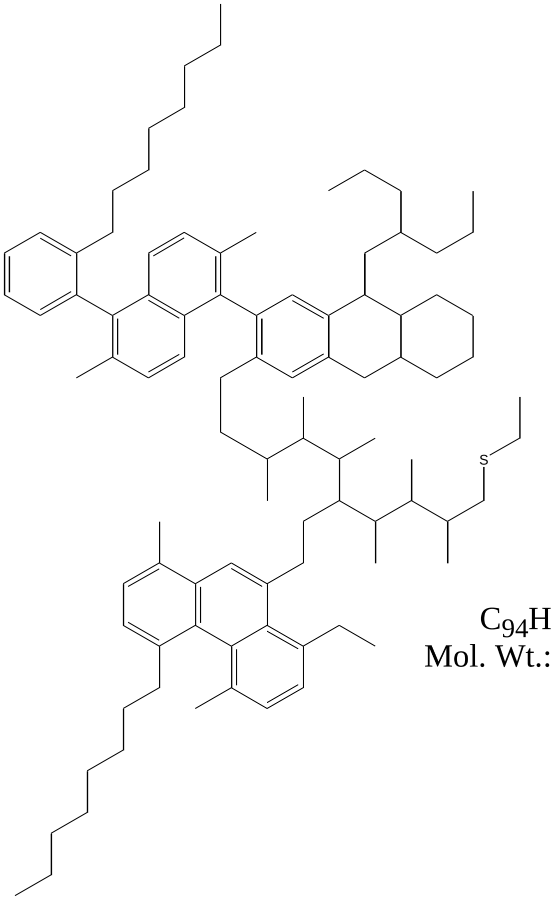

$C_{94}H_{136}S$
Mol. Wt.: 1298.15

Molecule # 5

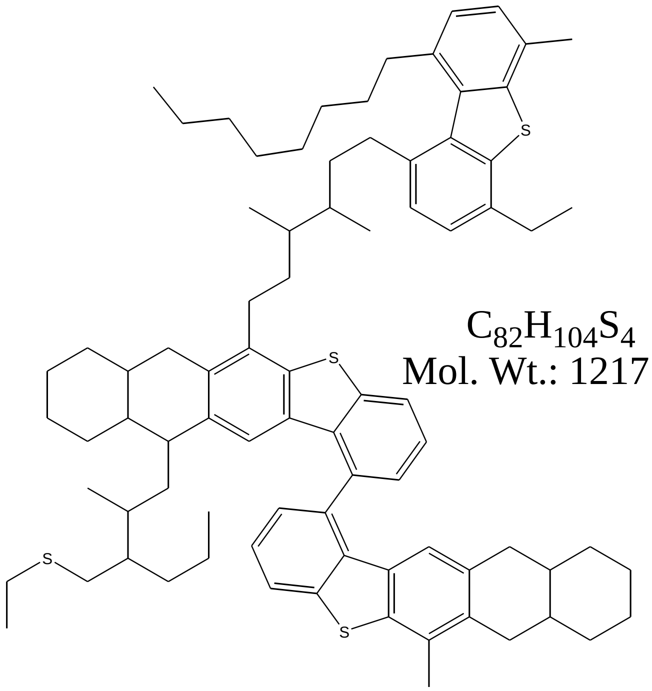

$C_{82}H_{104}S_4$
Mol. Wt.: 1217.97

Molecule # 6

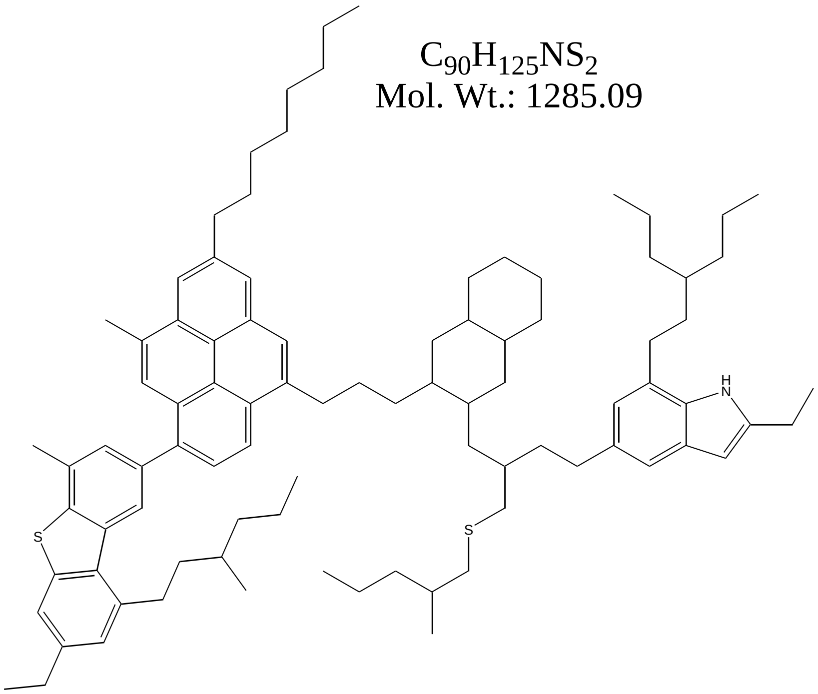

$C_{90}H_{125}NS_2$
Mol. Wt.: 1285.09

FRACTION 7

Molecule #1

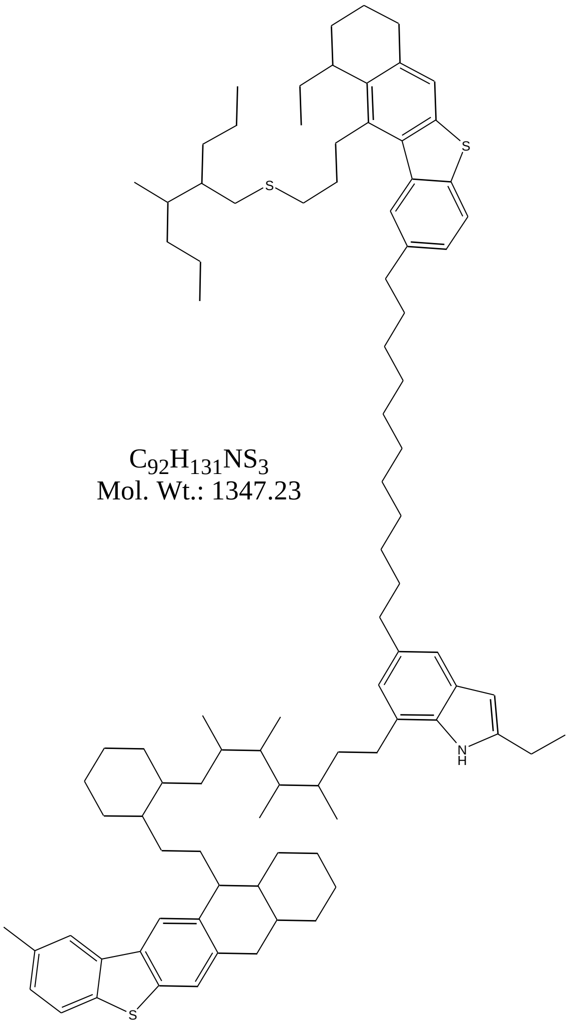

$C_{92}H_{131}NS_3$
Mol. Wt.: 1347.23

Molecule # 2

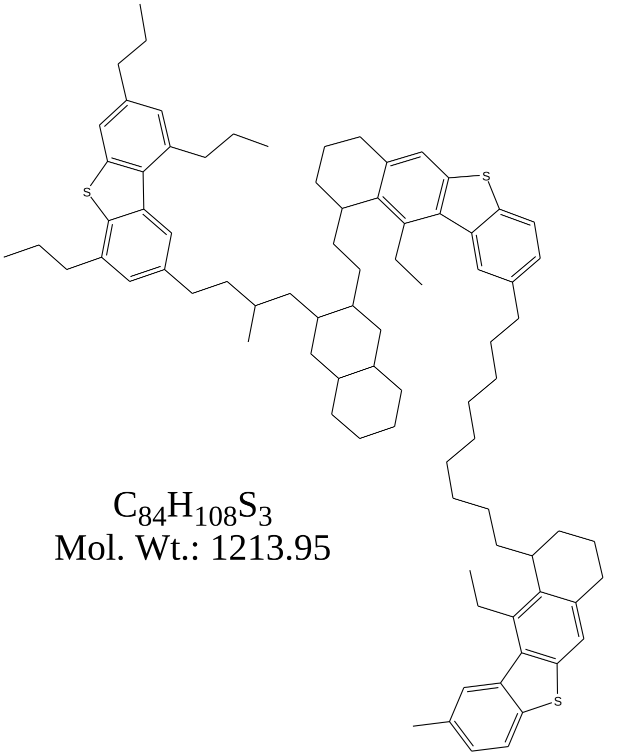

$C_{84}H_{108}S_3$
Mol. Wt.: 1213.95

Molecule #3

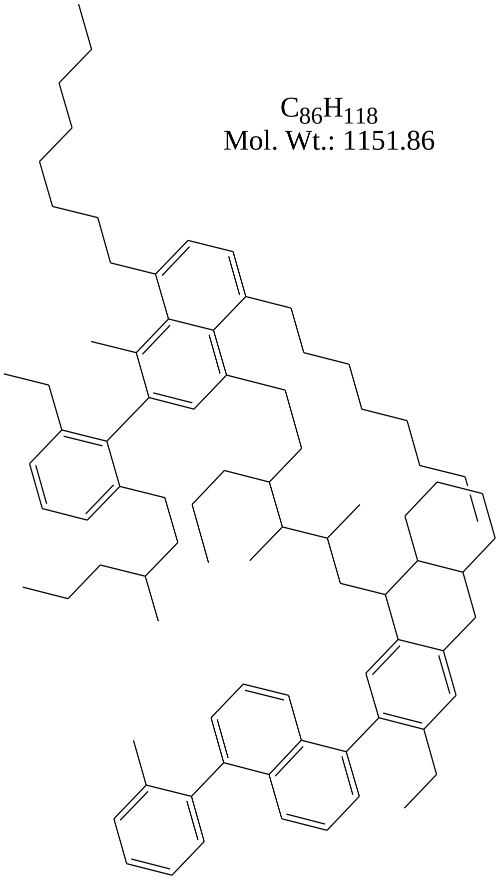

$C_{86}H_{118}$
Mol. Wt.: 1151.86

Molecule # 4

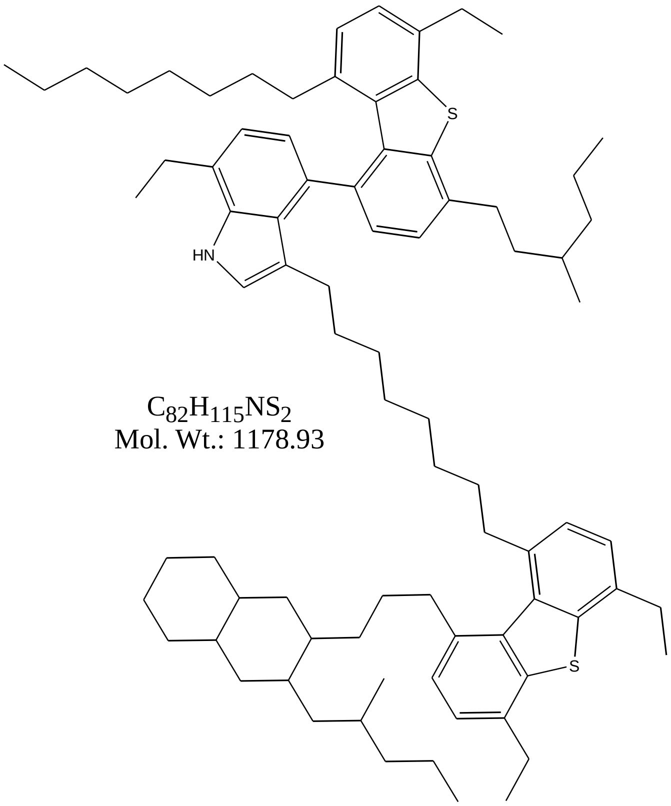

$C_{82}H_{115}NS_2$
Mol. Wt.: 1178.93

Molecule # 5

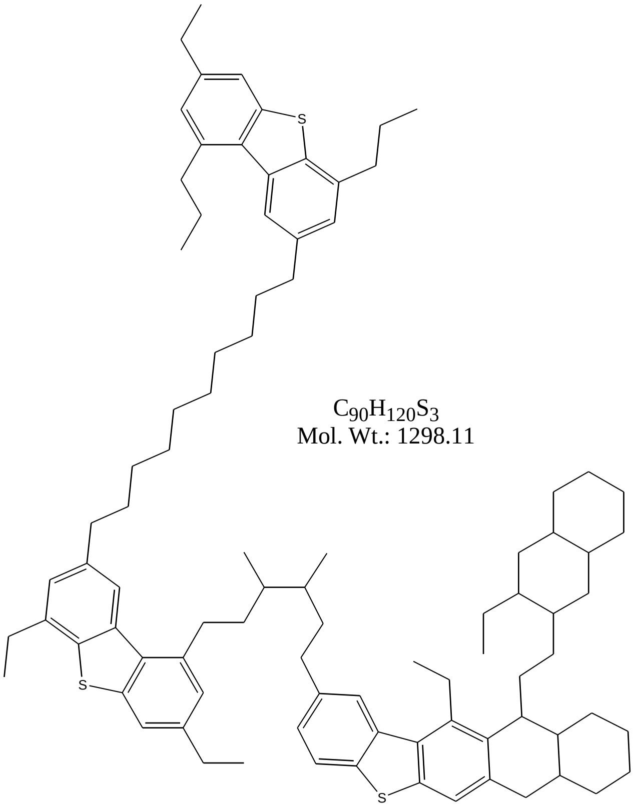

$C_{90}H_{120}S_3$
Mol. Wt.: 1298.11

Molecule # 6

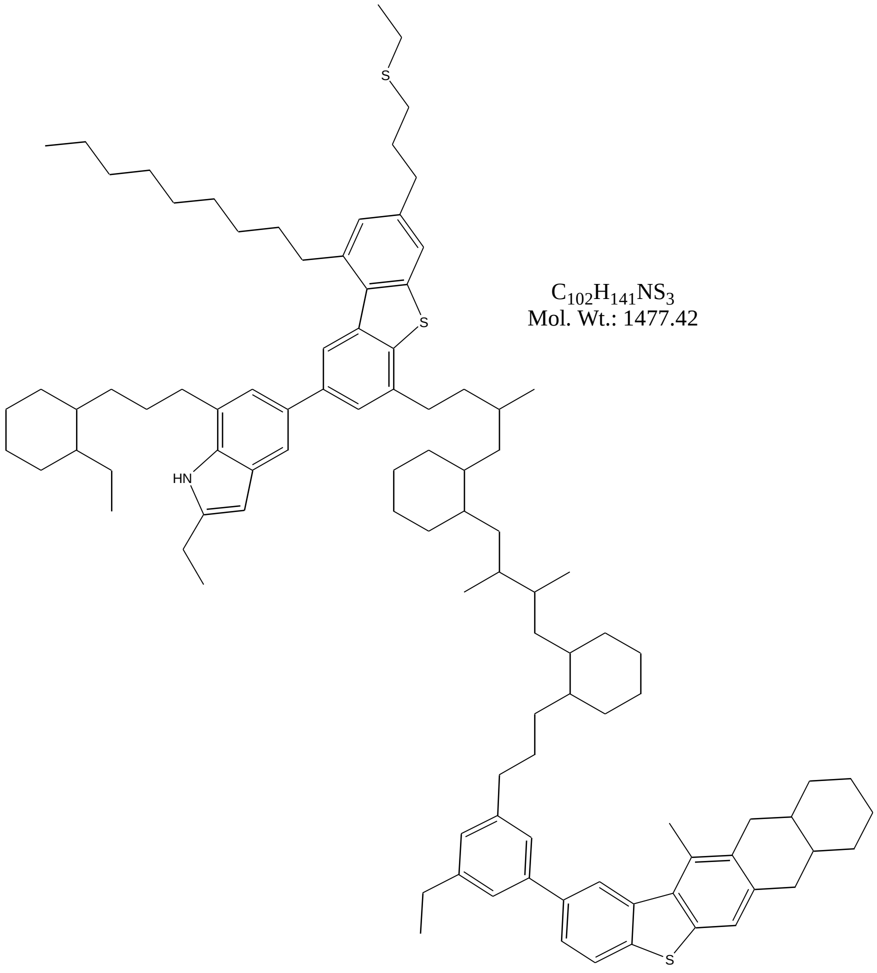

$C_{102}H_{141}NS_3$
Mol. Wt.: 1477.42

FRACTION 8

Molecule #1

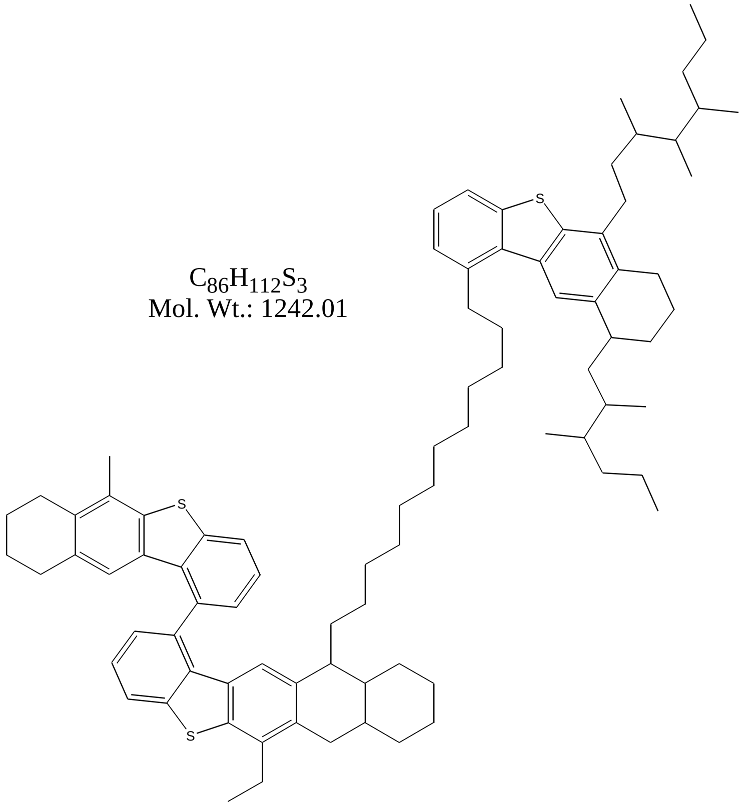

$C_{86}H_{112}S_3$
Mol. Wt.: 1242.01

Molecule #2

$C_{69}H_{107}NS_2$
Mol. Wt.: 1014.73

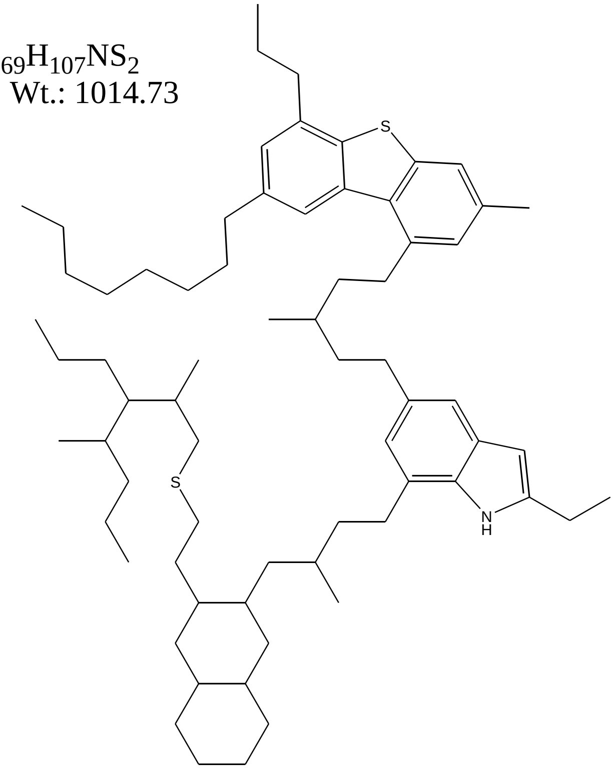

Molecule # 3

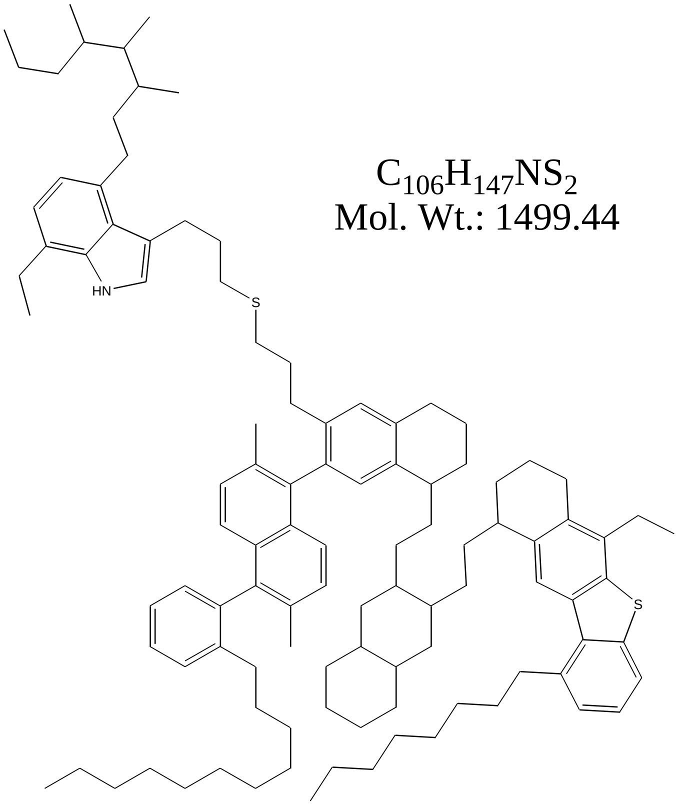

$C_{106}H_{147}NS_2$
Mol. Wt.: 1499.44

Molecule # 4

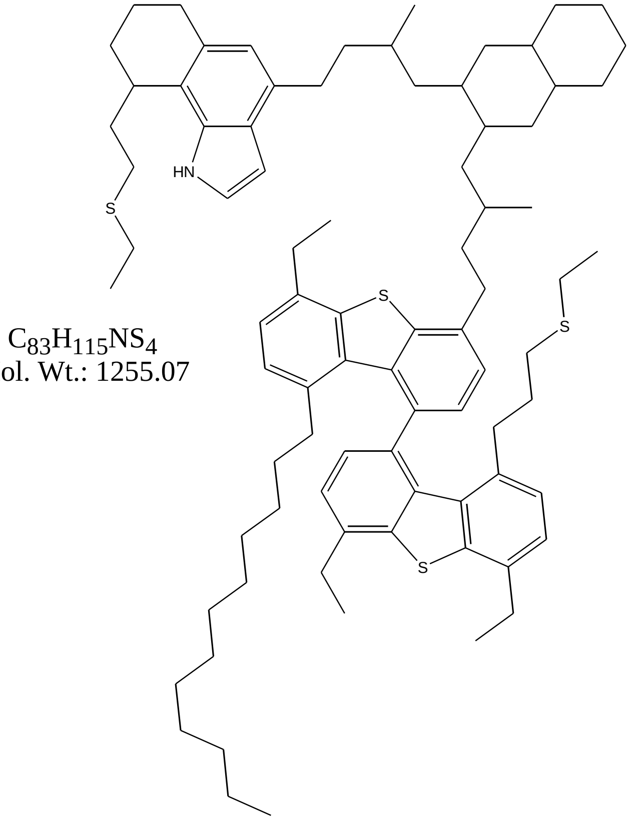

$C_{83}H_{115}NS_4$
Mol. Wt.: 1255.07

Molecule # 5

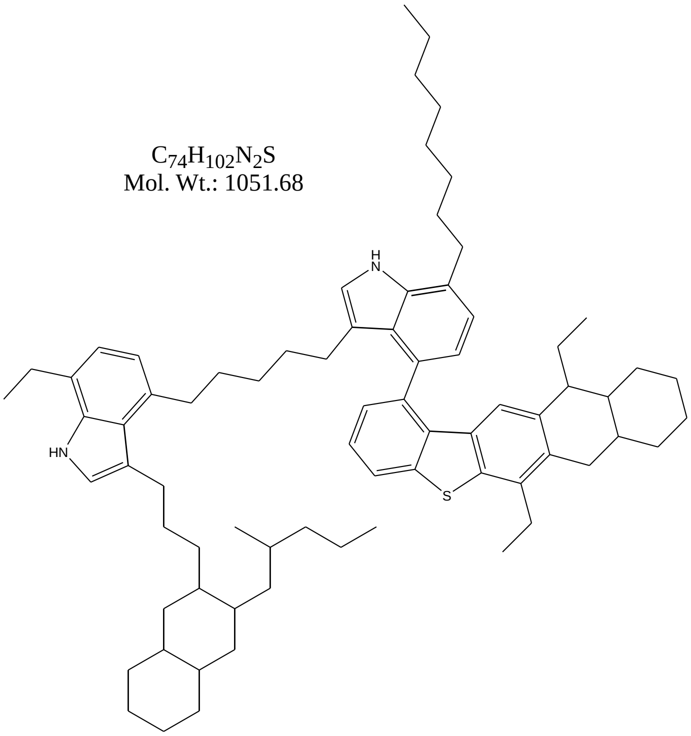

$C_{74}H_{102}N_2S$
Mol. Wt.: 1051.68

Molecule # 6

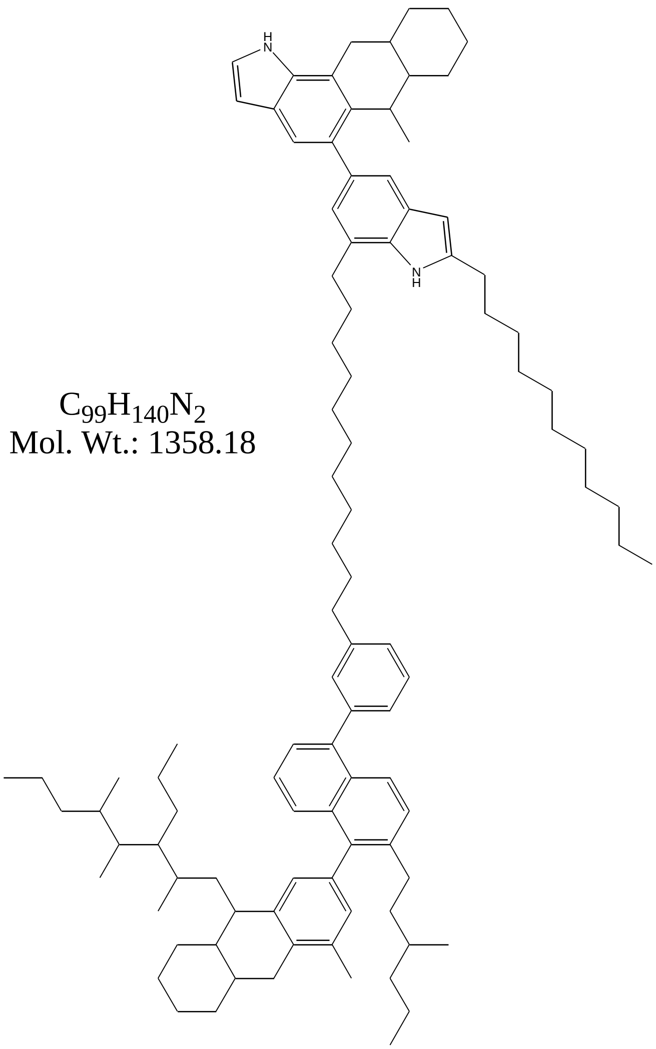

$C_{99}H_{140}N_2$
Mol. Wt.: 1358.18

FRACTION 9

Molecule #1

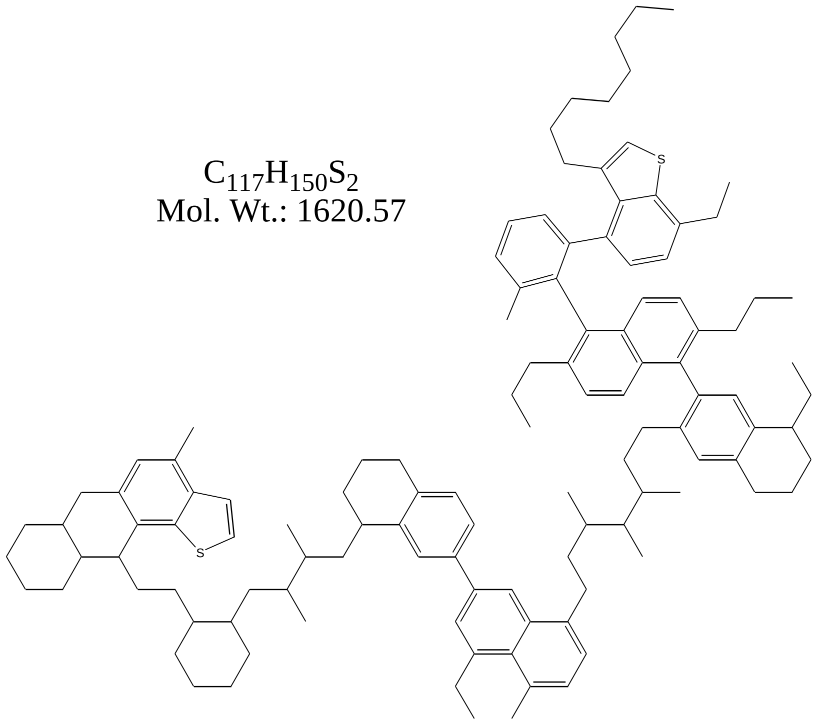

$C_{117}H_{150}S_2$
Mol. Wt.: 1620.57

Molecule #2

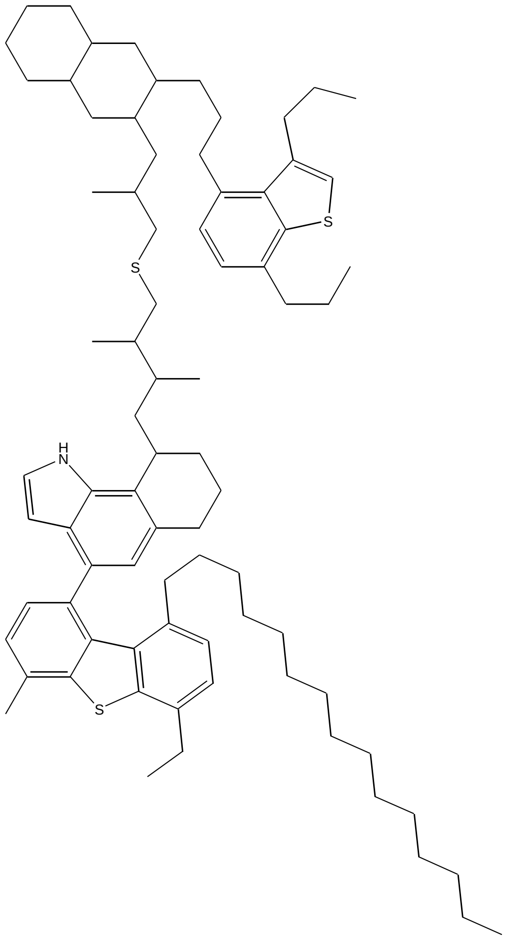

$C_{79}H_{113}NS_3$
Mol. Wt.: 1172.95

Molecule #3

$C_{78}H_{103}NS_3$
Mol. Wt.: 1150.86

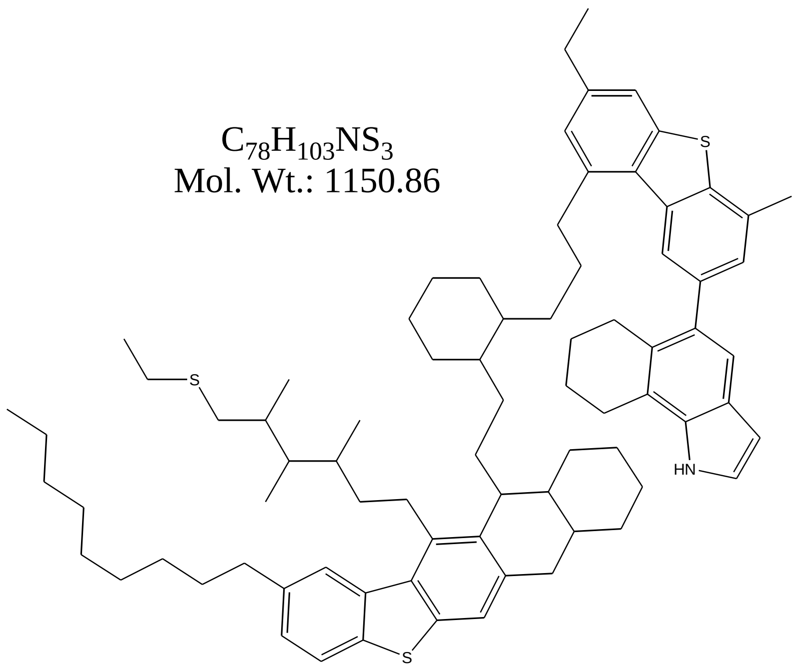

Molecule #4

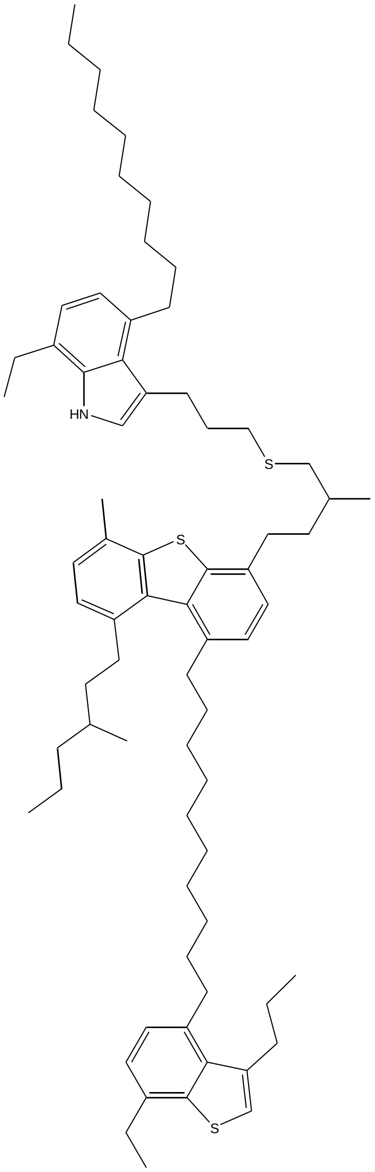

$C_{71}H_{103}NS_3$
Mol. Wt.: 1066.78

Molecule #5

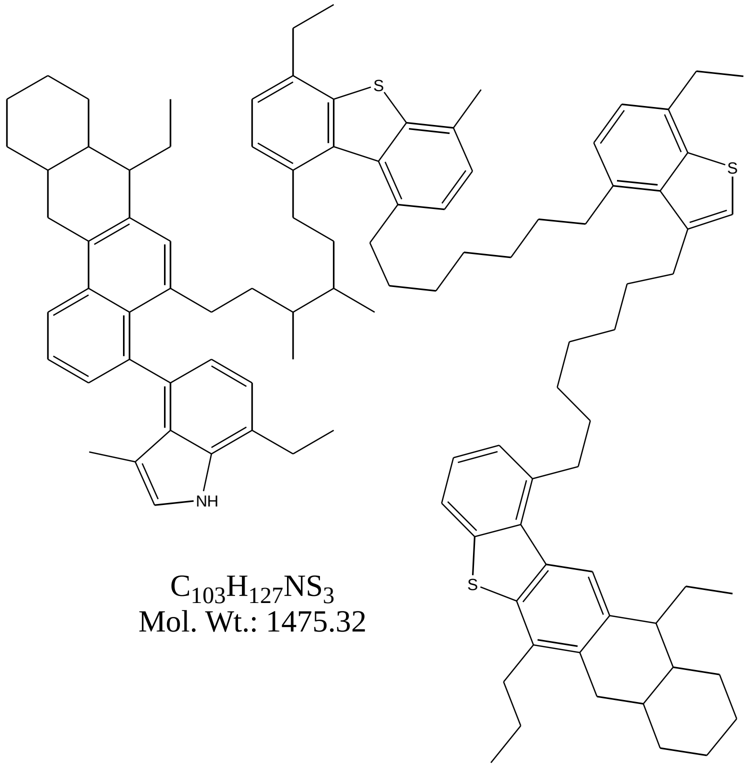

$C_{103}H_{127}NS_3$
Mol. Wt.: 1475.32

Molecule #6

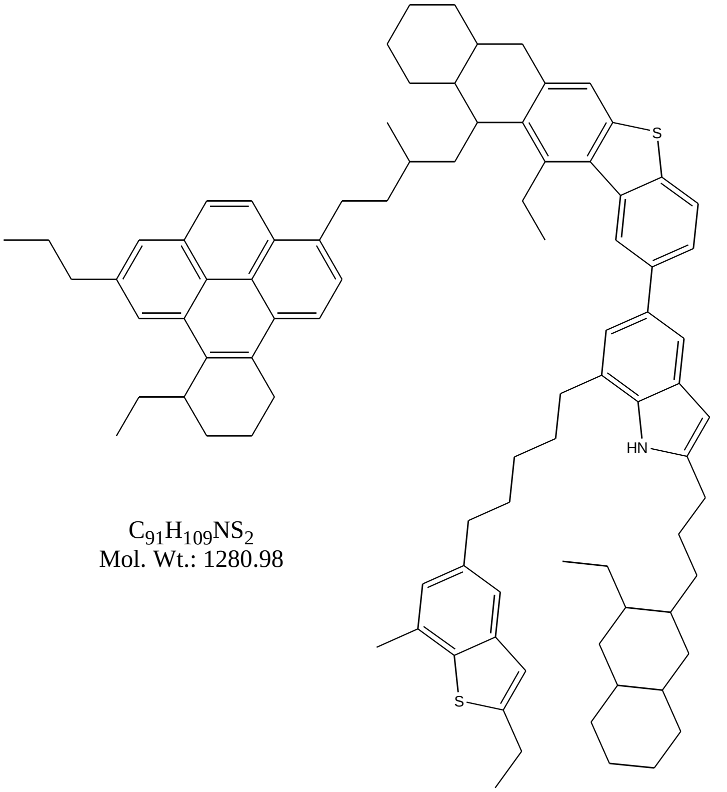

$C_{91}H_{109}NS_2$
Mol. Wt.: 1280.98

FRACTION 10

Molecule #1

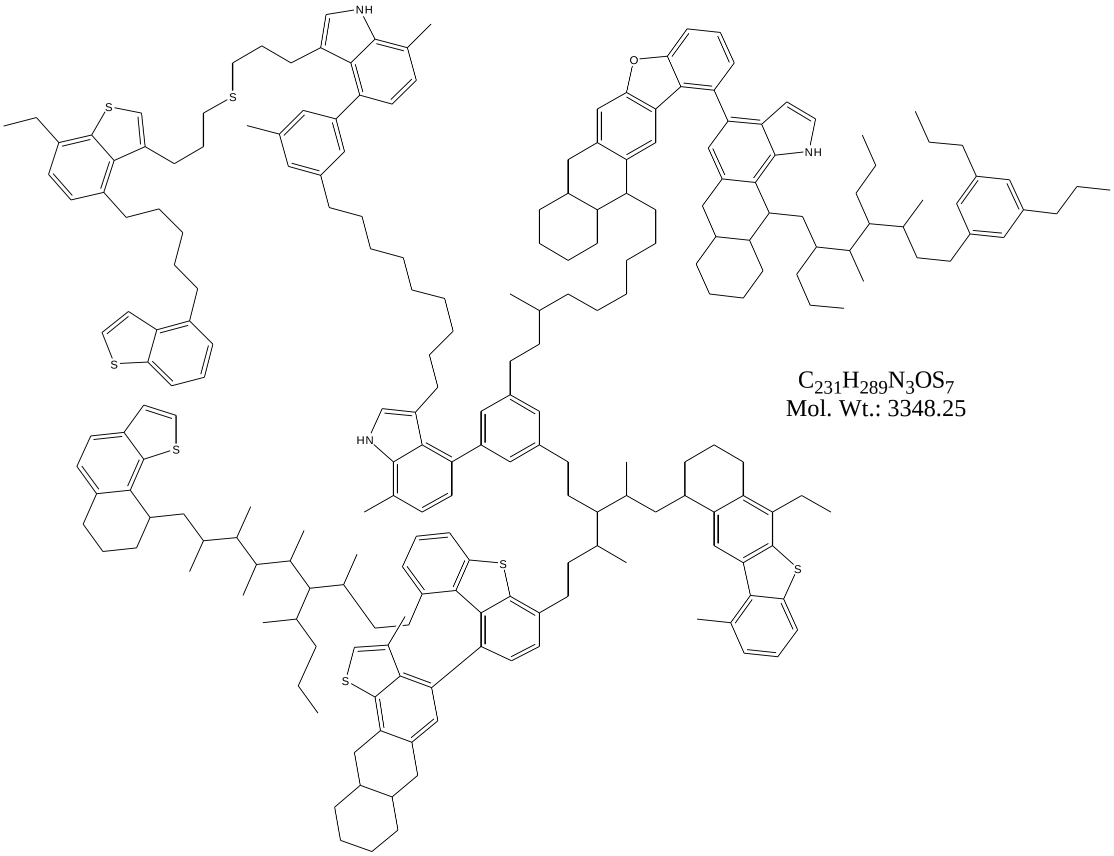

$C_{231}H_{289}N_3OS_7$
Mol. Wt.: 3348.25

Molecule # 2

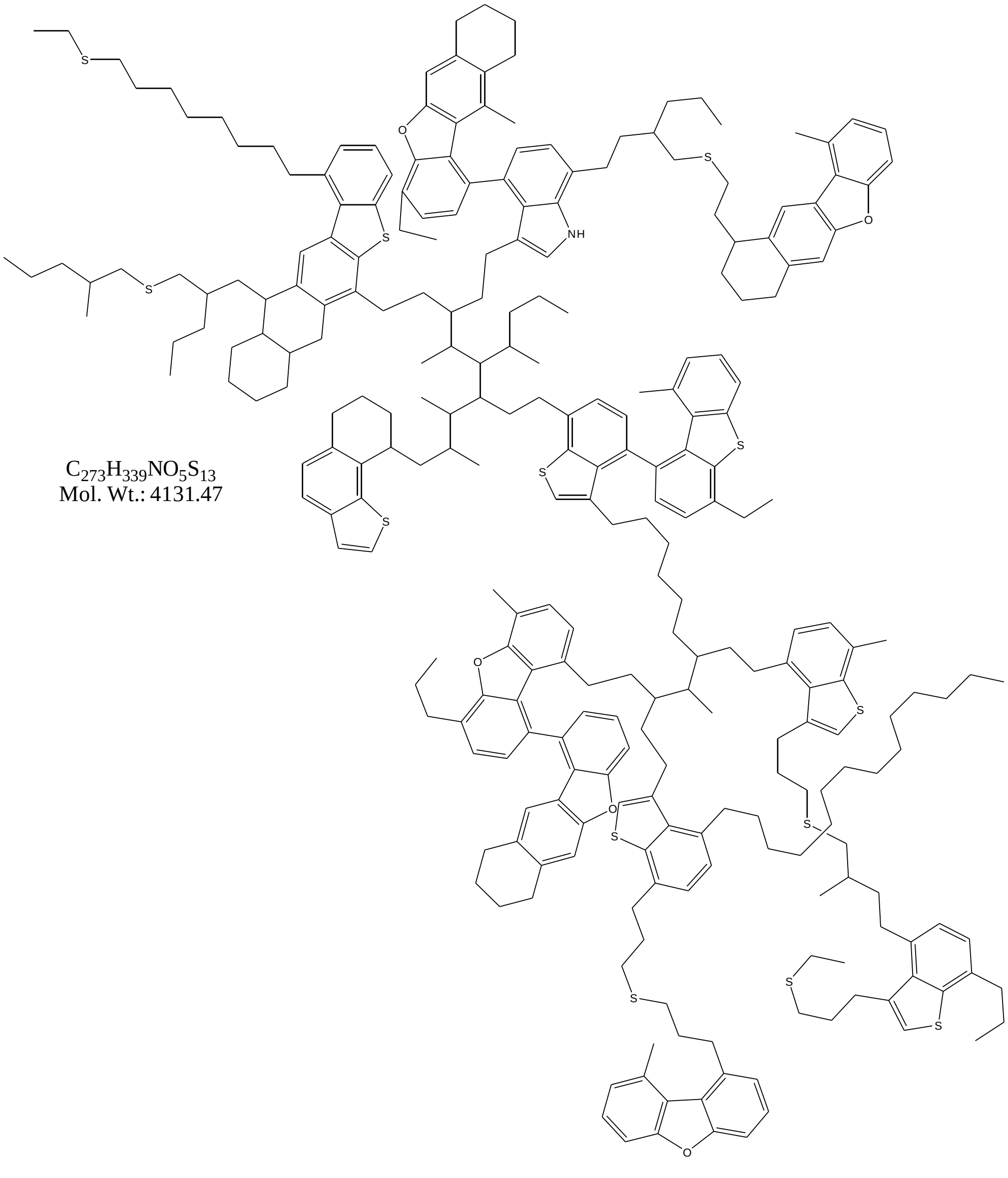

$C_{273}H_{339}NO_5S_{13}$
Mol. Wt.: 4131.47

Molecule #3

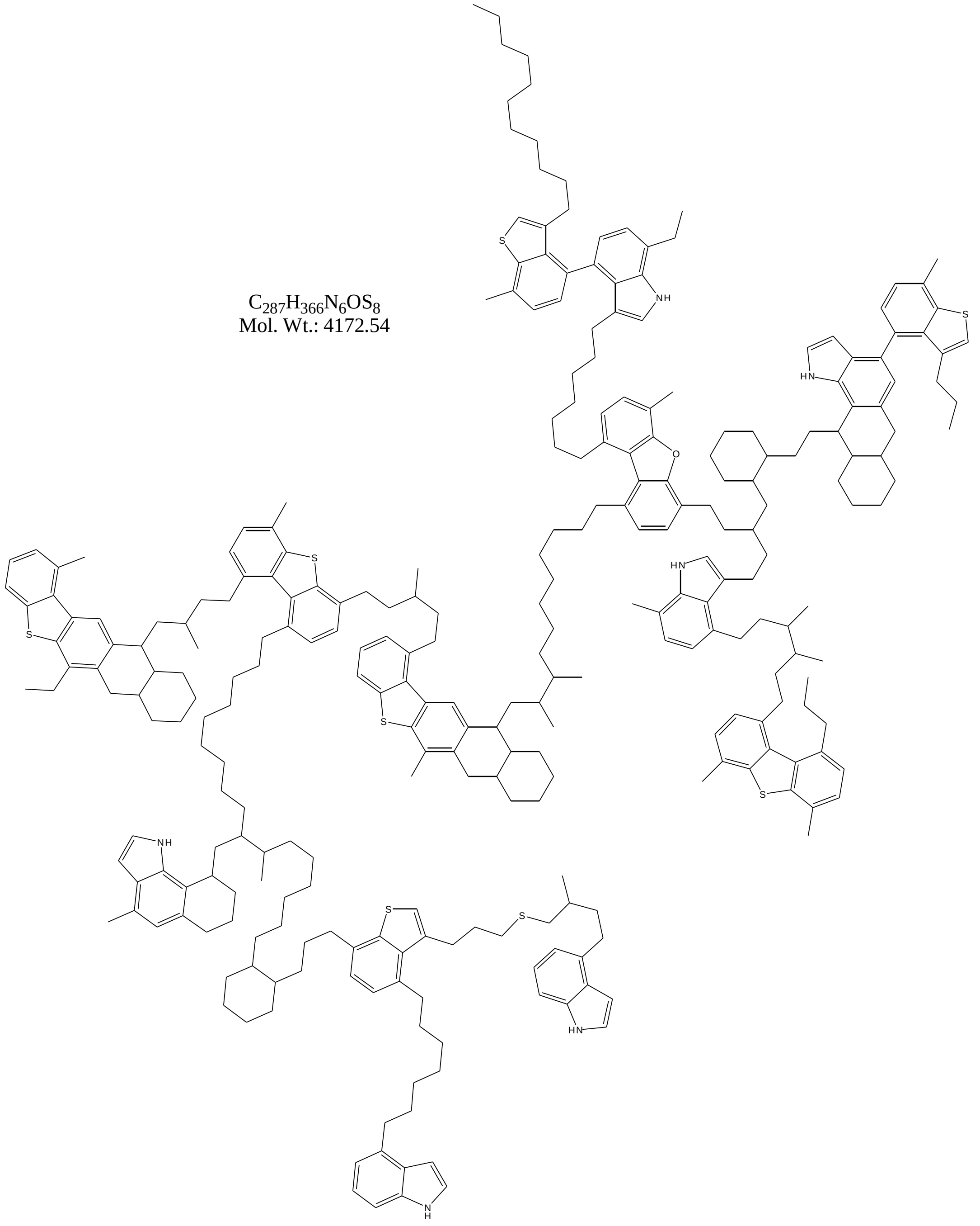

$C_{287}H_{366}N_6OS_8$
Mol. Wt.: 4172.54

Molecule # 4

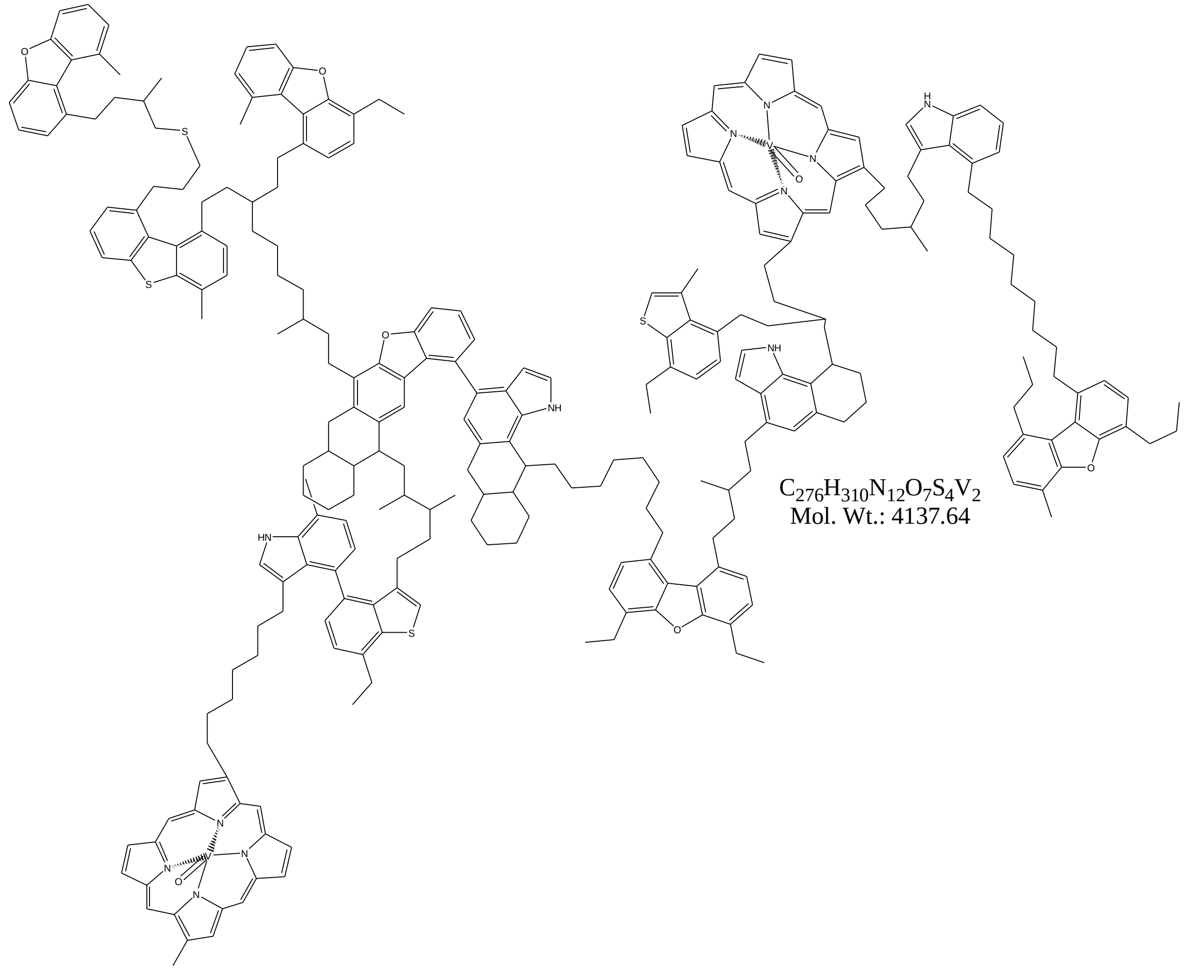

$C_{276}H_{310}N_{12}O_7S_4V_2$
Mol. Wt.: 4137.64

Molecule # 5

$C_{286}H_{351}N_3O_2S_8$
Mol. Wt.: 4119.39

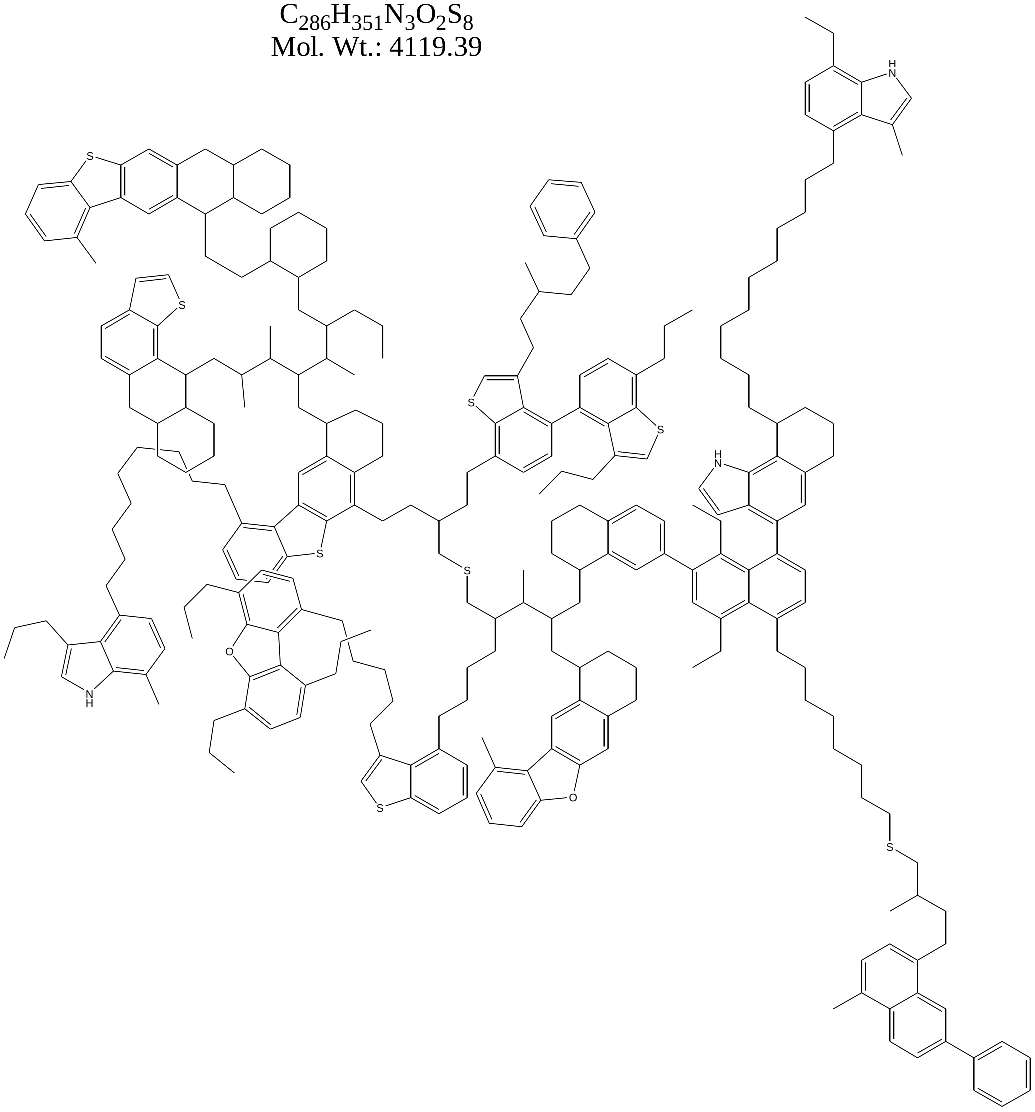

Molecule #6

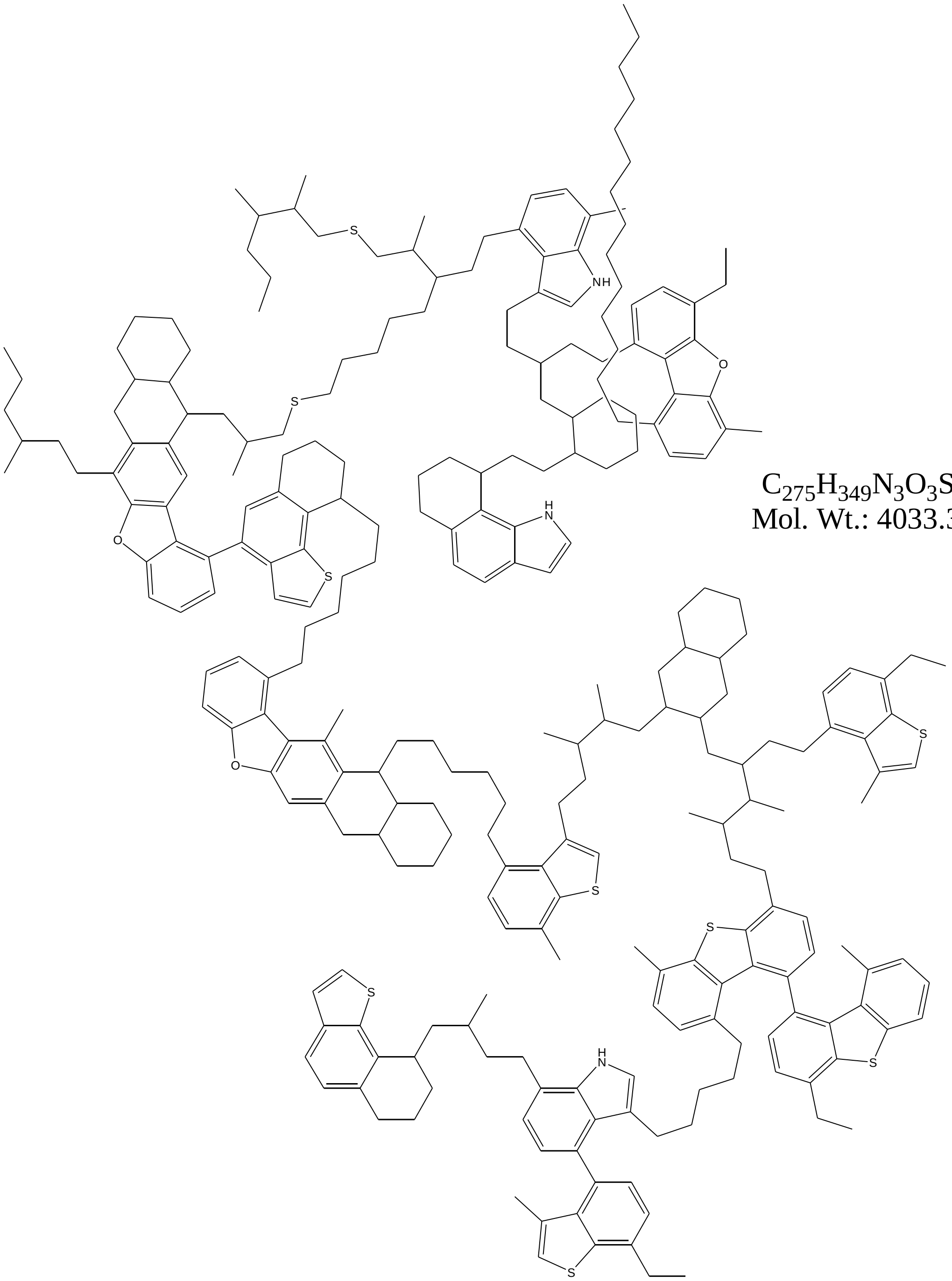

$C_{275}H_{349}N_3O_3S_9$
Mol. Wt.: 4033.33

Athabasca bitumen Molecules

Molecule #1

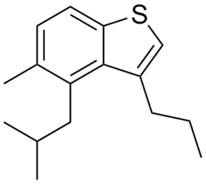

Chemical Formula: $C_{16}H_{22}S$
Molecular Weight: 246.41

Molecule #2

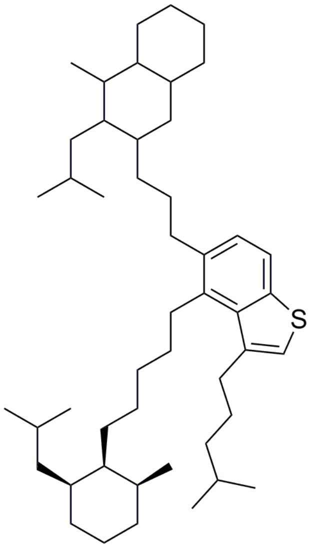

Chemical Formula: $C_{48}H_{80}S$
Molecular Weight: 689.21

Molecule #3

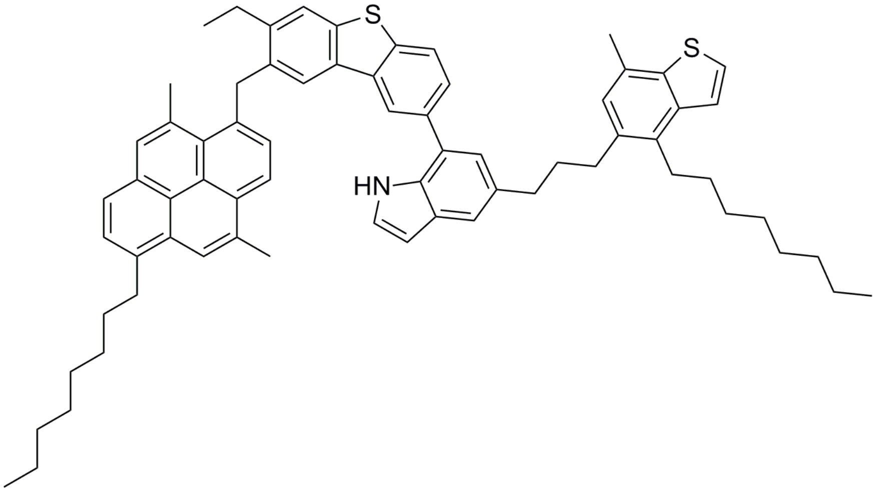

Chemical Formula: $C_{69}H_{75}NS_2$
Molecular Weight: 982.47

Molecule #4

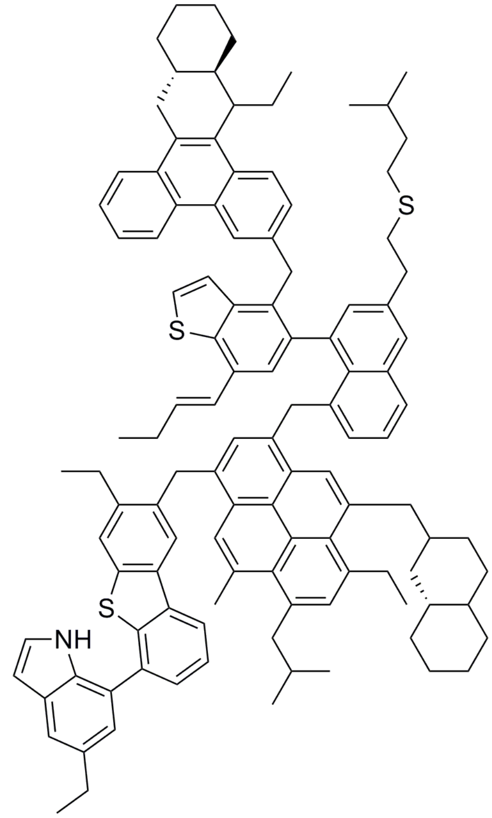

Chemical Formula: $C_{114}H_{121}NS_3$
Molecular Weight: 1601.38

Molecule #5

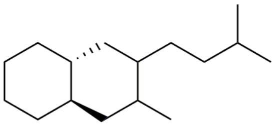

Chemical Formula: $C_{16}H_{30}$
Molecular Weight: 222.41

Molecule #6

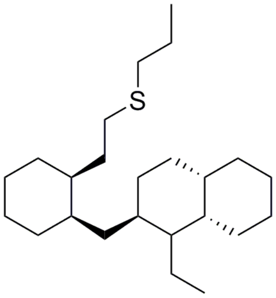

Chemical Formula: $C_{24}H_{44}S$
Molecular Weight: 364.67

Molecule #7

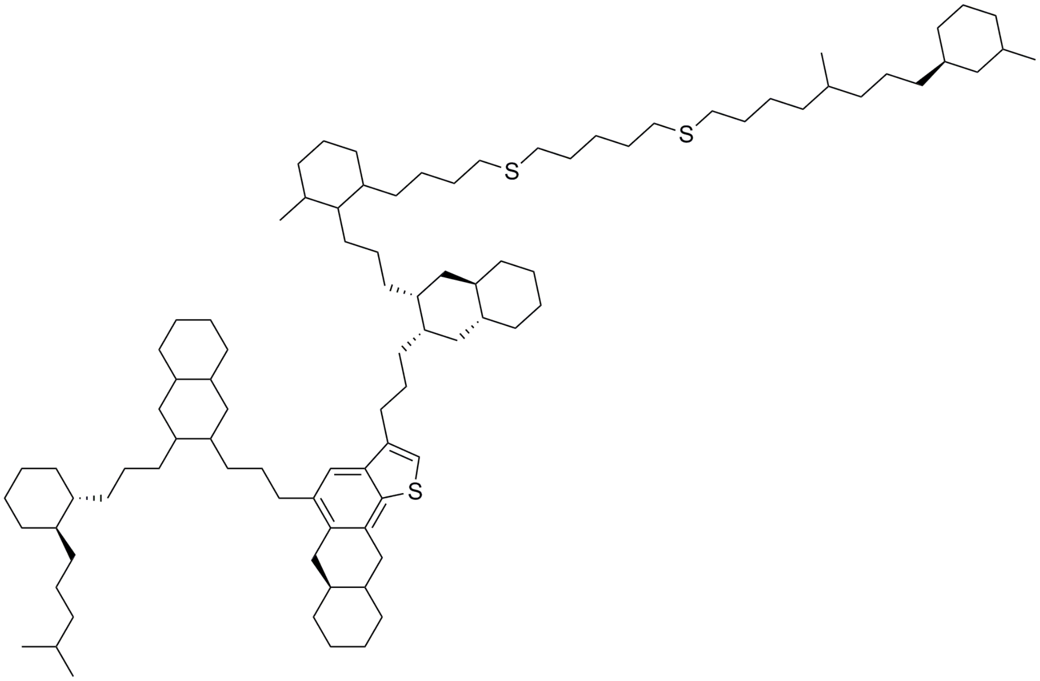

Chemical Formula: $C_{92}H_{156}S_3$
Molecular Weight: 1358.42

Molecule #8

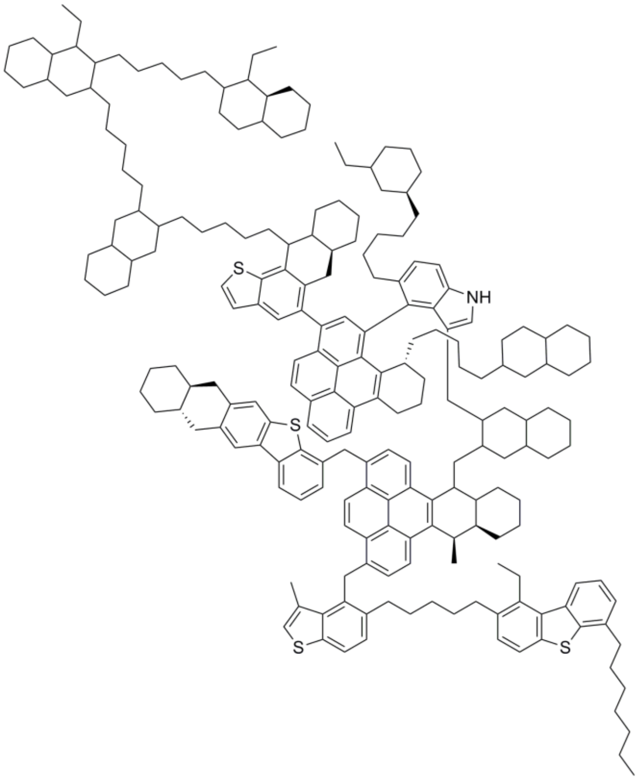

Chemical Formula: $C_{215}H_{277}NS_4$
Molecular Weight: 3003.77

Molecule #9

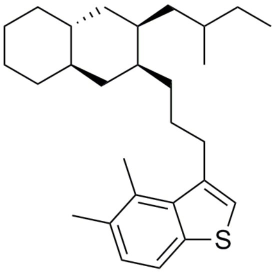

Chemical Formula: $C_{28}H_{42}S$
Molecular Weight: 410.70

Molecule #10

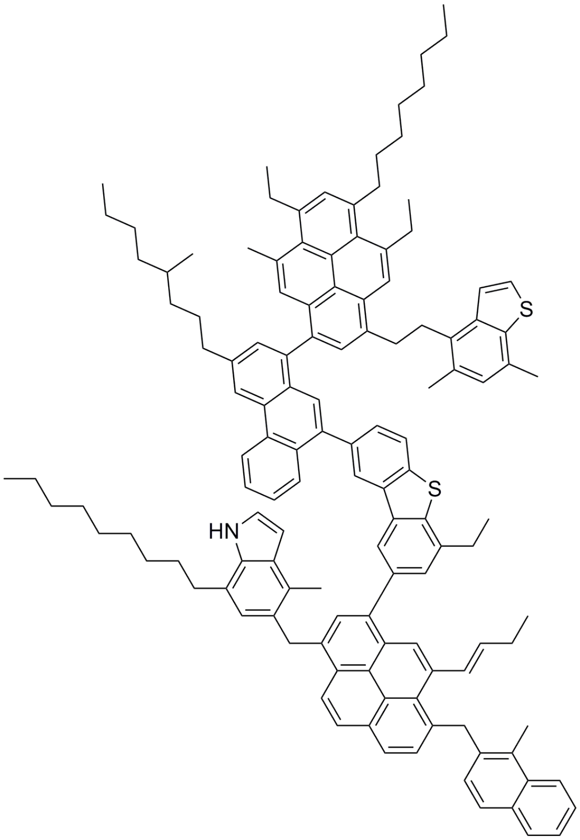

Chemical Formula: $C_{129}H_{135}NS_2$
Molecular Weight: 1763.59

Molecule #11

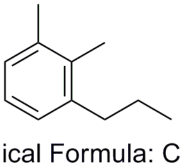

Chemical Formula: $C_{11}H_{16}$
Molecular Weight: 148.24

Molecule #12

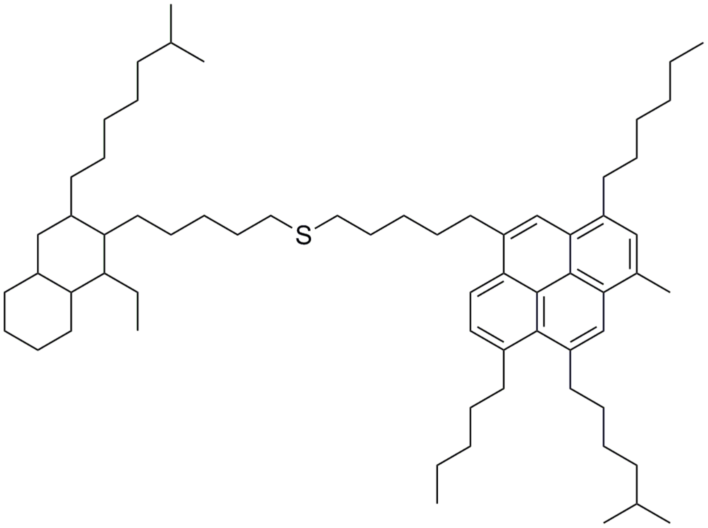

Chemical Formula: $C_{65}H_{104}S$
Molecular Weight: 917.59

Molecule #13

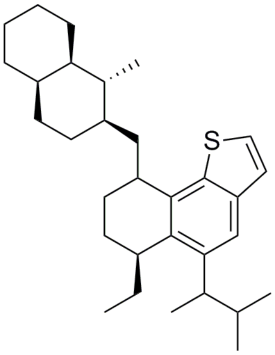

Chemical Formula: $C_{31}H_{46}S$
Molecular Weight: 450.76

Molecule #14

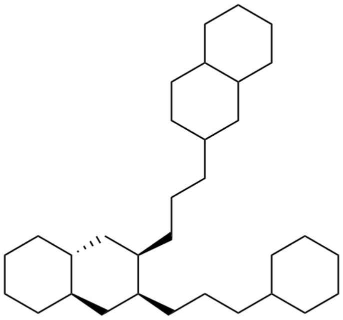

Chemical Formula: $C_{32}H_{56}$
Molecular Weight: 440.79

Molecule #15

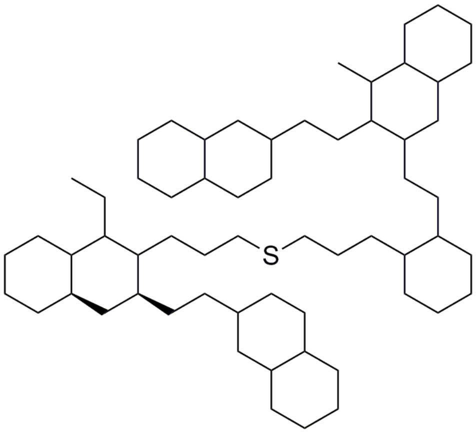

Chemical Formula: $C_{61}H_{106}S$
Molecular Weight: 871.56

Molecule #16

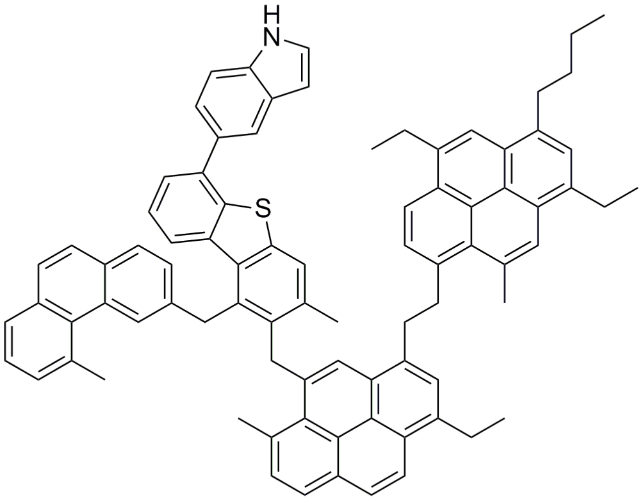

Chemical Formula: $C_{84}H_{73}NS$
Molecular Weight: 1128.55

Molecule #17

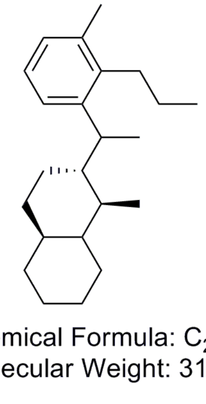

Chemical Formula: $C_{23}H_{36}$
Molecular Weight: 312.53

Structural representation of Athabasca vacuum residue with fifteen ensemble molecules (developed running Sheremata's codes)

Molecule #1

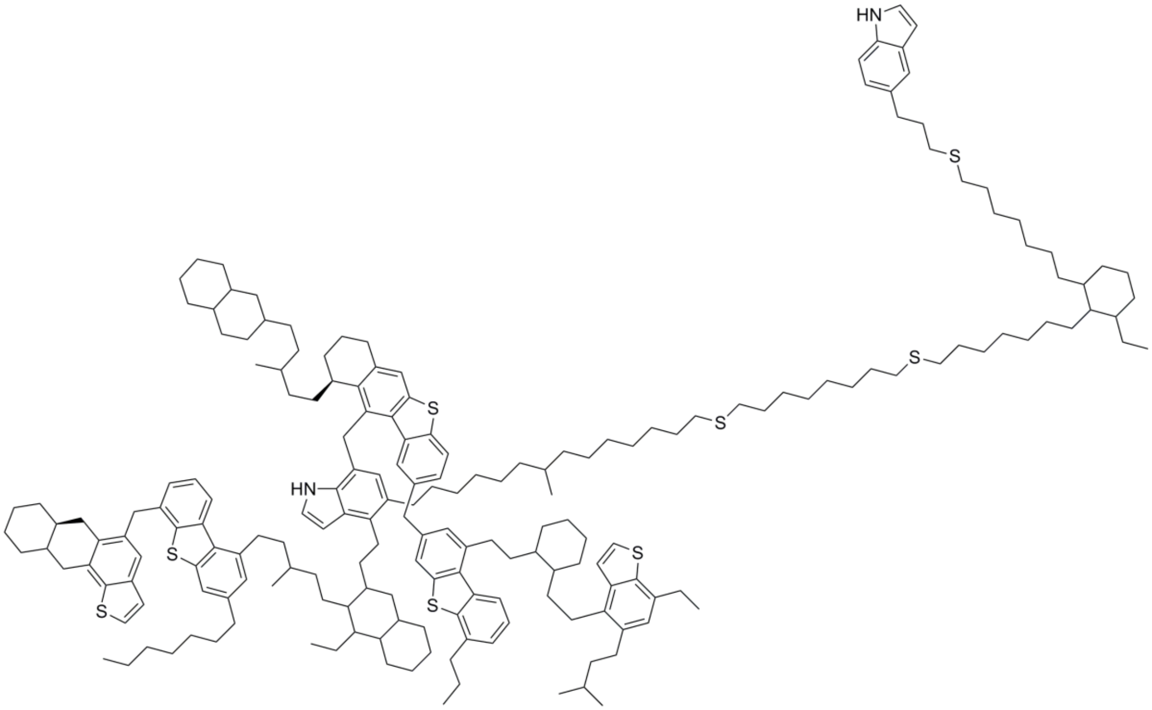

Molecule #2

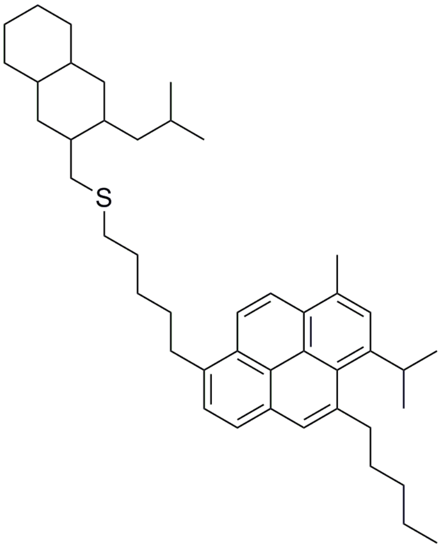

Molecule #3

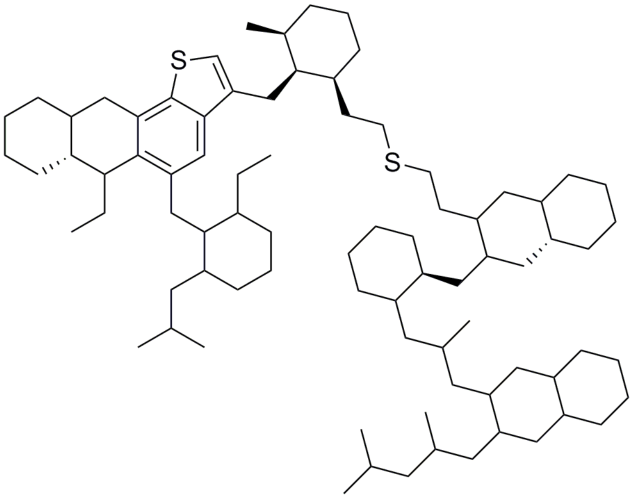

Molecule #4

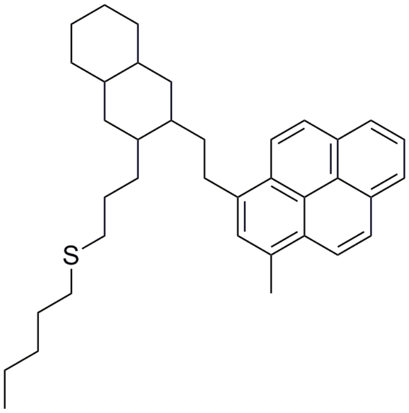

Molecule #5

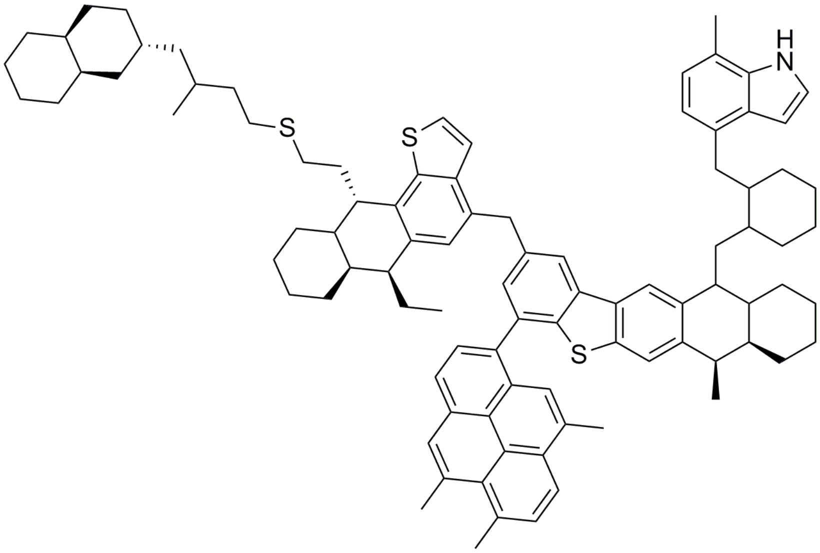

Molecule #6

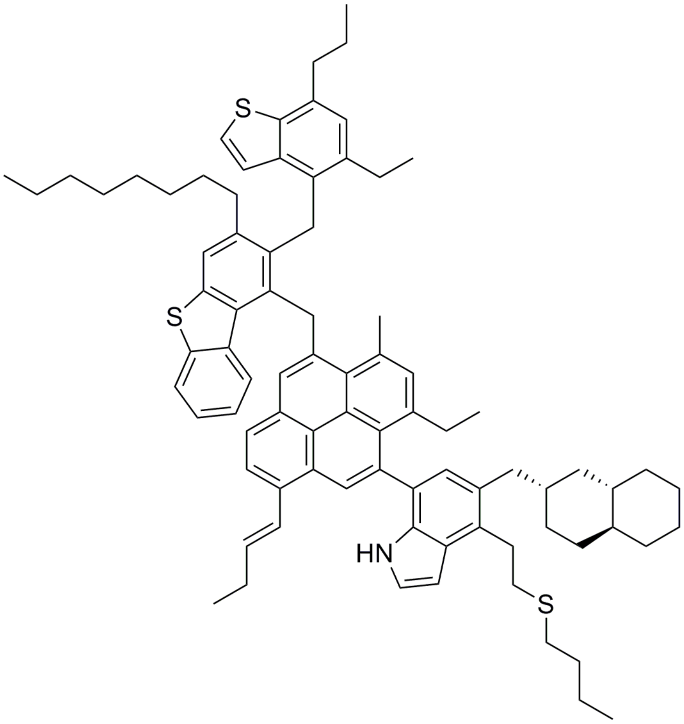

Molecule #7

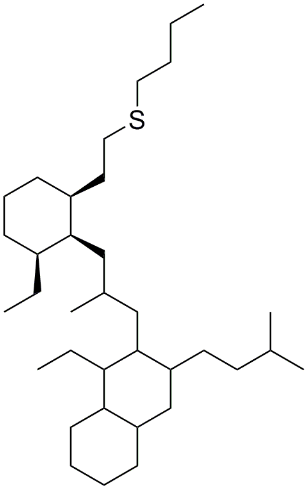

Molecule #9

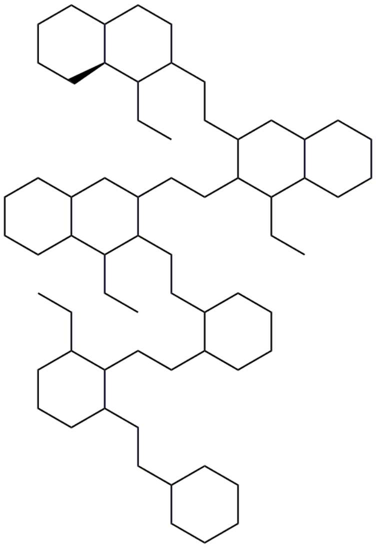

Molecule #10

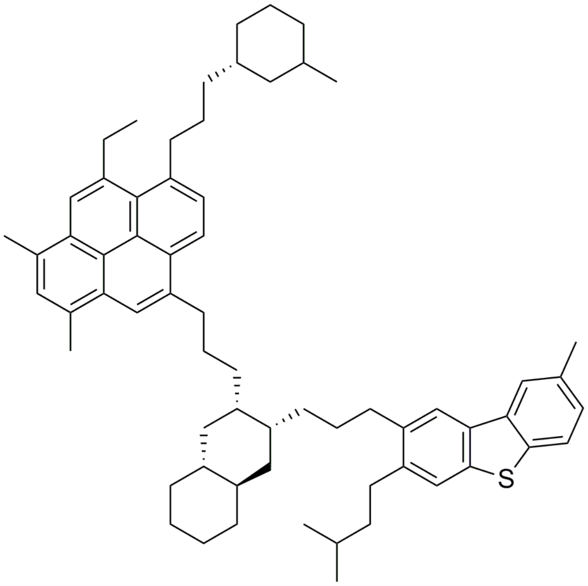

Molecule #11

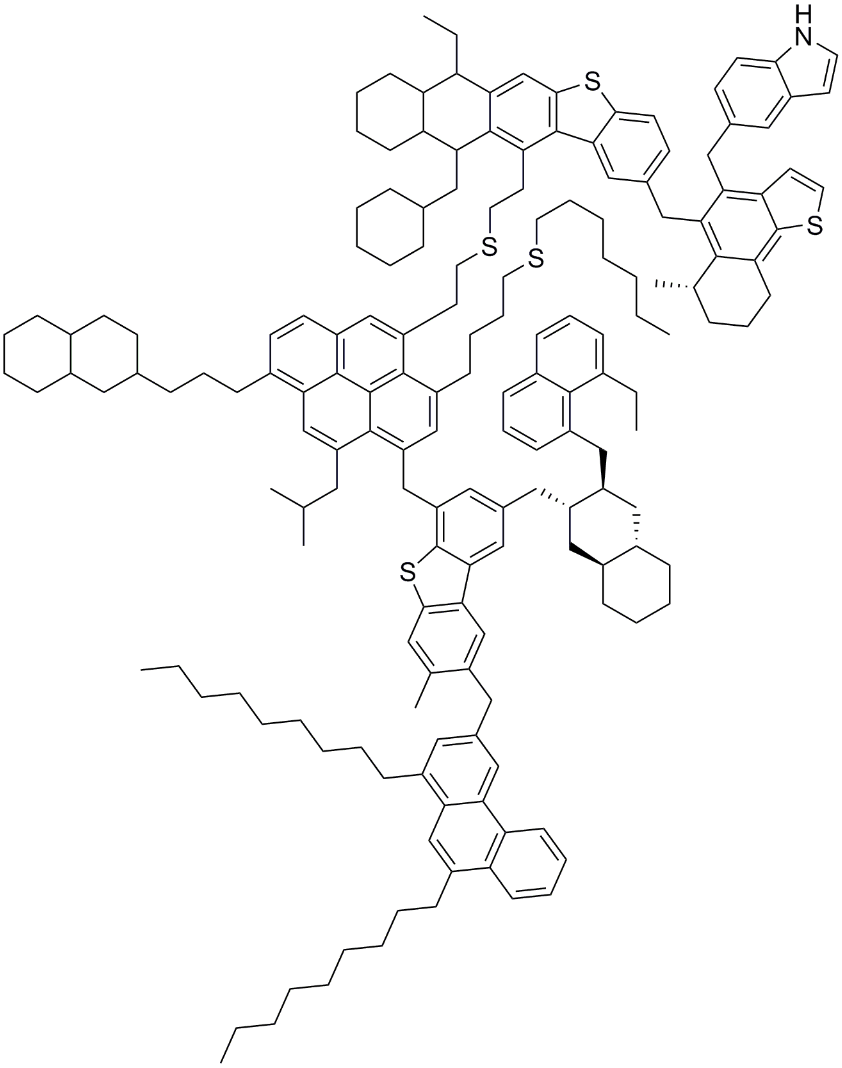

Molecule #12

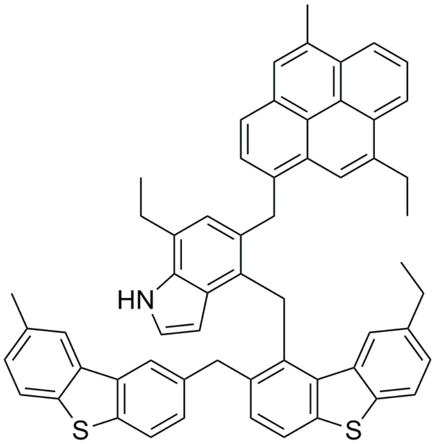

Molecule #13

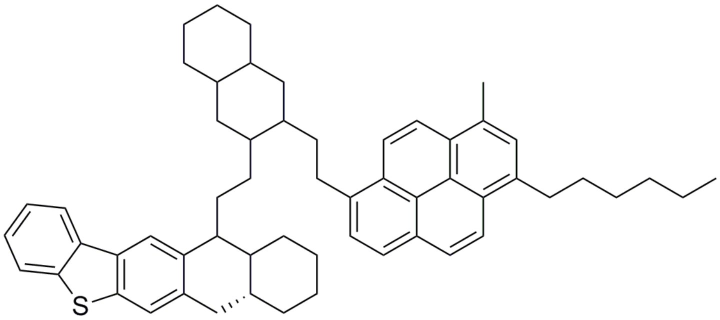

Molecule #14

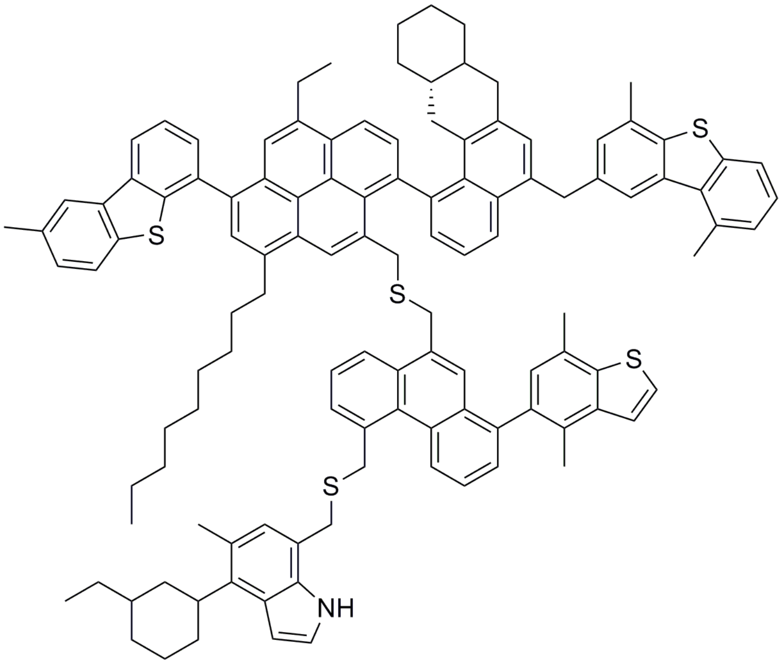

Molecule #15